
Nitsche-based enforcement of Dirichlet boundary conditions for the Hodge Laplacian

Thesis to obtain the degree of
Master of Science (MSc)

Carried out at
Seminar for Applied Mathematics (SAM), ETH Zürich

Author:

Camilo TELLO FACHIN

Mat. Nr. ETHZ:

17-671-579

Mat. Nr. TUW:

12127084

Supervisors:

Prof. Dr. Ralf HIPTMAIR

(SAM-ETHZ)

Wouter Rens TONNON

(SAM-ETHZ)

Dr. Enrico ZAMPA

(Faculty of Mathematics - University of Vienna)

Dr. Wietse Marijn BOON

(NORCE)

Prof. Dr. Joachim SCHÖBERL

(ASC-TUW)

Zürich, April 19, 2025

Camilo TELLO FACHIN

Abstract

This thesis investigates the discrete Hodge Laplace equation with Nitsche-type Dirichlet boundary conditions. Within the Finite Element Exterior Calculus framework we establish well-posedness, consistency, convergence, and a sub-optimal a-priori error estimate. For 1-forms in 2D we sharpen this to an optimal estimate, confirmed by numerical tests.

Further experiments in 3D for both 1- and 2-forms show the same convergence trend, still half an order below the theoretical bound. All results can be reproduced by cloning this repository.

We also demonstrate robustness on non-convex domains and study the effect of different perturbation factors, hinting at applications to compressible Stokes flow.

Zusammenfassung

Diese Arbeit untersucht die diskrete Hodge Laplace Gleichung mit Dirichlet-Randbedingungen vom Nitsche-Typ. Im Rahmen des Finite Element Exterior Calculus zeigen wir Wohlgestelltheit, Konsistenz, Konvergenz sowie eine suboptimale a-priori-Fehlerschranke.

Für 1-Formen in 2D verschärfen wir diese Schranke zu einer optimalen a-priori-Schranke, was durch numerische Tests bestätigt wird.

Weitere 3D-Experimente für 1- und 2-Formen weisen den gleichen Konvergenztrend auf, bleiben jedoch um eine halbe Ordnung unter der theoretischen Schranke. Alle Ergebnisse lassen sich reproduzieren, indem man dieses Repository klonet.

Wir demonstrieren zudem die Robustheit auf nicht-konvexen Mannigfaltigkeiten und untersuchen den Einfluss verschiedener Störparameter, was auf Anwendungen in der kompressiblen Stokes-Strömung hindeutet.

Acknowledgement

First of all, I'd like to thank Prof. Dr. Ralf Hiptmair for the opportunity to conduct my thesis at ETH and allowing me to work in an office among the brilliant minds at SAM and explore such an interesting topic.

Wouter, Enrico, and Wietse, you have been amazing. I am forever grateful for all the knowledge you have shared with me while remaining humble and patient. The way you supervised me was something many students can only wish for, and I hope we will collaborate in the future if I am given the chance to continue this journey in academia.

A big thanks also goes to Prof. Dr. Joachim Schöberl, not only for creating NGSolve but also for accepting me into the CSE program. This master's program has given me so much. For the first time in my life, I felt that I truly belonged to a larger community of people with similar interests, comparable values, and a nonjudgmental attitude towards me.

A huge thanks goes to Prof. Dr. Andreas Witzig. You started as merely my boss at the Institute of Computational Physics at ZHAW, but you grew into a fatherlike mentor and eventually a friend. Without you, none of this would have been possible.

Special thanks go to Edoardo Bonetti, whom I consider one of my best friends. You have been of tremendous help with NGSolve bugs and questions, and I am deeply grateful for your feedback and critique of my mathematical work throughout the process of this thesis. I did not anticipate you becoming such a friend and role model for me.

I would like to thank Paul Genest, Simon König, Dominik Freinberger, Manuela Raidl, Markus Renoldner, Eva Doloszeski, Leonid Ricker, Carmen Halbeisen, Leonie Greber, Alexander Kurt, Tobias Slowiak, Peter Unger, Johannes Reck and Hans Ruckdäschel, You have been great friends, and I hope our paths never part.

A big thank you to my parents for always supporting me, for creating me and my dear sister Melody, for being who you are, and for always believing in me. I would literally not be here without you.

My flatmates Jakob Schleenvoigt, Adrian Lindenthal, I am very happy that you came into my life and contribute to my happiness every time I come home. I hope we remain like family forever. Victoria Wiltos, you are not my flatmate but I sure hope you become one again one day, you are a friend I hold very dear.

Last but not least, thanks to Lisa Sophie Brunhilde Rosenthal, my girlfriend, whom I met two years ago. I love you, and I hope I can be as good a boyfriend to you as you are a girlfriend to me. Without you, everything would be sad; when you are here, everything is good.

Contents

1	Introduction	1
1.1	Prior Work	1
1.2	Foundational work	2
2	Theory and preliminaries	3
2.1	Exterior algebra	3
2.2	Exterior calculus on manifolds	5
2.3	Finite Element Exterior Calculus	8
2.4	Some preliminaries for discrete analysis	9
2.5	Trace operators	11
2.6	Deriving the variational formulation	12
2.6.1	Discrete Hodge Laplace Nitsche method for 1-forms in $\Omega \subset \mathbb{R}^3$	14
2.6.2	Discrete Hodge Laplace Nitsche method for 2-forms in $\Omega \subset \mathbb{R}^3$	15
3	Analysis	16
3.1	Preliminary results & definitions	16
3.2	Saddle-point problem well-posedness	18
3.2.1	Semi positive-definiteness of $a_h(\mathbf{v}_h, \mathbf{v}_h)$	20
3.2.2	Continuity of $a_h(\mathbf{u}, \mathbf{v}_h)$	21
3.2.3	Coercivity of $a_h(\mathbf{v}_h, \mathbf{v}_h)$	22
3.2.4	Continuity & coercivity of $c(\cdot, \cdot)$	23
3.2.5	Continuity and inf-sup stability of $b(\mathbf{v}_h, q_h)$	24
3.3	Babuška-Nečas-Brezzi Well-posedness	25
3.3.1	1-form vector proxy BNB well-posedness	26
3.3.2	Well-posedness in the context of FEEC	30
3.4	Consistency	35
3.4.1	1-form vector proxy consistency	35
3.4.2	FEEC consistency	36
3.5	A priori error analysis	37
3.5.1	A suboptimal error bound	38

3.5.2	A sharp error bound for the 1-form 2D method	39
4	Numerical Experiments	42
4.1	Discrete Hodge Laplace for $\Lambda^1(\Omega)$ in \mathbb{R}^2	42
4.1.1	First order solution visualizations	46
4.1.2	Nitsche penalty parameter C_w impact on errors	47
4.1.3	h -convergence rates in the L^2 norms	48
4.1.4	h -convergence in the $\#$ -norm and its components	49
4.1.5	h -convergence in the X -norm and its components	50
4.2	Discrete Hodge Laplace for $\Lambda^1(\Omega)$ in \mathbb{R}^3	51
4.2.1	Nitsche penalty parameter C_w impact on errors	53
4.2.2	h -convergence in the L^2 norms	54
4.2.3	h -convergence in the $\#$ norm	55
4.2.4	h -convergence in the X norm	56
4.3	Discrete Hodge Laplace for $\Lambda^2(\Omega)$ in \mathbb{R}^3	57
4.3.1	Nitsche penalty parameter C_w impact on errors	59
4.3.2	h -convergence in the L^2 -norms	60
4.3.3	h -convergence in the $\#$ -norm	61
4.3.4	h -convergence in the X -norm	62
4.4	Experiments with non-convex geometries	63
4.4.1	Singularities in reentrant corners	63
4.4.2	Reentrant corner 1-forms in 2D	64
4.4.3	3D Reentrant corner geometry experiments	65
4.5	Perturbation factor experiments	66
5	Conclusion & Outlook	68
	References	70
	Appendix	70
A	In-silico environment 1	71
B	In-silico environment 2	72
C	Differential operators on \mathfrak{g}	73

Chapter 1

Introduction

We want to find a differential k -form $\omega \in \Lambda^k(\Omega)$ in a bounded smooth Lipschitz domain $\Omega \subset \mathbb{R}^d$ with boundary Γ such that the Hodge Laplace Equation (1.0.1) with boundary conditions (1.0.2) and (1.0.3) is satisfied. We introduce the exterior calculus notation in the beginning of the theory chapter.

$$(\mathbf{d}\delta + \delta\mathbf{d})\omega = f, \quad \text{in } \Omega, \quad (1.0.1)$$

$$\text{tr } \omega = 0, \quad \text{on } \Gamma, \quad (1.0.2)$$

$$\text{tr } \star \omega = 0, \quad \text{on } \Gamma. \quad (1.0.3)$$

A variational formulation for (1.0.1) that satisfies (1.0.2) and (1.0.3) needs to be well chosen to yield a well posed system. by applying the Nitsche method [Ern21b, Ch.37] to boundary condition (1.0.2), we can devise a well-posed discrete variational formulation that naturally satisfies (1.0.3) and penalizes deviations from (1.0.2), while preserving discrete De Rham exactness.

The main goal of this thesis is to rigorously establish well-posedness (existence and uniqueness), consistency, convergence, and a priori error estimates for this method. All of these properties are proven using the Finite Element Exterior Calculus (FEEC) framework, demonstrating that the approach is robust for a family of vector proxy space methods, both in 2- and 3D.

1.1 Prior Work

Arnold et. al [Arnold12] have proven well-posedness and derived error bounds for the 2D vector Laplacian (the Hodge-Laplacian can be identified with the vector Laplacian through vector proxies) in a 2D mixed method in $H^1(\Omega) \times \mathbf{H}^0(\text{div}, \Omega)$ where the tangential part of the boundary condition arises naturally and the normal one essentially in $\mathbf{H}^0(\text{div}, \Omega)$.

Boon et. al [Boon24] have investigated the Vorticity-Velocity-Pressure Stokes formulation in 2D, which can be posed in the discrete subspaces of $\mathbf{H}(\text{curl}, \Omega) \times H^1(\Omega)$, satisfying the 2D De Rham complex (most of their results are applicable in 3D as well). Their approaches differ not only in the boundary conditions but also in the formulation of the auxiliary equation. In our work, we introduce an auxiliary variable to derive the mixed method, whereas they employ the zero divergence equation from Stokes.

A recent publication by Wang et. al [Wang25] has also delivered well-posedness and optimal a-priori error estimates for a mixed method for the 2D vector Laplacian with Dirichlet boundary conditions. However, in that work the authors additionally solve for the divergence and the rotation of \mathbf{u} thereby increasing complexity

and seeking $(\mathbf{u}, \gamma, \delta) \in [H^1(\Omega)]^2 \times [H^1(\Omega)]^2 \times \mathbf{H}(\text{div}, \Omega)$. The advantage of this approach is that the well-posedness proof can be done in the continuous setting, whereas our method can only be shown to be well-posed in the discrete setting.

1.2 Foundational work

In the 1980s, Bossavit pioneered using differential forms for discretizing electromagnetic fields, emphasizing geometric accuracy [Bossavit88]. Raviart and Thomas introduced the now-classic Raviart–Thomas elements for enforcing flux continuity in elliptic problems [Raviart77], while Nédélec devised the edge elements tailored to $\mathbf{H}(\text{curl}, \Omega)$ type constraints in electromagnetics [Nédélec80]. Brezzi and Fortin formalized mixed and hybrid finite elements, showing how “exact” sequences and stability principles aid robust numerical methods [Brezzi91].

Building on these foundations, Hiptmair worked on the theory of discrete Hodge operators, making it possible to rigorously connect the continuous de Rham complex with its finite element counterparts [Hiptmair01]. Arnold, Falk, and Winther synthesized these developments into Finite Element Exterior Calculus (FEEC): a unifying framework that explains why classic elements (Lagrange, Nédélec, Raviart–Thomas etc.) fit together so naturally, and shows how preserving exactness in discrete differential forms leads to stable and accurate solutions of variational problems [Arnold18]. In this work, they already showed well-posedness for the continuous variational form of the Hodge Laplacian, but with $\text{tr} \star \mathbf{d}\omega = 0$ and $\text{tr} \star \omega = 0$ as boundary conditions.

Chapter 2

Theory and preliminaries

In the next two sections, we give a brief overview of the relevant definitions, lemmas & theorems, covered in [Arnold06, Chap. 2]. Afterwards we will cover a brief introduction to Finite Element Exterior Calculus and some relevant inequalities that will be used throughout the thesis. The last section in this chapter is dedicated to the derivation of the variational formulations, both for differential k -forms in \mathbb{R}^n , as well as the vector proxy space of 1-forms and 2-forms in \mathbb{R}^3 .

2.1 Exterior algebra

Definition 2.1.1 (Alternating algebraic forms on a vector space). Let V be a real vector space. For each integer $k \geq 0$, define

$$\text{Alt}^k V := \{ \omega : V^k \rightarrow \mathbb{R} \mid \omega \text{ is } k\text{-linear and } \omega \text{ changes sign upon swapping any two arguments} \}.$$

Equivalently,

$$\omega(v_1, \dots, v_i, \dots, v_j, \dots, v_k) = -\omega(v_1, \dots, v_j, \dots, v_i, \dots, v_k),$$

and ω is linear in each argument. By convention,

$$\text{Alt}^0 V = \mathbb{R}, \quad \text{and} \quad \text{Alt}^1 V = V^*.$$

With V^* denoting the dual of V .

Definition 2.1.2 (Exterior product). Given $\omega \in \text{Alt}^j V$ and $\eta \in \text{Alt}^k V$ the exterior product, or wedge product $\omega \wedge \eta \in \text{Alt}^{j+k} V$ is given by

$$(\omega \wedge \eta)(v_1, \dots, v_{j+k}) = \sum_{\sigma} (\text{sign } \sigma) \omega(v_{\sigma(1)}, \dots, v_{\sigma(j)}) \eta(v_{\sigma(j+1)}, \dots, v_{\sigma(j+k)}), \quad v_i \in V \quad (2.1.1)$$

where the sum is over all permutations σ of $\{1, \dots, j+k\}$, for which $\sigma(1) < \sigma(2) < \dots < \sigma(j)$ and $\sigma(j+1) < \sigma(j+2) < \dots < \sigma(j+k)$. The exterior product is bilinear and associative, and satisfies the anti-commutativity condition

$$\eta \wedge \omega = (-1)^{jk} \omega \wedge \eta, \quad \omega \in \text{Alt}^j V, \quad \eta \in \text{Alt}^k V \quad (2.1.2)$$

Definition 2.1.3 (Inner product on algebraic forms). $\langle \cdot, \cdot \rangle : \text{Alt}^k V \times \text{Alt}^k V \longrightarrow \mathbb{R}$

$$\langle \omega, \eta \rangle = \sum_{\sigma} \omega(v_{\sigma(1)}, \dots, v_{\sigma(k)}) \eta(v_{\sigma(1)}, \dots, v_{\sigma(k)}), \quad \omega, \eta \in \text{Alt}^k V. \quad (2.1.3)$$

where the sum runs over all increasing sequences $\sigma : \{1, \dots, k\} \rightarrow \{1, \dots, n\}$, and v_1, \dots, v_n is any orthonormal basis. The right-hand side is independent of the choice of basis.

For $n = \dim V$, the space $\text{Alt}^n(V)$ is one-dimensional. Any element $\omega \in \text{Alt}^n(V)$ is uniquely determined by its value on a single ordered basis, and its value on any list of n vectors (w_1, \dots, w_n) is given by:

$$\omega(w_1, \dots, w_n) = \omega(v_1, \dots, v_n) \cdot \det(A), \quad (2.1.4)$$

where A is the matrix expressing w_1, \dots, w_n in terms of the basis v_1, \dots, v_n . In particular, an algebraic n form is uniquely determined (up to sign) by requiring that it takes the value 1 on some orthonormal basis. Consequently, it will take values ± 1 on all orthonormal bases.

Definition 2.1.4 (Hodge star Operator). Let V be an n -dimensional real vector space equipped with a positive-definite inner product $\langle \cdot, \cdot \rangle$ and an orientation, giving rise to a volume form $\text{vol} \in \Lambda^n(V^*)$. For each $0 \leq k \leq n$, the *Hodge star* is the linear map

$$\star : \Lambda^k(V^*) \longrightarrow \Lambda^{n-k}(V^*),$$

characterized uniquely by the property

$$\omega \wedge (\star \eta) = \langle \omega, \eta \rangle \text{vol} \quad \text{for all } \omega, \eta \in \Lambda^k(V^*).$$

That is, $\star \eta$ is the unique $(n - k)$ -form whose wedge product with ω reproduces the inner product $\langle \omega, \eta \rangle$ up to the volume form vol . Furthermore we have

$$\text{Isometry: } \|\star \eta\| = \|\eta\|, \quad \text{Involution: } \star(\star \eta) = (-1)^{k(n-k)} \eta. \quad (2.1.5)$$

The definition of \star depends on the chosen orientation (through vol) and the positive-definite structure on V . In the context of an oriented Riemannian manifold one applies this construction pointwise to each tangent space, obtaining the Hodge star operator on differential forms.

2.2 Exterior calculus on manifolds

Definition 2.2.1 (Manifolds and tangent spaces). A smooth manifold Ω of dimension n is a topological space in which every point $x \in \Omega$ has a neighborhood homeomorphic to an open subset of \mathbb{R}^n . At each $x \in \Omega$, the tangent space $T_x\Omega$ is an n -dimensional real vector space, and the disjoint union of all tangent spaces forms the tangent bundle $T\Omega = \bigcup_{x \in \Omega} \{(x, v) \mid v \in T_x\Omega\}$.

A *vector field* on Ω is a smooth map $x \mapsto v(x)$ with $v(x) \in T_x\Omega$ for each $x \in \Omega$. Thus, each vector field picks out one tangent vector in $T_x\Omega$ at every point x .

If $\phi : \Omega \rightarrow \Omega'$ is a smooth map between manifolds, the differential (or tangent map) of ϕ at x , denoted $D\phi_x$, is a linear map

$$D\phi_x : T_x\Omega \longrightarrow T_{\phi(x)}\Omega'.$$

In particular, for a real-valued function $\phi : \Omega \rightarrow \mathbb{R}$, this differential at x evaluates directional derivatives of ϕ in any tangent direction $v \in T_x\Omega$.

Definition 2.2.2 (Differential forms on manifolds). Let Ω be a smooth manifold. A differential k -form on Ω is a smooth section of the bundle $\Lambda^k(T^*\Omega)$. Concretely, for each point $x \in \Omega$, it assigns an alternating k -linear map

$$\omega_x : T_x\Omega \times \cdots \times T_x\Omega \longrightarrow \mathbb{R},$$

and this assignment varies smoothly in x . The space of all such k -forms on Ω is denoted by $\Lambda^k(\Omega)$.

Definition 2.2.3 (traces of k -forms). For a differential k -form ω in \mathbb{R}^n we define

$$\omega^{\text{tan}} = \text{tr } \omega, \tag{2.2.1}$$

$$\omega^{\text{nor}} = \hat{\star}^{-1} \text{tr } \star \omega. \tag{2.2.2}$$

Where \star^{-1} is the inverse operation of \star , and $\hat{\star}$ is the Hodge star operator at the boundary Γ .

Formally, if we have ω , a 1-form in \mathbb{R}^3 , then $\text{tr } \omega$ gives the behavior of ω on Γ in direction tangential to Γ . This quantity can still be interpreted as "tangential to Γ " in \mathbb{R}^2 , although it is represented as scalar.

A 2-form in \mathbb{R}^3 is something that assigns an oriented area to pairs of tangent vectors. The trace of such a 2-form, yields a 2-form on a 2-dimensional surface, which is a top form on Γ and directly represents an area element on the boundary and can be interpreted as the flux density across Γ .

Intuitively, the term $\hat{\star}^{-1} \text{tr } \star \omega$ for 2-forms in 3D, applying \star on ω yields a 1-form, if one thinks of ω as a flux (which is a 2-form in 3D), then $\star \omega$ is the vector representation of that flux, the trace of this gives the flux tangential to Γ . $\hat{\star}^{-1}$ then "rotates back" the restricted 1-form into another 1-form on Γ , that now represents the flux normal to Γ .

Definition 2.2.4 (Exterior Derivative \mathbf{d}). Let $\Omega \subset \mathbb{R}^n$ be a smooth manifold, and let $\omega \in \Lambda^k(\Omega)$ be a smooth k -form. The exterior derivative is the linear map

$$\mathbf{d} : \Lambda^k(\Omega) \rightarrow \Lambda^{k+1}(\Omega)$$

defined by

$$\mathbf{d}\omega_x(\nu_1, \dots, \nu_{k+1}) = \sum_{i=1}^{k+1} (-1)^{i+1} \partial_{\nu_i} \omega_x(\nu_1, \dots, \widehat{\nu_i}, \dots, \nu_{k+1}),$$

where $\{\nu_1, \dots, \nu_{k+1}\}$ are vectors and the hat $\widehat{\nu_i}$ indicates omission of ν_i from the list of arguments.

\mathbf{d} satisfies the Leibniz rule with respect to the wedge product

$$\mathbf{d}(\alpha \wedge \beta) = (\mathbf{d}\alpha) \wedge \beta + (-1)^k \alpha \wedge (\mathbf{d}\beta),$$

for $\alpha \in \Lambda^k(\Omega)$ and $\beta \in \Lambda^\ell(\Omega)$. Note that we have formally introduced the exterior product of differential forms, which is just the pointwise applied exterior product of algebraic forms.

Remark 2.2.5 (Integration of differential forms). Let Ω be a k -dimensional Manifold. If ω is a differential k -form, then the integral $\int_\Omega \omega$ is well defined. Formally, 0-forms are evaluated at points, 1-forms integrated over curves, 2-forms integrated over oriented surfaces and 3-forms integrated over oriented volumes.

Theorem 2.2.6 (Stokes' Theorem and Integration by Parts). Let Ω be an oriented n -dimensional manifold with boundary Γ , and let $\omega \in \Lambda^{n-1}(\Omega)$. Then Stokes' Theorem states

$$\int_\Omega \mathbf{d}\omega = \int_\Gamma \text{tr } \omega.$$

Using the Leibniz rule for the exterior derivative, we obtain the integration by parts formula for $\omega \in \Lambda^k(\Omega)$ and $\eta \in \Lambda^{n-k-1}(\Omega)$

$$\int_\Omega \mathbf{d}\omega \wedge \eta = (-1)^k \int_\Omega \omega \wedge \mathbf{d}\eta + \int_\Gamma \text{tr}(\omega) \wedge \text{tr}(\eta).$$

Definition 2.2.7 (Inner Product on k -forms). Let Ω be an oriented manifold in \mathbb{R}^n , for $\omega, \eta \in \Lambda^k(\Omega)$, define their L^2 -inner product by the integral of their local inner product

$$\langle \omega, \eta \rangle_{L^2} = \int_\Omega \langle \omega_x, \eta_x \rangle_x \text{vol} = \int_\Omega \omega \wedge \star \eta.$$

Definition 2.2.8 (Sobolev Spaces of Differential Forms). Let Ω be an oriented Riemannian manifold. For an integer $s \geq 0$, we define the Sobolev space $H^s(\Omega)$ (resp. $W^{p,s}(\Omega)$) of real-valued functions whose weak derivatives up to order s lie in $L^2(\Omega)$ (resp. $L^p(\Omega)$). Extending this to k -forms, we write $H^s \Lambda^k(\Omega)$ for the space of k -forms whose components (in local coordinates) have all weak derivatives up to order s in $L^2(\Omega)$. Define the weaker space where H does not have a superscript

$$H \Lambda^k(\Omega) = \{ \omega \in L^2 \Lambda^k(\Omega) \mid \mathbf{d}\omega \in L^2 \Lambda^{k+1}(\Omega) \},$$

equipped with the norm

$$\|\omega\|_{H\Lambda^k(\Omega)}^2 = \|\omega\|_{L^2\Lambda^k(\Omega)}^2 + \|\mathbf{d}\omega\|_{L^2\Lambda^{k+1}(\Omega)}^2.$$

So we require only the exterior derivative to be in $L^2(\Omega)$ instead of every partial derivative of each component of the k -form.

Definition 2.2.9 (Closed Hilbert Complex). A Hilbert complex (W^k, d^k) is closed if for every k , the image $\text{im}(d^k)$ is a closed subspace of W^{k+1} . Equivalently this means, $\mathbf{d} \circ \mathbf{d} = 0$.

Definition 2.2.10 (Sobolev de Rham Complex). Let Ω be an oriented Riemannian manifold. For $0 \leq k \leq n$, consider the Sobolev space $H\Lambda^k(\Omega)$ and the exterior derivative. Since $\mathbf{d} \circ \mathbf{d} = 0$, we have

$$\text{Im}(\mathbf{d} : H\Lambda^{k-1}(\Omega) \rightarrow H\Lambda^k(\Omega)) \subset \text{Ker}(\mathbf{d} : H\Lambda^k(\Omega) \rightarrow H\Lambda^{k+1}(\Omega)).$$

This yields the Sobolev de Rham complex

$$0 \longrightarrow H\Lambda^0(\Omega) \xrightarrow{\mathbf{d}} H\Lambda^1(\Omega) \xrightarrow{\mathbf{d}} \dots \xrightarrow{\mathbf{d}} H\Lambda^n(\Omega) \longrightarrow 0.$$

Definition 2.2.11 (Coderivative δ). In an L^2 setting, the coderivative $\delta : H\Lambda^k(\Omega) \rightarrow H\Lambda^{k-1}(\Omega)$ is defined as the formal L^2 -adjoint of \mathbf{d} . Concretely, if $\omega \in H\Lambda^k(\Omega)$ and $\eta \in H\Lambda^{k-1}(\Omega)$ are compactly supported, then

$$\langle \mathbf{d}\omega, \eta \rangle_{L^2(\Omega)} = \langle \omega, \delta\eta \rangle_{L^2(\Omega)},$$

When Ω is oriented of dimension n , one can also write

$$\delta = (-1)^{n(k+1)+1} \star \mathbf{d} \star,$$

In particular, δ lowers the form degree by one, while \mathbf{d} raises it by one, and $\delta \circ \delta = 0$ as well.

Definition 2.2.12 (Dual Sobolev Complex). Define the space

$$H^*\Lambda^k(\Omega) := \{ \omega \in L^2\Lambda^k(\Omega) \mid \delta\omega \in L^2\Lambda^{k-1}(\Omega) \},$$

We have $H^*\Lambda^k(\Omega) = \star(H\Lambda^{n-k}(\Omega))$ by the definition of δ and the properties of the Hodge star \star . Consequently, we have the dual de Rham complex

$$0 \longleftarrow H^*\Lambda^0(\Omega) \xleftarrow{\delta} H^*\Lambda^1(\Omega) \xleftarrow{\delta} \dots \xleftarrow{\delta} H^*\Lambda^n(\Omega) \longleftarrow 0$$

which contains the same information as the de Rham complex.

Theorem 2.2.13 (Hodge Decomposition without Harmonic Forms). *Let W be a closed Hilbert complex. In a topologically trivial setting where the harmonic spaces vanish, we have the following orthogonal decompositions:*

$$W = \bar{b} \oplus \bar{c}.$$

With $\bar{b} = \overline{\text{Im}(\mathbf{d})}$ and $\bar{c} = \overline{\text{Im}(\boldsymbol{\delta})}$. The Hodge decomposition can be interpreted as a generalized Helmholtz decomposition. For $\omega \in H\Lambda^k(\Omega)$ we have

$$\omega = \mathbf{d}\alpha + \boldsymbol{\delta}\beta, \quad \alpha \in H\Lambda^{k-1}(\Omega), \quad \beta \in H\Lambda^{k+1}(\Omega), \quad \langle \mathbf{d}\alpha, \boldsymbol{\delta}\beta \rangle_{L^2(\Omega)} = 0.$$

[Arnold18, Thm. 4.5].

Theorem 2.2.14 (Poincaré inequality). *For any closed Hilbert Complex $\exists C_{P_\alpha}, C_{P_\beta} > 0$ such that*

$$\alpha \perp \text{Ker}(\mathbf{d}), \beta \perp \text{Ker}(\boldsymbol{\delta}), \quad \|\alpha\|_{L^2(\Omega)} \leq C_{P_\alpha} \|\mathbf{d}\alpha\|_{L^2(\Omega)}, \quad \|\beta\|_{L^2(\Omega)} \leq C_{P_\beta} \|\boldsymbol{\delta}\beta\|_{L^2(\Omega)}, \quad (2.2.3)$$

Where $\mathbf{d}\alpha, \boldsymbol{\delta}\beta$ are the components of the Hodge decomposition [Arnold18, Thm. 4.6].

We will regularly use the discrete counterpart of Theorem 2.2.13 and 2.2.14 in the analysis part.

2.3 Finite Element Exterior Calculus

The De Rham and proxy space picture in 3D

$$\begin{array}{ccccccc}
 H\Lambda^0(\Omega) & \xrightarrow{\mathbf{d}} & H\Lambda^1(\Omega) & \xrightarrow{\mathbf{d}} & H\Lambda^2(\Omega) & \xrightarrow{\mathbf{d}} & H\Lambda^3(\Omega) \\
 \updownarrow \cong & & \updownarrow \cong & & \updownarrow \cong & & \updownarrow \cong \\
 H^1(\Omega) & \xrightarrow{\nabla} & \mathbf{H}(\text{curl}; \Omega) & \xrightarrow{\nabla \times} & \mathbf{H}(\text{div}; \Omega) & \xrightarrow{\nabla \cdot} & L^2(\Omega) \\
 \downarrow \Pi_h^0 & & \downarrow \Pi_h^1 & & \downarrow \Pi_h^2 & & \downarrow \Pi_h^3 \\
 V_h^{\text{CG}} & \xrightarrow{\nabla} & V_h^{\text{ND1}} & \xrightarrow{\nabla \times} & V_h^{\text{RT}} & \xrightarrow{\nabla \cdot} & V_h^{\text{DG}}
 \end{array}$$

Figure 2.1: 3D De Rham complex for differential forms & vector proxies.

Shown figure in 2.1, the Sobolev spaces of differential forms, the isomorphisms to their according proxy Sobolev spaces and the commuting projectors to their discrete finite element spaces, which guarantee the discrete spaces inherit the "exactness" of the continuous spaces.

Whitney elements are the lowest order elements that can represent differential forms of degree k in the De Rham complex. In the literature, there is also often made the distinction between "trimmed" and "non-trimmed" Whitney forms. E.g. the first kind Nédélec elements [Nédélec80] would be trimmed, while the second kind would be non-trimmed for $k = 1$ and the Raviart-Thomas elements [Raviart77] would be trimmed while the BDM elements [Brezzi85] would be non-trimmed for $k = 2$. Standard Lagrange elements [Ciarlet72] of first order represent the Whitney forms trimmed space for 0-forms.

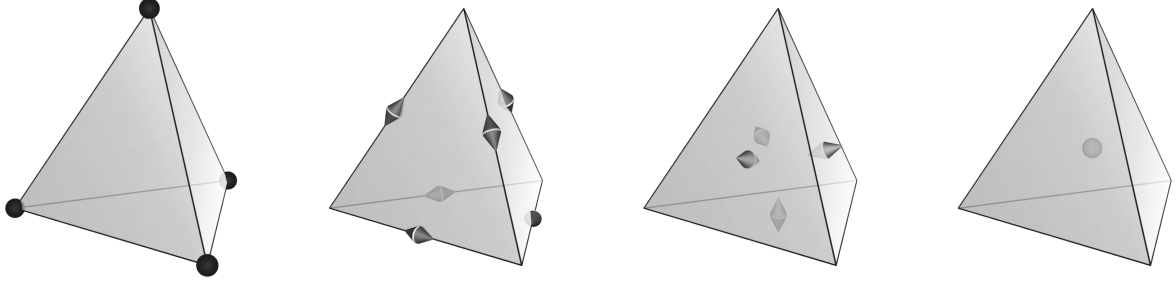


Figure 2.2: DOF's for the Whitney forms in 3D for $k = \{0, 1, 2, 3\}$. From left to right, Lagrange, Nédélec, Raviart-Thomas and discontinuous Galerkin elements [Arnold18].

In this thesis, we will work with the trimmed spaces only and denote them as follows

- V_h^{CG} : Continuous Galerkin or Lagrange (CG) elements for 0-forms,
- V_h^{ND1} : Nédélec (ND) elements of the first kind for 1-forms,
- V_h^{RT} : Raviart-Thomas (RT) elements for 2-forms,
- V_h^{DG} : Discontinuous Galerkin (DG) elements for 3-forms.

These spaces are available in  NGSolve . We will present numerical results in the according chapter.

2.4 Some preliminaries for discrete analysis

Since our method works only in the discrete setting, naturally, we define the generalized setting and present theoretical results that are valid in this setting.

Definition 2.4.1 (Mesh and mesh uniformity). Let Ω be a bounded domain. A mesh (or triangulation) of Ω is a collection of elements and faces denoted by

$$\mathcal{T}_h = \{K\}, \quad \mathcal{F}_K = \{F \in \partial K\}$$

where K is an open subset of Ω (e.g. tetrahedra in 3D or triangles in 2D). The elements K cover the domain without overlapping. A face F_K of an element K is a $d - 1$ dimensional entity (e.g. edge in 2D or face in 3D)

which forms part of the boundary of that element. If \mathcal{T}_h is uniform, there exist positive h, c_1, c_2 such that

$$c_1 h \leq h_K \leq c_2 h, \quad \forall K \in \mathcal{T}_h.$$

This uniformity has as a consequence that the faces F are also uniform (they have sizes comparable to the other faces of their according element).

Definition 2.4.2 (Family of uniform meshes).

$$\mathcal{H} = \{\mathcal{T}_h\}_{h>0}, \quad h \rightarrow 0.$$

Definition 2.4.3 (Boundary adjacent elements). The set of boundary adjacent elements \mathcal{T}_Γ can be defined as

$$\mathcal{T}_\Gamma = \{K \in \mathcal{T}_h \mid \partial K \cap \Gamma \neq \emptyset\}. \quad (2.4.1)$$

Theorem 2.4.4 (Inverse trace inequality). [Ern21a, Lemma 12.8] In a uniform family of meshes there holds

$$\exists C > 0 : \|v\|_{L^p(F_K, \mathbb{R}^q)} \leq C h_K^{-\frac{1}{p} + d\left(\frac{1}{p} - \frac{1}{r}\right)} \|v\|_{L^r(K, \mathbb{R}^q)}, \quad \forall p, r < \infty, \quad \forall K \in \mathcal{T}_h, \forall F \in \mathcal{F}_K, \forall h \in \mathcal{H}, \forall v \in \mathcal{P}_K.$$

For $p = r = 2$ we have

$$\|v\|_{L^2(F_K)} \leq C h_K^{-\frac{1}{2}} \|v\|_{L^2(K)}.$$

Theorem 2.4.5 (Inverse inequality for Sobolev seminorm). [Ern21a, Lemma 12.3] Let $l \in \mathbb{N}$ such that $\hat{P} \subset W^{l, \infty}(\hat{K}, \mathbb{R}^q)$, where the \hat{P} and \hat{K} denote the finite dimensional space P on the physical element K in the reference configuration. Then there exists $C > 0$ for every integer $m \in 0 : l$ and the following holds true

$$|v|_{W^{l, p}(K; \mathbb{R}^q)} \leq C h_K^{m-l+d\left(\frac{1}{p} - \frac{1}{r}\right)} |v|_{W^{m, r}(K; \mathbb{R}^q)}, \quad \forall p, r < \infty, \quad \forall K \in \mathcal{T}_h, \forall v \in P_K, \forall h \in \mathcal{H}.$$

For $l = 1, m = 0$ and $p = 2$ we therefore have

$$\|\nabla v\|_{L^2(K)} \leq C h_K^{-1} \|v\|_{L^2(K)}.$$

Most importantly, one can show for $k = \{0, 1, 2\}, n = 2$ and $k = \{0, 1, 2, 3\}, n = 3$ that there exist $C > 0$ such that

$$\|\mathbf{d}\omega_h\|_{L^2(K)} \leq C h_K^{-1} \|\omega_h\|_{L^2(K)}, \quad \forall \omega_h \in V_h \subset H\Lambda^k(K), \quad K \subset \mathbb{R}^n.$$

Only considering trimmed spaces, we use a reduced form of a result by Arnold et al.

Theorem 2.4.6. *Let Ω be a smooth Lipschitz domain, and let $r \geq 1$. Suppose $V_h^k \subset L^2\Lambda^k(\Omega)$ is the finite element space built from the trimmed polynomial forms of degree r on a uniform mesh of size h . Then there exists positive constants C and a linear projection operator*

$$\pi_h^k : L^2\Lambda^k(\Omega) \longrightarrow V_h^k, \quad (2.4.2)$$

such that for all differential k -forms ω there holds

$$\|\omega - \pi_h^k \omega\|_{L^2\Lambda^k(\Omega)} \leq Ch^s |\omega|_{H^s\Lambda^k(\Omega)}, \quad (2.4.3)$$

$$\|\mathbf{d}(\omega - \pi_h^k \omega)\|_{L^2\Lambda^k(\Omega)} \leq Ch^s |\mathbf{d}\omega|_{H^s\Lambda^{k+1}(\Omega)}, \quad 0 \leq s \leq r, \quad (2.4.4)$$

$$\mathbf{d}\pi_h^k = \pi_h^{k+1} \mathbf{d}, \quad (2.4.5)$$

provided $\omega \in H^s\Lambda^k(\Omega)$ and $\mathbf{d}\omega \in H^s\Lambda^{k+1}(\Omega)$.

Proof. The proof can be found in [Arnold06, Thm. 5.8]. We can verify the Theorem in a handwavy manner by taking the Lagrange, the Nédélec as well as the Raviart-Thomas elements and note that they themselves have h^r approximation property, while the gradient, the curl and the divergence applied to them respectively still yield h^r approximation property. \square

2.5 Trace operators

For Ω , a smooth Lipschitz domain, we have the following two trace operators

Definition 2.5.1 (Trace operator $\gamma_{||}(\mathbf{v})$). Let $L_{||}^2(\Gamma) := \{\zeta \in \mathbf{L}^2(\Gamma) | \zeta \cdot \mathbf{n} = 0\}$, then we have the following trace operator

$$\gamma_{||} : \mathbf{C}^\infty(\Omega) \longrightarrow \mathbf{L}_{||}^2(\Gamma), \quad \gamma_{||}(\mathbf{v}) := \mathbf{n} \times (\mathbf{v}|_\Gamma \times \mathbf{n}) \quad \forall \mathbf{v} \in \mathbf{C}^\infty(\Omega). \quad (2.5.1)$$

Definition 2.5.2 (Trace operator $\gamma_n(\mathbf{v})$). Under the same assumptions as 2.5.1 we have the trace operator

$$\gamma_n : \mathbf{C}^\infty(\Omega) \longrightarrow \mathbf{L}_{||}^2(\Gamma), \quad \gamma_n(\mathbf{v}) := \mathbf{n} \times (\nabla \times \mathbf{v})|_\Gamma, \quad \forall \mathbf{v} \in \mathbf{C}^\infty(\Omega). \quad (2.5.2)$$

With \mathbf{t} the tangent vector on Γ , in $\Omega \subset \mathbb{R}^2$ the operator becomes

$$\gamma_n : \mathbf{C}^\infty(\Omega) \longrightarrow \mathbf{L}_{||}^2(\Gamma), \quad \gamma_n(\mathbf{v}) := -\text{rot}(\mathbf{v})|_\Gamma \cdot \mathbf{t}, \quad \forall \mathbf{v} \in \mathbf{C}^\infty(\Omega). \quad (2.5.3)$$

Remark 2.5.3. There is academic literature on the analysis of trace maps, for example Buffa et al. [Buffa02], have shown

$$\gamma_{\parallel}(\mathbf{v}) := \mathbf{n} \times (\mathbf{v}|_{\Gamma} \times \mathbf{n}), \quad \gamma_{\parallel} : \mathbf{H}(\text{curl}, \Omega) \longrightarrow \mathbf{H}^{-\frac{1}{2}}(\text{curl}_{\Gamma}, \Gamma), \quad (2.5.4)$$

$$\gamma_n(\mathbf{v}) := \mathbf{n} \times (\nabla \times \mathbf{v})|_{\Gamma}, \quad \gamma_n : \mathbf{H}(\text{curl}, \Omega) \longrightarrow \mathbf{H}^{-\frac{1}{2}}(\Gamma). \quad (2.5.5)$$

Additionally, there exists formal trace theory from Arnold et al. [Arnold18, Thm. 6.3]

$$(\cdot)^{\text{tan}} : H\Lambda^k(\Omega) \longrightarrow H^{-\frac{1}{2}}\Lambda^k(\Gamma), \quad (\cdot)^{\text{nor}} : H\Lambda^k(\Omega) \longrightarrow H^{-\frac{1}{2}}\Lambda^{k-1}(\Gamma). \quad (2.5.6)$$

However, our analysis is done in the discrete setting where the L^2 inner products on the boundary are well-defined. For the parts of the analysis where we use continuous arguments, namely continuity proofs and error analysis, we require them to have sufficient regularity, such that the L^2 inner products involving our trace operators are well defined.

2.6 Deriving the variational formulation

Recall the Hodge Laplace equation (1.0.1) and its associated boundary conditions that we combine to $\omega = g$ on Γ , to cover non-zero Dirichlet cases $g \neq 0$ as well. We now aim to derive a variational formulation and start with the introduction of an auxiliary variable, a $(k-1)$ -form $\sigma = \delta\omega$.

Find $(\omega, \sigma) \in H\Lambda^k(\Omega) \times H\Lambda^{k-1}(\Omega)$ such that

$$\delta\mathbf{d}\omega + \mathbf{d}\sigma = f, \quad \text{in } \Omega, \quad (2.6.1)$$

$$\delta\omega - \sigma = 0, \quad \text{in } \Omega, \quad (2.6.2)$$

$$\omega = g, \quad \text{on } \Gamma. \quad (2.6.3)$$

The analogue of multiplying by a function in exterior calculus is wedging by a differential form of the same degree. In order for the wedge product to be integrable over a manifold of dimension n , the resulting wedge product must be a n -form, this can be achieved with the Hodge Star operator. Let $(\eta, \tau) \in H\Lambda^k(\Omega) \times H\Lambda^{k-1}(\Omega)$

$$\delta\mathbf{d}\omega \wedge \star\eta + \mathbf{d}\sigma \wedge \star\eta = f \wedge \star\eta, \quad \text{in } \Omega, \quad (2.6.4)$$

$$\delta\omega \wedge \star\tau - \sigma \wedge \star\tau = 0, \quad \text{in } \Omega. \quad (2.6.5)$$

We rewrite them as inner products according to definition 2.2.7 and integrate them over Ω . Then we have

$$\int_{\Omega} \langle \delta\mathbf{d}\omega, \eta \rangle + \int_{\Omega} \langle \mathbf{d}\sigma, \eta \rangle = \int_{\Omega} \langle f, \eta \rangle, \quad (2.6.6)$$

$$\int_{\Omega} \langle \delta\omega, \tau \rangle - \int_{\Omega} \langle \sigma, \tau \rangle = 0. \quad (2.6.7)$$

Applying integration by parts from Theorem 2.2.6 to the first term in (2.6.6) we obtain

$$\int_{\Omega} \langle \delta \mathbf{d}\omega, \eta \rangle = \int_{\Omega} \langle \mathbf{d}\omega, \mathbf{d}\eta \rangle + \int_{\Gamma} \langle (\mathbf{d}\omega)^{\text{nor}}, \eta^{\text{tan}} \rangle. \quad (2.6.8)$$

We apply integration by parts to the first term in (2.6.7) to get

$$\int_{\Omega} \langle \delta \omega, \tau \rangle = \int_{\Omega} \langle \omega, \mathbf{d}\tau \rangle + \int_{\Gamma} \langle \omega^{\text{nor}}, \tau^{\text{tan}} \rangle. \quad (2.6.9)$$

From this previous step, we can bring the boundary term to the right hand side and incorporate part of the Dirichlet data, then the problem reads

Find $(\omega, \sigma) \in \text{H}\Lambda^k(\Omega) \times \text{H}\Lambda^{k-1}(\Omega)$ such that

$$\begin{aligned} \int_{\Omega} \langle \mathbf{d}\omega, \mathbf{d}\eta \rangle + \int_{\Gamma} \langle (\mathbf{d}\omega)^{\text{nor}}, \eta^{\text{tan}} \rangle + \int_{\Omega} \langle \mathbf{d}\sigma, \eta \rangle &= \int_{\Omega} \langle f, \eta \rangle & \forall \eta \in \text{H}\Lambda^k(\Omega), \\ \int_{\Omega} \langle \omega, \mathbf{d}\tau \rangle - \int_{\Omega} \langle \sigma, \tau \rangle &= - \int_{\Gamma} \langle g^{\text{nor}}, \tau^{\text{tan}} \rangle, & \forall \tau \in \text{H}\Lambda^{k-1}(\Omega). \end{aligned}$$

We have decomposed $g|_{\Gamma} = g^{\text{nor}} + g^{\text{tan}}$. From our previous step we see, that we have incorporated half of the Dirichlet data. For the other half, we use the Nitsche method. We add a term that symmetrizes the system, while maintaining consistency. We also add the Nitsche term that penalizes deviations from our desired g^{tan} at the boundary. At this point, we switch to the discrete setting, since the Nitsche method can only be employed discretely. Our discrete variational formulation for the Hodge-Laplacian with Dirichlet boundary condition then reads

Mixed method for Nitsche Hodge Laplace k-forms for $\Omega \subset \mathbb{R}^n, n \leq k$.

Find $(\omega_h, \eta_h) \in (V_h \subset \text{H}\Lambda^k(\Omega)) \times (Q_h \subset \text{H}\Lambda^{k-1}(\Omega))$ such that

$$\begin{aligned} \int_{\Omega} \langle \mathbf{d}\omega_h, \mathbf{d}\eta_h \rangle - \int_{\Gamma} \langle (\mathbf{d}\omega_h)^{\text{nor}}, \eta_h^{\text{tan}} \rangle + \int_{\Omega} \langle \mathbf{d}\sigma_h, \eta_h \rangle \\ - \int_{\Gamma} \langle (\mathbf{d}\eta_h)^{\text{nor}}, \omega_h^{\text{tan}} \rangle + \frac{C_w}{h} \int_{\Gamma} \langle \eta_h^{\text{tan}}, \omega_h^{\text{tan}} \rangle &= \int_{\Omega} \langle f, \eta_h \rangle - \int_{\Gamma} \langle (\mathbf{d}\eta_h)^{\text{nor}}, g^{\text{tan}} \rangle \\ &\quad + \frac{C_w}{h} \int_{\Gamma} \langle \eta_h^{\text{tan}}, g^{\text{tan}} \rangle, \end{aligned} \quad (2.6.10)$$

$$\int_{\Omega} \langle \omega_h, \mathbf{d}\tau_h \rangle - \int_{\Omega} \langle \sigma_h, \tau_h \rangle = - \int_{\Gamma} \langle g^{\text{nor}}, \tau_h^{\text{tan}} \rangle, \quad (2.6.11)$$

$$\forall (\eta_h, \tau_h) \in V_h \times Q_h.$$

Either we evaluate the exterior calculus definitions to derive the proxy methods from the final variational formulation, or we start with the strong form definition (1.0.1). We illustrate this with 1-forms as an example and then present the final variational formulation for 2-forms.

2.6.1 Discrete Hodge Laplace Nitsche method for 1-forms in $\Omega \subset \mathbb{R}^3$

For 1- and 2-forms in \mathbb{R}^3 , the Hodge Laplace equation translates to the vector Laplacian. In the 2D method, curl curl changes to curl rot in the strong form.

$$\nabla \times \nabla \times \mathbf{u} - \nabla(\nabla \cdot \mathbf{u}) = \mathbf{f}, \quad \text{in } \Omega, \quad (2.6.12)$$

$$\mathbf{u} = \mathbf{g} \quad \text{on } \Gamma. \quad (2.6.13)$$

For 2-forms, we would introduce the vectorial auxiliary variable $\mathbf{p} = \nabla \times \mathbf{u}$, but for 1-forms, we have the scalar $p = -\nabla \cdot \mathbf{u}$. We multiply by testfunctions and integrate to obtain

$$\int_{\Omega} (\nabla \times \nabla \times \mathbf{u}) \cdot \mathbf{v} \, dx + \int_{\Omega} \nabla p \cdot \mathbf{v} \, dx = \int_{\Omega} \mathbf{f} \cdot \mathbf{v} \, dx, \quad (2.6.14)$$

$$\int_{\Omega} (\nabla \cdot \mathbf{u}) q \, dx + \int_{\Omega} p q \, dx = 0. \quad (2.6.15)$$

If we perform integration by parts on the curl-curl term in (2.6.14) and on the divergence term in (2.6.15) we get

$$\int_{\Omega} (\nabla \times \mathbf{u}_h) \cdot (\nabla \times \mathbf{v}_h) \, dx + \int_{\Gamma} \gamma_n(\mathbf{u}_h) \cdot \gamma_{\parallel}(\mathbf{v}_h) \, ds + \int_{\Omega} \nabla p_h \cdot \mathbf{v}_h \, dx = \int_{\Omega} \mathbf{f} \cdot \mathbf{v}_h \, dx, \quad (2.6.16)$$

$$\int_{\Omega} \mathbf{u}_h \cdot \nabla q_h \, dx - \int_{\Omega} p_h q_h \, dx = \int_{\Gamma} (\mathbf{g} \cdot \mathbf{n}) q_h \, ds. \quad (2.6.17)$$

We choose the spaces based on the discrete De Rham complex, add the symmetrization term and the Nitsche term.

Mixed method for Nitsche Hodge Laplace 1-forms

Let $V_h \subset \mathbf{H}(\text{curl}, \Omega)$ and $Q_h \subset H^1(\Omega)$. Find $(\mathbf{u}_h, p_h) \in V_h \times Q_h$ such that

$$\begin{aligned} & \int_{\Omega} (\nabla \times \mathbf{u}_h) \cdot (\nabla \times \mathbf{v}_h) \, dx + \int_{\Gamma} \gamma_n(\mathbf{u}_h) \cdot \gamma_{\parallel}(\mathbf{v}_h) \, ds + \int_{\Omega} \nabla p_h \cdot \mathbf{v}_h \, dx \\ & + \int_{\Gamma} \gamma_n(\mathbf{v}_h) \cdot \gamma_{\parallel}(\mathbf{u}_h) \, ds + \frac{C_{\omega}}{h} \int_{\Gamma} \gamma_{\parallel}(\mathbf{u}_h) \cdot \gamma_{\parallel}(\mathbf{v}_h) \, ds = \int_{\Omega} \mathbf{f} \cdot \mathbf{v}_h \, dx + \frac{C_{\omega}}{h} \int_{\Gamma} \gamma_{\parallel}(\mathbf{g}) \cdot \gamma_{\parallel}(\mathbf{v}_h) \, ds \\ & + \int_{\Gamma} \gamma_n(\mathbf{v}_h) \cdot \gamma_{\parallel}(\mathbf{g}) \, ds, \end{aligned} \quad (2.6.18)$$

$$\int_{\Omega} \mathbf{u}_h \cdot \nabla q_h \, dx - \int_{\Omega} p_h q_h \, dx = \int_{\Gamma} (\mathbf{g} \cdot \mathbf{n}) q_h \, ds, \quad (2.6.19)$$

$$\forall (\mathbf{v}_h, q_h) \in V_h \times Q_h.$$

2.6.2 Discrete Hodge Laplace Nitsche method for 2-forms in $\Omega \subset \mathbb{R}^3$

In the same way as for the 1-forms, we start with the vector Laplacian. But now, we introduce $\mathbf{p}_h \in Q_h \subset \mathbf{H}(\text{curl}, \Omega)$ such that $\mathbf{p}_h = \nabla \times \mathbf{u}_h$. Multiplying by test functions, integrating by parts the grad div term in the first equation, adding the symmetrization and Nitsche terms and integrating by parts the curl term in the second equation to finally obtain

Mixed method for Nitsche Hodge Laplace 2-forms

Let $V_h \subset \mathbf{H}(\text{div}, \Omega)$ and $\subset \mathbf{H}(\text{curl}, \Omega)$. Find $(\mathbf{u}_h, \mathbf{p}_h) \in V_h \times$ such that

$$\begin{aligned} \int_{\Omega} (\nabla \cdot \mathbf{u}_h) \cdot (\nabla \cdot \mathbf{v}_h) \, dx - \int_{\Gamma} (\nabla \cdot \mathbf{u}_h) \cdot (\mathbf{v}_h \cdot \mathbf{n}) \, ds + \int_{\Omega} (\nabla \times \mathbf{p}_h) \cdot \mathbf{v}_h \, dx \\ - \int_{\Gamma} (\nabla \cdot \mathbf{v}_h) \cdot (\mathbf{u}_h \cdot \mathbf{n}) \, ds + \frac{C_{\omega}}{h} \int_{\Gamma} (\mathbf{u}_h \cdot \mathbf{n}) \cdot (\mathbf{v}_h \cdot \mathbf{n}) \, ds = \int_{\Omega} \mathbf{f} \cdot \mathbf{v}_h \, dx + \frac{C_{\omega}}{h} \int_{\Gamma} (\mathbf{g} \cdot \mathbf{n}) \cdot (\mathbf{v}_h \cdot \mathbf{n}) \, ds \\ - \int_{\Gamma} (\nabla \cdot \mathbf{v}_h) \cdot (\mathbf{g} \cdot \mathbf{n}) \, ds, \end{aligned} \quad (2.6.20)$$

$$\int_{\Omega} (\nabla \times \mathbf{q}_h) \cdot \mathbf{u}_h \, dx - \int_{\Omega} \mathbf{p} \cdot \mathbf{q} \, dx = \int_{\Gamma} (\mathbf{n} \times \mathbf{q}_h) \cdot \mathbf{g} \, ds, \quad (2.6.21)$$

$$\forall (\mathbf{v}_h, \mathbf{q}_h) \in V_h \times.$$

Since we have that both the 1-forms and the 2-forms case originally are derived from the vector Laplacian, we observe that in the 2-forms mixed method, the tangential part of \mathbf{g} is incorporated naturally and the normal part via the Nitsche penalization while in the 1-forms method, it is the other way around.

Chapter 3

Analysis

This chapter contains a formal analysis. First we present a section of preliminary results and definitions that are used throughout the analysis. Readers who consider themselves numerical analysis experts may skip this section and immediately go to section 3.2 and refer to it during the reading process if necessary.

3.1 Preliminary results & definitions

Lemma 3.1.1 (Upper bound on norms of boundary adjacent elements). *Fix a finite dimensional Hilbert space $V_h \subset V$, $V = \{H^1(\Omega), \mathbf{H}(\text{curl}, \Omega), \mathbf{H}(\text{div}, \Omega)\}$. If we have a uniform mesh we can bound the norms on the boundary adjacent elements by*

$$\sum_{K \in \mathcal{T}_\Gamma} \frac{1}{h_K} \|\mathbf{v}_h\|_{L^2(K)}^2 \leq \sum_{K \in \mathcal{T}} \frac{1}{h_K} \|\mathbf{v}_h\|_{L^2(K)}^2 \leq \frac{C}{h} \|\mathbf{v}_h\|_{L^2(\Omega)}^2, \quad \forall \mathbf{v}_h \in V_h. \quad (3.1.1)$$

Proof.

$$\frac{1}{h} \|\mathbf{v}_h\|_{L^2(\Omega)}^2 = \frac{1}{h} \int_{\Omega} |\mathbf{v}_h|^2 dx = \frac{1}{h} \sum_{K \in \mathcal{T}} \int_K |\mathbf{v}_h|^2 dx = \frac{1}{h} \sum_{K \in \mathcal{T}} \|\mathbf{v}_h\|_{L^2(K)}^2. \quad (3.1.2)$$

We make use of the mesh uniformity 2.4.1 which implies

$$\frac{1}{h} \geq \frac{C}{h_k}, \quad \forall K \in \mathcal{T}. \quad (3.1.3)$$

$$\frac{1}{h} \|\mathbf{v}_h\|_{L^2(\Omega)}^2 \geq \sum_{K \in \mathcal{T}} \frac{C}{h_K} \|\mathbf{v}_h\|_{L^2(K)}^2 \geq C \sum_{K \in \mathcal{T}_\Gamma} \frac{1}{h_K} \|\mathbf{v}_h\|_{L^2(K)}^2. \quad (3.1.4)$$

The same can also be done for $\nabla \times \mathbf{v}_h$ and $\nabla \cdot \mathbf{v}_h$ analogously. \square

Lemma 3.1.2 (Upper bound on norm of $\gamma_n(\mathbf{v}_h)$). *In a uniform mesh there holds*

$$\|\gamma_n(\mathbf{v}_h)\|_{L^2(\Gamma)}^2 \leq \frac{C_{\text{tr}}^2}{h} \|\nabla \times \mathbf{v}_h\|_{L^2(\Omega)}^2, \quad \forall \mathbf{v}_h \in V_h \subset \mathbf{H}(\text{curl}, \Omega). \quad (3.1.5)$$

Additionally, there holds as well

$$\|(\mathbf{d}\omega_h)^{\text{nor}}\|_{L^2(\Gamma)}^2 \leq \frac{C_{\text{tr}}^2}{h} \|\mathbf{d}\omega_h\|_{L^2(\Omega)}^2, \quad \forall \omega_h \in V_h \subset H\Lambda^k(\Omega). \quad (3.1.6)$$

Proof. On the boundary Γ there holds pointwise $|\mathbf{n} \times \mathbf{v}_h| \leq |\mathbf{v}_h|$ which implies $|\mathbf{n} \times (\nabla \times \mathbf{v}_h)| \leq |\nabla \times \mathbf{v}_h|$. Let $\mathbf{v}_h \in V_h \subset \mathbf{H}(\text{curl}, \Omega)$. We use inverse inequality 2.4.4 and Lemma 3.1.1 to derive the following bound

$$\|\gamma_n(\mathbf{v}_h)\|_{L^2(\Gamma)}^2 \leq \|\nabla \times \mathbf{v}_h\|_{L^2(\Gamma)}^2 \leq \sum_{K \in \mathcal{T}_\Gamma} \frac{C_{\text{tr}}^2}{h_K} \|\nabla \times \mathbf{v}_h\|_{L^2(K)}^2 \leq \sum_{K \in \mathcal{T}} \frac{C_{\text{tr}}^2}{h_K} \|\nabla \times \mathbf{v}_h\|_{L^2(K)}^2 \leq \frac{C_{\text{tr}}^2}{h} \|\nabla \times \mathbf{v}_h\|_{L^2(\Omega)}^2. \quad (3.1.7)$$

We omit the analogous proof for differential forms. \square

Again on the boundary Γ , a trivial but relevant inequality used in the thesis is

$$|\mathbf{n} \times (\mathbf{v}_h \times \mathbf{n})| \leq |\mathbf{v}_h|, \quad \forall \mathbf{v}_h \text{ on } \Gamma. \quad (3.1.8)$$

The inequality can be shown by decomposing $|\mathbf{n} \times (\mathbf{v}_h \times \mathbf{n})|$ into normal and tangential part with respect to Γ . The left-hand side is exactly the tangential part of the decomposition. This yields the following

Lemma 3.1.3 (Upper bound on norm of $\gamma_{\parallel}(\mathbf{v}_h)$ bound). *In a uniform mesh there holds*

$$\|\gamma_{\parallel}(\mathbf{v}_h)\|_{L^2(\Gamma)}^2 \leq \frac{C_{\text{tr}}^2}{h} \|\mathbf{v}_h\|_{L^2(\Omega)}^2, \quad \forall \mathbf{v}_h \in \mathbf{H}(\text{curl}, \Omega). \quad (3.1.9)$$

Proof. Using 3.1.8, inverse inequality 2.4.4 and Lemma 3.1.1

$$\|\gamma_{\parallel}(\mathbf{v}_h)\|_{L^2(\Gamma)}^2 \leq \|\mathbf{v}_h\|_{L^2(\Gamma)}^2 \leq \sum_{K \in \mathcal{T}_\Gamma} \frac{C_{\text{tr}}^2}{h} \|\mathbf{v}_h\|_{L^2(K)}^2 \leq \frac{C_{\text{tr}}^2}{h} \|\mathbf{v}_h\|_{L^2(\Omega)}^2, \quad \forall \mathbf{v}_h \in \mathbf{H}(\text{curl}, \Omega). \quad (3.1.10)$$

\square

Lemma 3.1.4 ($\gamma_{\parallel}(\mathbf{v}_h)$ - term equality). *The following equality holds true*

$$\langle \gamma_n(\mathbf{u}_h), \mathbf{v}_h \rangle_{L^2(\Gamma)} = \langle \gamma_n(\mathbf{u}_h), \gamma_{\parallel}(\mathbf{v}_h) \rangle_{L^2(\Gamma)}, \quad \forall \mathbf{u}_h, \mathbf{v}_h \in \mathbf{H}(\text{curl}, \Omega). \quad (3.1.11)$$

Proof. We can decompose any vector

$$\mathbf{u} = \mathbf{u}_t + \mathbf{u}_n = \mathbf{u}_t + \mathbf{n}(\mathbf{u} \cdot \mathbf{n}). \quad (3.1.12)$$

$$\begin{aligned} \langle \gamma_n(\mathbf{u}), \mathbf{v} \rangle_{L^2(\Gamma)} &= \int_{\Gamma} \mathbf{n} \times (\nabla \times \mathbf{u}) \cdot \mathbf{v} \, ds \\ &= \int_{\Gamma} \mathbf{n} \times (\nabla \times \mathbf{u}) \cdot (\mathbf{v}_t + \mathbf{n}(\mathbf{v} \cdot \mathbf{n})) \, ds \\ &= \int_{\Gamma} \mathbf{n} \times (\nabla \times \mathbf{u}) \cdot \mathbf{v}_t \, ds + \int_{\Gamma} \mathbf{n} \times (\nabla \times \mathbf{u}) \cdot \mathbf{n}(\mathbf{v} \cdot \mathbf{n}) \, ds \\ &= \int_{\Gamma} \mathbf{n} \times (\nabla \times \mathbf{u}) \cdot \mathbf{v}_t \, ds \end{aligned} \quad (3.1.13)$$

$$\gamma_{\parallel}(\mathbf{v}) = \mathbf{n} \times (\mathbf{v} \times \mathbf{n}) = (\mathbf{n} \cdot \mathbf{n})\mathbf{v} - (\mathbf{n} \cdot \mathbf{v})\mathbf{n} = \mathbf{v}_t. \quad (3.1.14)$$

\square

Definition 3.1.5 (Standard norms). If nothing else is mentioned, and we evaluate norms of functions from Q_h or V_h e.g. $\|\mathbf{u}_h\|_V$ or $\|p_h\|_Q$, we use the Sobolev norms that the continuous spaces are equipped with. E.g.

$$\mathbf{v}_h \in V_h \subset \mathbf{H}(\text{curl}, \Omega) \implies \|\mathbf{v}_h\|_{\mathbf{H}(\text{curl}, \Omega)}, \quad (3.1.15)$$

$$\mathbf{v}_h \in V_h \subset \mathbf{H}(\text{div}, \Omega) \implies \|\mathbf{v}_h\|_{\mathbf{H}(\text{div}, \Omega)}, \quad (3.1.16)$$

$$q_h \in Q_h \subset H^1(\Omega) \implies \|q_h\|_{H^1(\Omega)}. \quad (3.1.17)$$

$$(3.1.18)$$

Definition 3.1.6 (The #-norm). We endow the space $V_h \subset \mathbf{H}(\text{curl}, \Omega)$ with

$$\|\mathbf{u}_h\|_{\#}^2 = \|\mathbf{u}_h\|_{\mathbf{H}(\text{curl}, \Omega)}^2 + \frac{1}{h} \|\gamma_{\parallel}(\mathbf{u}_h)\|_{L^2(\Gamma)}^2 + h \|\gamma_n(\mathbf{u}_h)\|_{L^2(\Gamma)}^2, \quad \forall \mathbf{u}_h \in V_h. \quad (3.1.19)$$

The above norm can be extended to general k -forms and reads as

$$\|\omega_h\|_{\#}^2 = \|\omega_h\|_{L^2(\Omega)}^2 + \|\mathbf{d}\omega_h\|_{L^2(\Omega)}^2 + \frac{1}{h} \|\omega_h^{\text{tan}}\|_{L^2(\Gamma)}^2 + h \|\omega_h^{\text{nor}}\|_{L^2(\Gamma)}^2, \quad \forall \omega_h \in V_h. \quad (3.1.20)$$

Definition 3.1.7 (The X-norm). The space $X_h = V_h \times Q_h \subset \mathbf{H}(\text{curl}, \Omega) \times H^1(\Omega)$ is endowed with the following norm

$$\|(\mathbf{u}_h, q_h)\|_X^2 = \|\mathbf{u}_h\|_{\#}^2 + \|q_h\|_{L^2(\Omega)}^2 + h^2 \|\nabla q_h\|_{L^2(\Omega)}^2, \quad \forall (\mathbf{u}_h, q_h) \in X_h. \quad (3.1.21)$$

Analogous, the X-norm extended to pairs of k and $(k-1)$ forms. We have the space

$V_h \times Q_h \subset \text{H}\Lambda^k(\Omega) \times \text{H}\Lambda^{k-1}(\Omega)$ with the norm

$$\|(\omega_h, \sigma_h)\|_X^2 = \|\omega_h\|_{\#}^2 + \|\sigma_h\|_{L^2(\Omega)}^2 + h^2 \|\mathbf{d}\sigma_h\|_{L^2(\Omega)}^2, \quad \forall (\omega_h, \sigma_h) \in X_h. \quad (3.1.22)$$

3.2 Saddle-point problem well-posedness

In this section, we will show well-posedness for 1-forms in 3D and 2D. We begin by outlining the relevant definitions and theorems.

Definition 3.2.1 (Abstract discrete Perturbed saddle point problem). Find $(u_h, q_h) \in V_h \subset V \times Q_h \subset Q$ such that

$$a(u_h, v_h) + b(v_h, p_h) = \langle f, v_h \rangle_{V \times V'}, \quad \forall v_h \in V_h \quad (3.2.1)$$

$$b(u_h, q_h) - \lambda^2 c(p_h, q_h) = \langle g, q_h \rangle_{Q \times Q'}, \quad \forall q_h \in Q_h \quad (3.2.2)$$

Here $\lambda^2 c(p_h, q_h)$ is considered the perturbation.

Theorem 3.2.2 (Well-posedness of perturbed saddle point problems). *Assume that $a(\cdot, \cdot)$ and $c(\cdot, \cdot)$ are symmetric on V_h and Q_h respectively and $\lambda^2 > 0$. Let $\alpha_1, \alpha_2, \beta_1, \beta_2, \gamma_1, \gamma_2$ be positive constants such that*

SPD & Coercivity:

Continuity:

$$0 \leq a_h(u_h, u_h), \quad \forall u_h \in V_h, \quad (3.2.3) \quad a_h(u_h, v_h) \leq \alpha_2 \|u_h\|_V \|v_h\|_V, \quad \forall u_h, v_h \in V_h,$$

$$0 \leq c(p_h, p_h), \quad \forall p_h \in Q_h, \quad (3.2.4) \quad (3.2.7)$$

$$\alpha_1 \|v_h\|_V^2 \leq a_h(v_h, v_h), \quad \forall v_h \in K_h, \quad (3.2.5) \quad c(p_h, q_h) \leq \beta_2 \|p_h\|_V \|q_h\|_V, \quad \forall p_h, q_h \in Q_h,$$

$$\beta_1 \|q_h\|_Q^2 \leq c(q_h, q_h), \quad \forall q_h \in H_h. \quad (3.2.6) \quad (3.2.8)$$

$$b(v_h, q_h) \leq \gamma_2 \|v_h\|_V \|q_h\|_Q, \quad \forall q_h \in H_h, \forall v_h \in K_h. \quad (3.2.9)$$

Stability:

$$\inf_{q_h \in H_h^\perp} \sup_{v_h \in V_h} \frac{b(v_h, q_h)}{\|q_h\|_Q \|v_h\|_V} = \inf_{v_h \in K_h^\perp} \sup_{q_h \in Q_h} \frac{b(v_h, q_h)}{\|q_h\|_Q \|v_h\|_V} = \gamma_1 > 0. \quad (3.2.10)$$

Where we have

$$K_h = \text{Ker} B = \{v_h \in V_h \mid b(v_h, q_h) = 0, \forall q_h \in Q_h\}, \quad K_h^\perp = \{v_h \in V_h \mid (w_h, v_h)_{L^2(\Omega)} = 0, \forall w_h \in K_h\}, \quad (3.2.11)$$

$$H_h = \text{Ker} B^t = \{q_h \in Q_h \mid b(v_h, q_h) = 0, \forall v_h \in V_h\}, \quad H_h^\perp = \{q_h \in Q_h \mid (r_h, q_h)_{L^2(\Omega)} = 0, \forall r_h \in H_h\}. \quad (3.2.12)$$

Then, for every $f \in V'$ and $g \in Q'$, the discretized problem has a unique solution.

Proof. A detailed proof can be found in [Boffi13, Thm. 5.5.1]. □

Defining the following bilinear forms to go towards the structure of theorem 3.2.2.

Definition 3.2.3. We use the following bilinear forms in our mixed method (2.6.18).

$$\begin{aligned} a_h(\mathbf{u}_h, \mathbf{v}_h) &= \int_{\Omega} (\nabla \times \mathbf{u}_h) \cdot (\nabla \times \mathbf{v}_h) \, dx + \int_{\Gamma} \gamma_n(\mathbf{u}_h) \cdot \gamma_{||}(\mathbf{v}_h) \, ds + \int_{\Gamma} \gamma_n(\mathbf{v}_h) \cdot \gamma_{||}(\mathbf{u}_h) \, ds \\ &\quad + \frac{C_\omega}{h} \int_{\Gamma} \gamma_{||}(\mathbf{u}_h) \cdot \gamma_{||}(\mathbf{v}_h) \, ds, \end{aligned} \quad (3.2.13)$$

$$b(\mathbf{u}_h, p_h) = \int_{\Omega} \nabla p_h \cdot \mathbf{v}_h \, dx, \quad (3.2.14)$$

$$c(p, q) = \int_{\Omega} p_h q_h \, dx. \quad (3.2.15)$$

With the introduced bilinear forms we rewrite the mixed method equivalently as a perturbed saddle point problem with the perturbation factor $\lambda^2 = 1$.

$$a_h(\mathbf{u}_h, \mathbf{v}_h) + b(\mathbf{v}_h, p_h) = \int_{\Omega} \mathbf{f} \cdot \mathbf{v}_h \, dx + \frac{C_{\omega}}{h} \int_{\Gamma} \gamma_{\parallel}(\mathbf{g}) \cdot \gamma_{\parallel}(\mathbf{v}_h) \, ds + \int_{\Gamma} \gamma_n(\mathbf{v}_h) \cdot \gamma_{\parallel}(\mathbf{g}) \, ds, \quad (3.2.16)$$

$$b(\mathbf{u}_h, q_h) - c(p_h, q_h) = \int_{\Gamma} (\mathbf{g} \cdot \mathbf{n}) q_h \, ds, \quad (3.2.17)$$

$$\forall (\mathbf{v}_h, q_h) \in V_h \times Q_h.$$

Definition 3.2.4 ($\bar{H}^1(\Omega)$).

$$\bar{H}^1(\Omega) = \{\mathbf{v}_h \in H^1(\Omega) \mid \langle \mathbf{v}_h, 1 \rangle_{L^2(\Omega)} = 0\}$$

We start by having a closer look at the space H_h^{\perp} .

Lemma 3.2.5 (H_h^{\perp} coincides with $\bar{H}^1(\Omega)$). *Let $V_h \subset \mathbf{H}(\text{curl}, \Omega)$ and $Q_h \subset H^1(\Omega)$, then we have*

$$H_h^{\perp} = \{q_h \in Q_h \mid \langle r_h, q_h \rangle_{L^2(\Omega)} = 0, \forall r_h \in H_h\} \implies H_h^{\perp} \subset \bar{H}^1(\Omega), \quad (3.2.18)$$

$$\text{with } \bar{H}^1(\Omega) = \{q_h \in H^1(\Omega) \mid \langle q_h, 1 \rangle_{L^2(\Omega)} = 0\}. \quad (3.2.19)$$

Proof. The space H_h is the space of constants. The only nonzero q_h such that $\langle q_h, r_h \rangle_{L^2(\Omega)} = 0$ with $r_h \in \mathbb{R}$ is $q_h \in \bar{H}^1(\Omega)$. \square

Lemma 3.2.6 (Poincaré holds on K_h for topologically trivial domains). *Let Ω be a domain with Lipschitz boundary Γ and non-zero measure boundary part Γ_D and let $\mathbf{u}_h|_{\Gamma_D} \times \mathbf{n}$ be prescribed. Then there exists C_P such that*

$$\|\mathbf{u}_h\|_{L^2(\Omega)} \leq C_P \|\nabla \times \mathbf{u}_h\|_{L^2(\Omega)}, \quad \forall \mathbf{u}_h \in K_h. \quad (3.2.20)$$

Sometimes also referred to as the Maxwell-Poincaré inequality.

Proof. Discrete Poincaré [Arnold18, Thm. 5.3] and discrete Poincaré-Steklov [Ern21b, Thm. 44.6]. \square

3.2.1 Semi positive-definiteness of $a_h(\mathbf{v}_h, \mathbf{v}_h)$

Lemma 3.2.7. $a_h(\cdot, \cdot)$ is SPD on V_h , for sufficiently large C_w

$$0 \leq a_h(\mathbf{v}_h, \mathbf{v}_h) \quad \forall \mathbf{v}_h \in V_h. \quad (3.2.21)$$

The proof of Lemma 3.2.7 and also its extension to coercivity, coincides with a proof yet to be published by the supervisors of this thesis Prof. Hiptmair, Dr. Zampa, Mr. Tonnon and Dr. Boon [Boon25] who have been working on a similar method. Their support and guidance in arriving at the same result has been crucial.

Proof. The bilinear form $a_h(\mathbf{v}_h, \mathbf{v}_h)$ can be bounded in the following way

$$a_h(\mathbf{v}_h, \mathbf{v}_h) = \int_{\Omega} (\nabla \times \mathbf{v}_h) \cdot (\nabla \times \mathbf{v}_h) \, dx + 2 \int_{\Gamma} \gamma_n(\mathbf{v}_h) \cdot \gamma_{\parallel}(\mathbf{v}_h) \, ds + \frac{C_w}{h} \int_{\Gamma} \gamma_{\parallel}(\mathbf{v}_h) \gamma_{\parallel}(\mathbf{v}_h) \, ds \quad (3.2.22)$$

$$= \|\nabla \times \mathbf{v}_h\|_{L^2(\Omega)}^2 + 2 \int_{\Gamma} \gamma_n(\mathbf{v}_h) \cdot \gamma_{\parallel}(\mathbf{v}_h) \, ds + \frac{C_w}{h} \|\gamma_{\parallel}(\mathbf{v}_h)\|_{L^2(\Gamma)}^2. \quad (3.2.23)$$

We apply the Cauchy-Schwarz inequality to the remaining mixed boundary integral and apply Young's inequality to the result. In the $\gamma_n(\mathbf{v}_h)$ norm we use the Lemma 3.1.1.

$$\int_{\Gamma} \gamma_n(\mathbf{v}_h) \cdot \gamma_{\parallel}(\mathbf{v}_h) \, ds \geq -\|\gamma_n(\mathbf{v}_h)\|_{L^2(\Gamma)} \|\gamma_{\parallel}(\mathbf{v}_h)\|_{L^2(\Gamma)} \quad (3.2.24)$$

$$\geq -\frac{1}{2\epsilon_1} \|\gamma_n(\mathbf{v}_h)\|_{L^2(\Gamma)}^2 - \frac{\epsilon_1}{2} \|\gamma_{\parallel}(\mathbf{v}_h)\|_{L^2(\Gamma)}^2 \quad (3.2.25)$$

$$\geq -\frac{C_{\text{tr}}^2}{2\epsilon_1 h} \|\nabla \times \mathbf{v}_h\|_{L^2(\Omega)}^2 - \frac{\epsilon_1}{2} \|\gamma_{\parallel}(\mathbf{v}_h)\|_{L^2(\Gamma)}^2. \quad (3.2.26)$$

Using estimate (3.2.26) in (3.2.23).

$$a_h(\mathbf{v}_h, \mathbf{v}_h) \geq (1 - \frac{C_{\text{tr}}^2}{\epsilon_1 h}) \|\nabla \times \mathbf{v}_h\|_{L^2(\Omega)}^2 + (\frac{C_w}{h} - \epsilon_1) \|\gamma_{\parallel}(\mathbf{v}_h)\|_{L^2(\Gamma)}^2, \quad (3.2.27)$$

$$\text{Set } \epsilon_1 = \frac{2C_{\text{tr}}^2}{h}, \quad \text{Choose } C_w = 2\epsilon_1 h = 4C_{\text{tr}}^2,$$

$$a_h(\mathbf{v}_h, \mathbf{v}_h) \geq \frac{1}{2} \|\nabla \times \mathbf{v}_h\|_{L^2(\Omega)}^2 + \frac{2C_{\text{tr}}^2}{h} \|\gamma_{\parallel}(\mathbf{v}_h)\|_{L^2(\Gamma)}^2 \quad (3.2.28)$$

$$\geq 0. \quad (3.2.29)$$

□

3.2.2 Continuity of $a_h(\mathbf{u}, \mathbf{v}_h)$

Remark 3.2.8. The following definition will allow us to perform error analysis. If we chose our continuous solution to be in $[H^2(\Omega)]^d$, all the boundary terms arising in the subsequent proof are well-defined when evaluated with said chosen function.

Definition 3.2.9 ($V_{\#}$ space). Let $\mathbf{u} \in [H^2(\Omega)]^d$ and $V_h \subset \mathbf{H}(\text{curl}, \Omega)$ then we have the space

$$V_{\#} = V_h + [H^2(\Omega)]^d. \quad (3.2.30)$$

Definition 3.2.10 ($Q_{\#}$ space). Let $p \in H^1(\Omega)$ and $Q_h \subset H^1(\Omega)$ then we have the space

$$V_{\#} = Q_h + H^1(\Omega). \quad (3.2.31)$$

Lemma 3.2.11. There exists $\alpha_2 > 0$ independent of h such that

$$a_h(\mathbf{u}, \mathbf{v}_h) \leq \alpha_2 \|\mathbf{u}_h\|_{\#} \|\mathbf{v}_h\|_{\#}, \quad \forall \mathbf{u} \in V_{\#}, \forall \mathbf{v}_h \in V_h. \quad (3.2.32)$$

Proof.

$$\begin{aligned} a_h(\mathbf{u}, \mathbf{v}_h) &= \int_{\Omega} (\nabla \times \mathbf{u}) \cdot (\nabla \times \mathbf{v}_h) \, dx + \int_{\Gamma} \gamma_n(\mathbf{u}) \cdot \gamma_{\parallel}(\mathbf{v}_h) \, ds \\ &\quad + \int_{\Gamma} \gamma_n(\mathbf{v}_h) \cdot \gamma_{\parallel}(\mathbf{u}) \, ds + \frac{C_w}{h} \int_{\Gamma} \gamma_{\parallel}(\mathbf{v}_h) \gamma_{\parallel}(\mathbf{u}) \, ds \end{aligned} \quad (3.2.33)$$

$$\begin{aligned} &\leq \|\nabla \times \mathbf{u}\|_{L^2(\Omega)} \|\nabla \times \mathbf{v}_h\|_{L^2(\Omega)} + \|\gamma_n(\mathbf{u})\|_{L^2(\Gamma)} \|\gamma_{\parallel}(\mathbf{v}_h)\|_{L^2(\Gamma)} \\ &\quad + \|\gamma_n(\mathbf{v}_h)\|_{L^2(\Gamma)} \|\gamma_{\parallel}(\mathbf{u})\|_{L^2(\Gamma)} + \frac{C_w}{h} \|\gamma_{\parallel}(\mathbf{v}_h)\|_{L^2(\Gamma)} \|\gamma_{\parallel}(\mathbf{u})\|_{L^2(\Gamma)} \end{aligned} \quad (3.2.34)$$

$$\begin{aligned} &\leq \|\mathbf{u}\|_{\mathbf{H}(\text{curl}, \Omega)} \|\mathbf{v}_h\|_{\mathbf{H}(\text{curl}, \Omega)} + \|\gamma_n(\mathbf{u})\|_{L^2(\Gamma)} \|\gamma_{\parallel}(\mathbf{v}_h)\|_{L^2(\Gamma)} \\ &\quad + \|\gamma_n(\mathbf{v}_h)\|_{L^2(\Gamma)} \|\gamma_{\parallel}(\mathbf{u})\|_{L^2(\Gamma)} + \frac{C_w}{h} \|\gamma_{\parallel}(\mathbf{v}_h)\|_{L^2(\Gamma)} \|\gamma_{\parallel}(\mathbf{u})\|_{L^2(\Gamma)} \end{aligned} \quad (3.2.35)$$

$$\begin{aligned} &\leq \|\mathbf{u}\|_{\mathbf{H}(\text{curl}, \Omega)} \|\mathbf{v}_h\|_{\mathbf{H}(\text{curl}, \Omega)} + h^{\frac{1}{2}} \|\gamma_n(\mathbf{u})\|_{L^2(\Gamma)} h^{-\frac{1}{2}} \|\gamma_{\parallel}(\mathbf{v}_h)\|_{L^2(\Gamma)} \\ &\quad + h^{\frac{1}{2}} \|\gamma_n(\mathbf{v}_h)\|_{L^2(\Gamma)} h^{-\frac{1}{2}} \|\gamma_{\parallel}(\mathbf{u})\|_{L^2(\Gamma)} + \frac{C_w}{h} \|\gamma_{\parallel}(\mathbf{v}_h)\|_{L^2(\Gamma)} \|\gamma_{\parallel}(\mathbf{u})\|_{L^2(\Gamma)} \end{aligned} \quad (3.2.36)$$

$$\leq C_{\#} \|\mathbf{u}\|_{\#} \|\mathbf{v}_h\|_{\#}, \quad \forall \mathbf{u} \in V_{\#}, \forall \mathbf{v}_h \in V_h. \quad \implies \alpha_2 = C_{\#}. \quad (3.2.37)$$

□

3.2.3 Coercivity of $a_h(\mathbf{v}_h, \mathbf{v}_h)$

Lemma 3.2.12. *There exists $\alpha_1 > 0$ independent of h such that*

$$\alpha_1 \|\mathbf{v}_h\|_{\#}^2 \leq a_h(\mathbf{v}_h, \mathbf{v}_h) \quad \forall \mathbf{v}_h \in K_h. \quad (3.2.38)$$

The proof of Lemma 3.2.12 can be continued from the SPD result in line (3.2.29). We proceed in a manner that is equivalent to Boon et. al, although here we use a different justification. In their method, the full space V_h is divergence-free, which per definition of the method allows the use of

$$\{\mathbf{v}_h \in V_h \mid b(\mathbf{v}_h, q_h) = 0 \quad \forall q_h \in Q_h\} \quad (3.2.39)$$

In our setting, we can achieve the same property by exploiting the definition of the kernel space $\text{KerB} = K_h$ from the perturbed saddle point problem well-posedness theorem (3.2.11) which is precisely defined as (3.2.39).

Proof. Continuing from the final step of the SPD proof in (3.2.29)

$$a_h(\mathbf{v}_h, \mathbf{v}_h) \geq \frac{1}{2} \|\nabla \times \mathbf{v}_h\|_{L^2(\Omega)}^2 + \frac{2C_{\text{tr}1}^2}{h} \|\gamma_{\parallel}(\mathbf{v}_h)\|_{L^2(\Gamma)}^2, \quad \forall \mathbf{v}_h \in K_h. \quad (3.2.40)$$

Lemma 3.1.2 applied to the curl term to borrow norm of $\gamma_n(\mathbf{v}_h)$.

$$\frac{h}{C_{\text{tr}2}^2} \|\gamma_n(\mathbf{v}_h)\|_{L^2(\Gamma)}^2 \leq \|\nabla \times \mathbf{v}_h\|_{L^2(\Omega)}^2. \quad (3.2.41)$$

$$a_h(\mathbf{v}_h, \mathbf{v}_h) \geq \frac{1}{4} \|\nabla \times \mathbf{v}_h\|_{L^2(\Omega)}^2 + \frac{1}{4C_{\text{tr}2}^2} h \|\gamma_n(\mathbf{v}_h)\|_{L^2(\Gamma)}^2 + \frac{2C_{\text{tr}1}^2}{h} \|\gamma_{\parallel}(\mathbf{v}_h)\|_{L^2(\Gamma)}^2. \quad (3.2.42)$$

To obtain the $\|\mathbf{u}_h\|_{L^2(\Omega)}$ part of the $\mathbf{H}(\text{curl}, \Omega)$ norm we use Lemma 3.2.6

$$a_h(\mathbf{v}_h, \mathbf{v}_h) \geq \frac{1}{8} \|\nabla \times \mathbf{v}_h\|_{L^2(\Omega)}^2 + \frac{1}{8C_P^2} \|\mathbf{v}_h\|_{L^2(\Omega)}^2 + \frac{1}{4C_{\text{tr}2}^2} h \|\gamma_n(\mathbf{v}_h)\|_{L^2(\Gamma)}^2 + \frac{2C_{\text{tr}1}^2}{h} \|\gamma_{\parallel}(\mathbf{v}_h)\|_{L^2(\Gamma)}^2. \quad (3.2.43)$$

$$\alpha_1 = \min \left(\frac{1}{8}, \frac{1}{8C_P^2}, \frac{1}{4C_{\text{tr}2}^2}, 2C_{\text{tr}1}^2 \right), \quad \|\mathbf{v}_h\|_{\mathbf{H}(\text{curl}, \Omega)} = \|\nabla \times \mathbf{v}_h\|_{L^2(\Omega)} + \|\mathbf{v}_h\|_{L^2(\Omega)}.$$

$$a_h(\mathbf{v}_h, \mathbf{v}_h) \geq \alpha_1 \left(\|\mathbf{v}_h\|_{\mathbf{H}(\text{curl}, \Omega)}^2 + \sum_{\forall F \in \Gamma} \frac{1}{h} \|\gamma_{\parallel}(\mathbf{v}_h)\|_F^2 \sum_{\forall F \in \Gamma} h \|\gamma_n(\mathbf{v}_h)\|_F^2 \right) \quad (3.2.44)$$

$$\geq \alpha_1 \|\mathbf{v}_h\|_{\#}^2, \quad \forall \mathbf{v}_h \in K_h. \quad (3.2.45)$$

□

3.2.4 Continuity & coercivity of $c(\cdot, \cdot)$

Lemma 3.2.13 (Continuity of $c(\cdot, \cdot)$). *There exists $\beta_2 > 0$ independent of h such that*

$$c(p, q_h) \leq \beta_2 \|p\|_Q \|q_h\|_Q, \quad \forall p \in Q_{\#}, \forall q_h \in Q_h. \quad (3.2.46)$$

Proof.

$$c(p, q_h) = \int_{\Omega} p q_h \, dx \leq \|p\|_{L^2(\Omega)} \|q_h\|_{L^2(\Omega)} \quad (3.2.47)$$

$$\leq \|p\|_{H^1(\Omega)} \|q_h\|_{H^1(\Omega)}, \quad \forall p \in Q_{\#}, \forall q_h \in Q_h, \quad \implies \beta_2 = 1. \quad (3.2.48)$$

□

Lemma 3.2.14. *Coercivity. There exists $\beta_1 > 0$ independent of h such that*

$$c(q_h, q_h) \geq \beta_1 \|q_h\|_V^2, \quad \forall q_h \in H_h. \quad (3.2.49)$$

Proof. Since H_h is the space of constants, we can add the L2 norm of the gradients without affecting equality.

$$c(q_h, q_h) = \|q_h\|_{L^2(\Omega)}^2 = \|q_h\|_{L^2(\Omega)}^2 + \|\nabla q_h\|_{L^2(\Omega)}^2 = \|q_h\|_{H^1(\Omega)}^2, \quad \forall q_h \in H_h. \quad \implies \beta_1 = 1. \quad (3.2.50)$$

□

3.2.5 Continuity and inf-sup stability of $b(\mathbf{v}_h, q_h)$

Lemma 3.2.15 (Continuity of $b(\mathbf{v}_h, q_h)$). *There exists $\gamma_2 > 0$ independent of h such that*

$$b(\mathbf{v}, q) \leq \gamma_2 \|\mathbf{v}\|_{\#} \|q\|_{H^1(\Omega)}, \quad \forall (\mathbf{v}, q) \in V_{\#} \times Q_{\#}. \quad (3.2.51)$$

Proof. We use $\|q\|_{L^2(\Omega)} \leq \|q\|_{H^1(\Omega)}$ and $\|\mathbf{v}\|_{L^2(\Omega)} \leq \|\mathbf{v}\|_{\#}$

$$b(\mathbf{v}, q) = \int_{\Omega} \mathbf{v} \cdot \nabla q \, dx \leq \|\mathbf{v}\|_{L^2(\Omega)} \|\nabla q\|_{L^2(\Omega)} \quad (3.2.52)$$

$$\leq \|\mathbf{v}\|_{L^2(\Omega)} \|q\|_{H^1(\Omega)} \leq \|\mathbf{v}\|_{\#} \|q\|_{H^1(\Omega)}, \quad \forall (\mathbf{v}, q) \in V_{\#} \times Q_{\#}, \quad \implies \gamma_2 = 1. \quad (3.2.53)$$

□

Lemma 3.2.16. *There exists $\gamma_1 > 0$ (dependent on h) with $\mathbf{v}_h \neq 0$ and $q_h \neq 0$ such that*

$$\inf_{q_h \in H_h^{\perp}} \sup_{\mathbf{v}_h \in V_h} \frac{b(\mathbf{v}_h, q_h)}{\|q_h\|_{H^1(\Omega)} \|\mathbf{v}_h\|_{\#}} = \gamma_1 > 0. \quad (3.2.54)$$

Proof. The $\#$ -norm part in the denominator we bound from above using 3.1.3

$$\|\mathbf{v}_h\|_{\#}^2 = \|\mathbf{v}_h\|_{\mathbf{H}(\text{curl}, \Omega)}^2 + \sum_{\forall F \in \Gamma_h} \frac{1}{h_F} \|\gamma_{\parallel}(\mathbf{v}_h)\|_F^2 + \sum_{\forall F \in \Gamma_h} h_F \|\gamma_n(\mathbf{v}_h)\|_F^2 \quad (3.2.55)$$

$$\leq \|\mathbf{v}_h\|_{\mathbf{H}(\text{curl}, \Omega)}^2 + \frac{C_{\text{tr}}^2}{h_K^2} \|\mathbf{v}_h\|_{L^2(\Omega)}^2 + \sum_{\forall F \in \Gamma_h} h_F \|\gamma_n(\mathbf{v}_h)\|_F^2. \quad (3.2.56)$$

For non-negative scalars A, B, C there holds the inequality

$$\sqrt{A^2 + B^2 + C^2} \leq A + B + C. \quad (3.2.57)$$

Therefore

$$\|\mathbf{v}_h\|_{\#} = \sqrt{\|\mathbf{v}_h\|_{\mathbf{H}(\text{curl}, \Omega)}^2 + \frac{C_{\text{tr}}^2}{h_K^2} \|\mathbf{v}_h\|_{L^2(\Omega)}^2 + \sum_{\forall F \in \Gamma_h} h_F \|\gamma_n(\mathbf{v}_h)\|_F^2} \quad (3.2.58)$$

$$\leq \|\mathbf{v}_h\|_{\mathbf{H}(\text{curl}, \Omega)} + \frac{C_{\text{tr}}}{h} \|\mathbf{v}_h\|_{L^2(\Omega)} + \sum_{\forall F \in \Gamma_h} \sqrt{h_F} \|\gamma_n(\mathbf{v}_h)\|_F. \quad (3.2.59)$$

We introduce the choice $\mathbf{v}_h(q_h) = \nabla q_h$ which yields a lower bound for the supremum over $\mathbf{v}_h \in V_h$. This choice, will make the last term in the bounded norm (3.2.59) vanish as well as the curl part of the $\mathbf{H}(\text{curl}, \Omega)$ norm.

$$\|\nabla q_h\|_{\#} \leq \|\nabla q_h\|_{\mathbf{H}(\text{curl}, \Omega)} + \frac{C_{\text{tr}}}{h} \|\nabla q_h\|_{L^2(\Omega)} + \sum_{\forall F \in \Gamma_h} \sqrt{h_F} \|\gamma_n(\nabla q_h)\|_F \quad (3.2.60)$$

$$\leq \|\nabla q_h\|_{L^2(\Omega)} + \frac{C_{\text{tr}}}{h} \|\nabla q_h\|_{L^2(\Omega)}. \quad (3.2.61)$$

We use the established bounds in the norm in the denominator and use Lemma 3.2.5 to apply Poincaré-Friedrichs inequality

$$\gamma_1 \geq \inf_{q_h \in H_h^\perp} \frac{b(\nabla q_h, q_h)}{\left(1 + \frac{C_{\text{tr}}}{h}\right) \|\nabla q_h\|_{L^2(\Omega)} \|q_h\|_{H^1(\Omega)}} \quad (3.2.62)$$

$$\geq \inf_{q_h \in H_h^\perp} \frac{\|\nabla q_h\|_{L^2(\Omega)}^2}{\left(1 + \frac{C_{\text{tr}}}{h}\right) \|\nabla q_h\|_{L^2(\Omega)} \|q_h\|_{H^1(\Omega)}} \quad (3.2.63)$$

$$\geq \inf_{q_h \in H_h^\perp} \frac{\|\nabla q_h\|_{L^2(\Omega)}^2}{\left(1 + \frac{C_{\text{tr}}}{h}\right) \|\nabla q_h\|_{L^2(\Omega)} \left(\frac{1}{2} + \frac{C_p}{2}\right) \|\nabla q_h\|_{L^2(\Omega)}} \quad (3.2.64)$$

$$\geq \frac{1}{\left(1 + \frac{C_{\text{tr}}}{h}\right) \left(\frac{1}{2} + \frac{C_p}{2}\right)} > 0, \quad \implies \gamma_1 \propto h. \quad (3.2.65)$$

□

Which concludes well-posedness for the 1-form proxy method. A drawback from this approach is that some of the obtained bounds are only valid in the kernel spaces, which render them suboptimal for a-priori error estimates. That is why during the process of the thesis, we have decided to take an additional well-posedness approach.

3.3 Babuška-Nečas-Brezzi Well-posedness

We recall the following standard result; see [Nečas62, Thm. 3.1], [Babuška62, Thm. 2.1] for reference. Let $V_h \subset V$ and $Q_h \subset Q$ be finite-dimensional subspaces and define

$$X_h = V_h \times Q_h. \quad (3.3.1)$$

Suppose $B(\cdot, \cdot): X_h \times X_h \rightarrow \mathbb{R}$ is a bilinear form and $\mathcal{F}: X_h \rightarrow \mathbb{R}$ is a bounded linear functional. We wish to find

$$B(x_h, y_h) = \mathcal{F}(y_h), \quad \forall y_h \in X_h \quad (3.3.2)$$

Theorem 3.3.1 (BNB Well-posedness). *Suppose the following assumptions are fulfilled*

$$(\text{Continuity}) \quad \exists \beta > 0 : \quad |B(x_h, y_h)| \leq \beta \|x_h\|_X \|y_h\|_X, \quad \forall x_h, y_h \in X_h, \quad (3.3.3)$$

$$(\text{Stability}) \quad \exists \gamma > 0 : \quad \sup_{y_h \neq 0} \frac{B(x_h, y_h)}{\|y_h\|_X} \geq \gamma \|x_h\|_X, \quad \forall x_h \in X_h. \quad (3.3.4)$$

Then for every $\mathcal{F} \in X_h^*$ there holds

$$\exists! x_h \in X_h : \quad B(x_h, y_h) = \mathcal{F}(y_h), \quad \forall y_h \in X_h, \quad (3.3.5)$$

$$\|x_h\|_X \leq \beta^{-1} \|\mathcal{F}\|_{X^*}. \quad (3.3.6)$$

Proof. A complete proof can be found in [Nečas62, Chapter 3]. □

3.3.1 1-form vector proxy BNB well-posedness

The bilinear form $B(\cdot, \cdot)$ and right hand side $\mathcal{F}(\cdot)$ for our mixed method (2.6.18) then reads

$$B((\mathbf{u}_h, p_h); (\mathbf{v}_h, q_h)) = a_h(\mathbf{u}_h, \mathbf{v}_h) + b(\mathbf{v}_h, p_h) - b(\mathbf{u}_h, q_h) + c(p_h, q_h), \quad (3.3.7)$$

$$\begin{aligned} \mathcal{F}((\mathbf{v}_h, q_h)) &= \int_{\Omega} \mathbf{f} \cdot \mathbf{v}_h \, dx + \frac{C_{\omega}}{h} \int_{\Gamma} \gamma_{\parallel}(\mathbf{g}) \cdot \gamma_{\parallel}(\mathbf{v}_h) \, ds \\ &\quad + \int_{\Gamma} \gamma_n(\mathbf{v}_h) \cdot \gamma_{\parallel}(\mathbf{g}) \, ds - \int_{\Gamma} (\mathbf{g} \cdot \mathbf{n}) q_h \, ds. \end{aligned} \quad (3.3.8)$$

Definition 3.3.2 ($X_{\#}$ space). Recall the definitions 3.2.9 and 3.2.10. In anticipation of the error analysis, we define the following space for the 1-form proxy method.

$$X_{\#} = V_{\#} \times Q_{\#}. \quad (3.3.9)$$

For the proofwork in the FEEC framework, we define

$$(\omega, \sigma) \in H^2 \Lambda^k(\Omega) \times H^1 \Lambda^{k-1}(\Omega), \quad (\omega_h, \sigma_h) \in V_h \subset H \Lambda^k(\Omega) \times Q_h \subset H \Lambda^{k-1}(\Omega). \quad (3.3.10)$$

And finally

$$V_{\#} = V_h + H^2 \Lambda^k(\Omega), \quad Q_{\#} = Q_h + H^1 \Lambda^{k-1}(\Omega), \quad X_{\#} = V_{\#} \times Q_{\#}. \quad (3.3.11)$$

Theorem 3.3.3 (BNB continuity 1-forms). *For the 1-forms Nitsche Hodge Laplace method (3.3.7) there exists $\beta_h > 0$ such that*

$$\exists \beta_h > 0 : \quad |B((\mathbf{u}, p); (\mathbf{v}_h, q_h))| \leq \beta_h \|(\mathbf{u}, p)\|_X \|(\mathbf{v}_h, q_h)\|_X, \quad \forall (\mathbf{u}, p) \in X_{\#}, \forall (\mathbf{v}_h, q_h) \in X_h. \quad (3.3.12)$$

We denote the constant as β_h to emphasize its dependency on h . B is continuous with $\beta_h = \mathcal{O}(h^{-1})$

Proof. We use Lemma 3.2.11 to bound $a_h(\cdot, \cdot)$, Cauchy Schwarz, a scaling argument and the X -norm definition.

$$|B((\mathbf{u}, p); (\mathbf{v}_h, q_h))| = |a_h(\mathbf{u}, \mathbf{v}_h) + b(\mathbf{v}_h, p) + b(\mathbf{u}, q_h) - c(p, q_h)| \quad (3.3.13)$$

$$\leq |a_h(\mathbf{u}, \mathbf{v}_h)| + |b(\mathbf{v}_h, p)| + |b(\mathbf{u}, q_h)| + |c(p, q_h)| \quad (3.3.14)$$

$$\text{Using 3.2.11} \leq C_1 \|\mathbf{u}\|_{\#} \|\mathbf{v}_h\|_{\#} + |b(\mathbf{v}_h, p)| + |b(\mathbf{u}, q_h)| + |c(p, q_h)| \quad (3.3.15)$$

$$\leq C_1 \|\mathbf{u}\|_{\#} \|\mathbf{v}_h\|_{\#} + C_2 \|\mathbf{v}_h\|_{L^2(\Omega)} \|\nabla p\|_{L^2(\Omega)} + C_3 \|\mathbf{u}\|_{L^2(\Omega)} \|\nabla q_h\|_{L^2(\Omega)} + C_4 \|p\|_{L^2(\Omega)} \|q_h\|_{L^2(\Omega)} \quad (3.3.16)$$

$$\leq C'_1 \|(\mathbf{u}, p)\|_X \|(\mathbf{v}_h, q_h)\|_X + C'_2 h^{-1} \|(\mathbf{u}, p)\|_X \|(\mathbf{v}_h, q_h)\|_X + C'_3 h^{-1} \|(\mathbf{u}, p)\|_X \|(\mathbf{v}_h, q_h)\|_X + C'_4 \|(\mathbf{u}, p)\|_X \|(\mathbf{v}_h, q_h)\|_X. \quad (3.3.17)$$

$$0 < h \leq 1 \implies 1 + \frac{1}{h} \leq \frac{2}{h}. \quad (3.3.18)$$

$$C'_1 + C'_4 + (C'_2 + C'_3) \frac{1}{h} \leq \max(C'_1 + C'_4, C'_2 + C'_3) \left(1 + \frac{1}{h}\right) \leq 2 \max(C'_1 + C'_4, C'_2 + C'_3) \frac{1}{h}. \quad (3.3.19)$$

$$\beta = 2 \max(C'_1 + C'_4, C'_2 + C'_3), \quad \beta_h = \frac{\beta}{h}. \quad (3.3.20)$$

Which allows us to conclude the continuity proof

$$|B((\mathbf{u}, p); (\mathbf{v}_h, q_h))| \leq \beta_h \|(\mathbf{u}, p)\|_X \|(\mathbf{v}_h, q_h)\|_X, \quad \forall (\mathbf{u}, p) \in X_{\#}, \forall (\mathbf{v}_h, q_h) \in X_h. \quad (3.3.21)$$

□

Theorem 3.3.4 (BNB Stability 1-forms). *For the 1-forms Nitsche Hodge Laplace method (3.3.7), there exists $\gamma > 0$ independent of h such that*

$$\sup_{(\mathbf{v}_h, q_h) \neq 0} \frac{B((\mathbf{u}_h, p_h); (\mathbf{v}_h, q_h))}{\|(\mathbf{v}_h, q_h)\|_X} \geq \gamma \|(\mathbf{u}_h, p_h)\|_X, \quad \forall (\mathbf{u}_h, p_h) \in X_h. \quad (3.3.22)$$

Proof. In order to show the theorem, we pick T , a linear operator $(\mathbf{v}_h, q_h) = T((\mathbf{u}_h, p_h))$ such that

$$\|T((\mathbf{u}_h, p_h))\|_X \leq C_T \|(\mathbf{u}_h, p_h)\|_X, \quad (3.3.23)$$

$$B((\mathbf{u}_h, p_h); T((\mathbf{u}_h, p_h))) \geq \gamma \|(\mathbf{u}_h, p_h)\|_X^2, \quad \forall (\mathbf{u}_h, p_h) \in X_h. \quad (3.3.24)$$

which implies Lemma 3.3.4 by T -coercivity as in [Bonnet10, Thm. 2.1]. We chose

$$T((\mathbf{u}_h, p_h)) = \left(\mathbf{u}_h, p_h - \frac{1}{2C_p^2} \varphi \right). \quad (3.3.25)$$

Unsurprisingly, this choice coincides with D. Arnolds choice in the proof of the method without the Nitsche

terms and different boundary conditions [Arnold18, Thm. 4.9].

$$\sup_{(\mathbf{v}_h, q_h) \neq 0} B((\mathbf{u}_h, p_h); (\mathbf{v}_h, q_h)) \geq B((\mathbf{u}_h, p_h); T((\mathbf{u}_h, p_h))) = B\left((\mathbf{u}_h, p_h); \left(\mathbf{u}_h, p_h - \frac{1}{2C_P^2} \varphi\right)\right). \quad (3.3.26)$$

Applying linearity of B to decompose it to

$$B\left((\mathbf{u}_h, p_h); \left(\mathbf{u}_h, p_h - \frac{1}{2C_P^2} \varphi\right)\right) = B((\mathbf{u}_h, p_h); (\mathbf{u}_h, p_h)) + \frac{1}{2C_P^2} B((\mathbf{u}_h, p_h); (0, -\varphi)). \quad (3.3.27)$$

We bound the first term as follows

$$B((\mathbf{u}_h, p_h); (\mathbf{u}_h, p_h)) = a_h(\mathbf{u}_h, \mathbf{u}_h) + b(\mathbf{u}_h, p_h) - b(\mathbf{u}_h, p_h) + c(p_h, p_h) \quad (3.3.28)$$

$$= a_h(\mathbf{u}_h, \mathbf{u}_h) + \|p_h\|_{L^2(\Omega)}^2 \quad (3.3.29)$$

$$\geq a_h(\mathbf{u}_h, \mathbf{u}_h) + \frac{1}{2} \|p_h\|_{L^2(\Omega)}^2 + C_{\text{inv}} \frac{h}{2} \|\nabla p_h\|_{L^2(\Omega)}^2 \quad (3.3.30)$$

$$\begin{aligned} &= \|\nabla \times \mathbf{u}_h\|_{L^2(\Omega)}^2 + 2 \int_{\Gamma} \gamma_n(\mathbf{u}_h) \cdot \gamma_{\parallel}(\mathbf{u}_h) \, ds + \frac{C_w}{h} \|\gamma_{\parallel}(\mathbf{u}_h)\|_{L^2(\Gamma)}^2 \\ &\quad + \frac{1}{2} \|p_h\|_{L^2(\Omega)}^2 + C_{\text{inv}} \frac{h}{2} \|\nabla p_h\|_{L^2(\Omega)}^2. \end{aligned} \quad (3.3.31)$$

Bounding the mixed boundary term, by Cauchy-Schwartz, Young's inequality and Lemma 3.1.2

$$\int_{\Gamma} \gamma_n(\mathbf{u}_h) \cdot \gamma_{\parallel}(\mathbf{u}_h) \, ds \geq -\frac{1}{2\epsilon_2} \|\gamma_n(\mathbf{u}_h)\|_{L^2(\Gamma)}^2 - \frac{\epsilon_2}{2} \|\gamma_{\parallel}(\mathbf{u}_h)\|_{L^2(\Gamma)}^2, \quad (3.3.32)$$

$$\geq -\frac{C_{\text{tr}_1}^2}{2h\epsilon_2} \|\nabla \times \mathbf{u}_h\|_{L^2(\Omega)}^2 - \frac{\epsilon_2}{2} \|\gamma_{\parallel}(\mathbf{u}_h)\|_{L^2(\Gamma)}^2. \quad (3.3.33)$$

$$\text{Picking Young's constant } \epsilon_2 = \frac{2C_{\text{tr}_1}^2}{h},$$

$$2 \int_{\Gamma} \gamma_n(\mathbf{u}_h) \cdot \gamma_{\parallel}(\mathbf{u}_h) \, ds \geq -\frac{1}{2} \|\nabla \times \mathbf{u}_h\|_{L^2(\Omega)}^2 - \frac{2C_{\text{tr}}^2}{h} \|\gamma_{\parallel}(\mathbf{u}_h)\|_{L^2(\Gamma)}^2. \quad (3.3.34)$$

If we pick $C_w = 4C_{\text{tr}_1}^2$ we get

$$B((\mathbf{u}_h, p_h); (\mathbf{u}_h, p_h)) \geq \frac{1}{2} \|\nabla \times \mathbf{u}_h\|_{L^2(\Omega)}^2 + \frac{2C_{\text{tr}_1}^2}{h} \|\gamma_{\parallel}(\mathbf{u}_h)\|_{L^2(\Gamma)}^2 \quad (3.3.35)$$

$$+ \frac{1}{2} \|p_h\|_{L^2(\Omega)}^2 + C_{\text{inv}} \frac{h}{2} \|\nabla p_h\|_{L^2(\Omega)}^2. \quad (3.3.36)$$

Using Lemma 3.1.2 to bound the curl term from below

$$B((\mathbf{u}_h, p_h); (\mathbf{u}_h, p_h)) \geq \frac{1}{4} \|\nabla \times \mathbf{u}_h\|_{L^2(\Omega)}^2 + \frac{h}{4C_{\text{tr}_2}^2} \|\gamma_n(\mathbf{u}_h)\|_{L^2(\Gamma)}^2 + \frac{2C_{\text{tr}_1}^2}{h} \|\gamma_{\parallel}(\mathbf{u}_h)\|_{L^2(\Gamma)}^2 \quad (3.3.37)$$

$$+ \frac{1}{2} \|p_h\|_{L^2(\Omega)}^2 + C_{\text{inv}} \frac{h}{2} \|\nabla p_h\|_{L^2(\Omega)}^2. \quad (3.3.38)$$

Due to the Hodge decomposition 2.2.13 and the Poincaré inequality 2.2.14 we have

$$\|\mathbf{u}_h\|_{L^2(\Omega)}^2 = \|\mathbf{u}_h^{\perp}\|_{L^2(\Omega)}^2 + \|\nabla \varphi\|_{L^2(\Omega)}^2 \leq C_{P_1}^2 \|\nabla \times \mathbf{u}_h^{\perp}\|_{L^2(\Omega)}^2 + \|\nabla \varphi\|_{L^2(\Omega)}^2, \quad (3.3.39)$$

$$\implies \|\mathbf{u}_h^{\perp}\|_{L^2(\Omega)}^2 \leq C_{P_1}^2 \|\nabla \times \mathbf{u}_h^{\perp}\|_{L^2(\Omega)}^2. \quad (3.3.40)$$

Using the obtained bound on what's left of the curl term a third time

$$B((\mathbf{u}_h, p_h); (\mathbf{u}_h, p_h)) \geq \frac{1}{8} \|\nabla \times \mathbf{u}_h\|_{L^2(\Omega)}^2 + \frac{1}{8C_{P_1}^2} \|\mathbf{u}_h^\perp\|_{L^2(\Omega)}^2 + \frac{h}{4C_{\text{tr}_2}^2} \|\gamma_n(\mathbf{u}_h)\|_{L^2(\Gamma)}^2 \quad (3.3.41)$$

$$+ \frac{2C_{\text{tr}_1}^2}{h} \|\gamma_\parallel(\mathbf{u}_h)\|_{L^2(\Gamma)}^2 + \frac{1}{2} \|p_h\|_{L^2(\Omega)}^2 + C_{\text{inv}} \frac{h}{2} \|\nabla p_h\|_{L^2(\Omega)}^2. \quad (3.3.42)$$

Bounding the second term in equation (3.3.27)

$$B((\mathbf{u}_h, p_h)(0, -\varphi)) = b(\mathbf{u}_h, \varphi_h) - c(p_h, \varphi_h) \quad (3.3.43)$$

$$\geq \|\nabla \varphi_h\|_{L^2(\Omega)}^2 - \int_{\Omega} p_h \varphi_h \, \mathbf{d}\mathbf{x} \quad (3.3.44)$$

$$\geq \|\nabla \varphi_h\|_{L^2(\Omega)}^2 - \frac{1}{2\epsilon_3} \|p_h\|_{L^2(\Omega)}^2 - \frac{\epsilon_3}{2} \|\varphi_h\|_{L^2(\Omega)}^2, \quad (3.3.45)$$

$$\text{Picking Young's constant } \epsilon_3 = \frac{1}{C_{P_2}^2}$$

$$\geq \|\nabla \varphi_h\|_{L^2(\Omega)}^2 - \frac{C_{P_2}^2}{2} \|p_h\|_{L^2(\Omega)}^2 - \frac{1}{2C_{P_2}^2} \|\varphi_h\|_{L^2(\Omega)}^2, \quad (3.3.46)$$

Due to the Hodge decomposition 2.2.13 and the Poincaré inequality 2.2.14 we have

$$- \frac{1}{2C_{P_2}^2} \|\varphi_h\|_{L^2(\Omega)}^2 \geq - \frac{1}{2} \|\nabla \varphi_h\|_{L^2(\Omega)}^2. \quad (3.3.47)$$

Which yields the following lower bound

$$B((\mathbf{u}_h, p_h)(0, -\varphi_h)) \geq \frac{1}{2} \|\nabla \varphi_h\|_{L^2(\Omega)}^2 - \frac{C_{P_2}^2}{2} \|p_h\|_{L^2(\Omega)}^2. \quad (3.3.48)$$

Now we successfully obtained both parts of the Hodge decomposition and we can combine them to get the missing norm on \mathbf{u}_h .

$$\begin{aligned} B\left((\mathbf{u}_h, p_h); \left(\mathbf{u}_h, p_h - \frac{1}{2C_{P_2}^2} \varphi\right)\right) &\geq \frac{1}{8} \|\nabla \times \mathbf{u}_h\|_{L^2(\Omega)}^2 + \frac{1}{8C_{P_1}^2} \|\mathbf{u}_h^\perp\|_{L^2(\Omega)}^2 + \frac{h}{4C_{\text{tr}_2}^2} \|\gamma_n(\mathbf{u}_h)\|_{L^2(\Gamma)}^2 \\ &\quad + \frac{2C_{\text{tr}_1}^2}{h} \|\gamma_\parallel(\mathbf{u}_h)\|_{L^2(\Gamma)}^2 + \frac{1}{2} \|p_h\|_{L^2(\Omega)}^2 + C_{\text{inv}} \frac{h}{2} \|\nabla p_h\|_{L^2(\Omega)}^2 \\ &\quad + \frac{1}{2C_{P_2}^2} \left(\frac{1}{2} \|\nabla \varphi_h\|_{L^2(\Omega)}^2 - \frac{C_{P_2}^2}{2} \|p_h\|_{L^2(\Omega)}^2 \right) \end{aligned} \quad (3.3.49)$$

$$\begin{aligned} &\geq \frac{1}{8} \|\nabla \times \mathbf{u}_h\|_{L^2(\Omega)}^2 + \frac{1}{8C_{P_1}^2} \|\mathbf{u}_h^\perp\|_{L^2(\Omega)}^2 + \frac{h}{4C_{\text{tr}_2}^2} \|\gamma_n(\mathbf{u}_h)\|_{L^2(\Gamma)}^2 \\ &\quad + \frac{2C_{\text{tr}_1}^2}{h} \|\gamma_\parallel(\mathbf{u}_h)\|_{L^2(\Gamma)}^2 + \frac{1}{4} \|p_h\|_{L^2(\Omega)}^2 + C_{\text{inv}} \frac{h}{2} \|\nabla p_h\|_{L^2(\Omega)}^2 \\ &\quad + \frac{1}{4C_{P_2}^2} \|\nabla \varphi_h\|_{L^2(\Omega)}^2. \end{aligned} \quad (3.3.50)$$

$$\gamma = \min \left(\frac{1}{8}, \frac{1}{8C_{P_1}^2}, \frac{1}{4C_{\text{tr}_2}^2}, 2C_{\text{tr}_1}^2, \frac{C_{\text{inv}}}{2}, \frac{1}{4C_{P_2}^2} \right). \quad (3.3.51)$$

And we conclude the proof

$$\begin{aligned}
 B\left((\mathbf{u}_h, p_h); \left(\mathbf{u}_h, p_h - \frac{1}{2C_{P_2}^2}\varphi\right)\right) &\geq \gamma(\|\nabla \times \mathbf{u}_h\|_{L^2(\Omega)} + \|\mathbf{u}_h^\perp\|_{L^2(\Omega)}^2 + \|\nabla \varphi_h\|_{L^2(\Omega)}^2 \\
 &\quad + h\|\gamma_n(\mathbf{u}_h)\|_{L^2(\Gamma)} + \frac{1}{h}\|\gamma_\parallel(\mathbf{u}_h)\|_{L^2(\Gamma)} \\
 &\quad + \|p_h\|_{L^2(\Omega)}^2 + h\|\nabla p_h\|_{L^2(\Omega)}^2) \tag{3.3.52}
 \end{aligned}$$

$$= \gamma(\|\mathbf{u}_h\|_\#^2 + \|p_h\|_{L^2(\Omega)}^2 + h\|\nabla p_h\|_{L^2(\Omega)}^2) \tag{3.3.53}$$

$$= \gamma\|(\mathbf{u}_h, p_h)\|_X^2. \tag{3.3.54}$$

□

3.3.2 Well-posedness in the context of FEEC

In this section, we prove well-posedness within the framework of Finite Element Exterior Calculus, which will allow us to conclude well-posedness for all the vector proxy choices that can be correctly employed. We have the norms from definition 3.1.6 and 3.1.7. Let $X_h = V_h \times Q_h$ and $V_h \subset H\Lambda^k(\Omega)$, $Q_h \subset H\Lambda^{k-1}(\Omega)$ and the following bilinear forms defined as

$$a_h(\cdot, \cdot) : V_h \times V_h \longrightarrow \mathbb{R}, \quad b(\cdot, \cdot) : Q_h \times V_h \longrightarrow \mathbb{R}, \quad c(\cdot, \cdot) : Q_h \times Q_h \longrightarrow \mathbb{R}. \tag{3.3.55}$$

$$\begin{aligned}
 a_h(\omega_h, \eta_h) &= \langle \mathbf{d}\omega_h, \mathbf{d}\eta_h \rangle_{L^2(\Omega)} - \langle (\mathbf{d}\omega_h)^{\text{nor}}, \eta_h^{\text{tan}} \rangle_{L^2(\Gamma)} \\
 &\quad - \langle (\mathbf{d}\eta_h)^{\text{nor}}, \omega_h^{\text{tan}} \rangle_{L^2(\Gamma)} + \frac{C_w}{h} \langle \omega_h^{\text{tan}}, \eta_h^{\text{tan}} \rangle_{L^2(\Gamma)}, \tag{3.3.56}
 \end{aligned}$$

$$b(\sigma_h, \eta_h) = \langle \mathbf{d}\sigma_h, \eta_h \rangle_{L^2(\Omega)}, \tag{3.3.57}$$

$$c(\sigma_h, \tau_h) = \langle \sigma_h, \tau_h \rangle_{L^2(\Omega)}. \tag{3.3.58}$$

The (bi)linear forms are defined as follows

$$B(\cdot, \cdot) : X_h \times X_h \longrightarrow \mathbb{R}, \quad \mathcal{F}(\cdot) : X_h \longrightarrow \mathbb{R}. \tag{3.3.59}$$

$$B((\omega_h, \sigma_h), (\eta_h, \tau_h)) = a_h(\omega_h, \eta_h) + b(\sigma_h, \eta_h) - b(\tau_h, \omega_h) + c(\sigma_h, \tau_h), \tag{3.3.60}$$

$$\mathcal{F}((\eta_h, \tau_h)) = \langle f, \eta_h \rangle_{L^2(\Omega)} - \langle (\mathbf{d}\eta_h)^{\text{nor}}, g^{\text{tan}} \rangle_{L^2(\Gamma)} + \frac{C_w}{h} \langle g^{\text{tan}}, \eta_h^{\text{tan}} \rangle_{L^2(\Gamma)} \tag{3.3.61}$$

$$+ \langle \omega^{\text{nor}}, \tau^{\text{tan}} \rangle_{L^2(\Gamma)}. \tag{3.3.62}$$

We want to find $(\omega_h, \sigma_h) \in X_h$ such that

$$B((\omega_h, \sigma_h), (\eta_h, \tau_h)) = \mathcal{F}((\eta_h, \tau_h)), \quad \forall (\eta_h, \tau_h) \in X_h. \tag{3.3.63}$$

We also want to subject problem (3.3.63) to BNB well-posedness analysis.

Lemma 3.3.5 (Continuity of $a_h(\cdot, \cdot)$ FEEC). *There exists $C > 0$ such that*

$$a_h(\omega_h, \eta_h) \leq C \|\omega_h\|_{\#} \|\eta_h\|_{\#}, \quad \forall \omega_h \in V_{\#}, \forall \eta_h \in V_h.$$

Proof. This proof is similar to the proof of Lemma 3.2.11. Cauchy-Schwarz, norm definitions and scaling arguments. \square

Theorem 3.3.6 (BNB Continuity FEEC). *For the FEEC Nitsche Hodge Laplace method (3.3.56), there exists $\beta_h > 0$ such that*

$$|B(x, y_h)| \leq \beta_h \|x\|_X \|y_h\|_X, \quad \forall x \in X_{\#}, \forall y_h \in X_h. \quad (3.3.64)$$

Proof. The procedure of the proof is analogous to the vector proxy continuity proof, which is why it also yields an h dependent constant β_h .

$$|B((\omega, \sigma); (\eta_h, \tau_h))| = |a_h(\omega, \eta_h) + b(\eta_h, \sigma) + b(\omega, \tau_h) - c(\sigma, \tau_h)| \quad (3.3.65)$$

$$\leq |a_h(\omega, \eta_h)| + |b(\eta_h, \sigma)| + |b(\omega, \tau_h)| + |c(\sigma, \tau_h)| \quad (3.3.66)$$

$$\text{Using 3.3.5} \quad \leq C_1 \|\omega\|_{\#} \|\eta_h\|_{\#} + |b(\eta_h, \sigma)| + |b(\omega, \tau_h)| + |c(\sigma, \tau_h)| \quad (3.3.67)$$

$$\begin{aligned} &\leq C_1 \|\omega\|_{\#} \|\eta_h\|_{\#} + C_2 \|\eta_h\|_{L^2(\Omega)} \|\mathbf{d}\sigma\|_{L^2(\Omega)} \\ &\quad + C_3 \|\omega\|_{L^2(\Omega)} \|\mathbf{d}\tau_h\|_{L^2(\Omega)} + C_4 \|\sigma\|_{L^2(\Omega)} \|\tau_h\|_{L^2(\Omega)} \end{aligned} \quad (3.3.68)$$

$$\begin{aligned} &\leq C'_1 \|(\omega, \sigma)\|_X \|(\eta_h, \tau_h)\|_X + C'_2 h^{-1} \|(\omega, \sigma)\|_X \|(\eta_h, \tau_h)\|_X \\ &\quad C'_3 h^{-1} \|(\omega, \sigma)\|_X \|(\eta_h, \tau_h)\|_X + C'_4 \|(\omega, \sigma)\|_X \|(\eta_h, \tau_h)\|_X. \end{aligned} \quad (3.3.69)$$

$$0 < h \leq 1 \implies 1 + \frac{1}{h} \leq \frac{2}{h}. \quad (3.3.70)$$

$$C'_1 + C'_4 + (C'_2 + C'_3) \frac{1}{h} \leq \max(C'_1 + C'_4, C'_2 + C'_3) \left(1 + \frac{1}{h}\right) \leq 2 \max(C'_1 + C'_4, C'_2 + C'_3) \frac{1}{h}. \quad (3.3.71)$$

$$\beta = 2 \max(C'_1 + C'_4, C'_2 + C'_3), \quad \beta_h = \frac{\beta}{h}. \quad (3.3.72)$$

Which allows us to conclude the continuity proof.

$$|B((\omega, \sigma); (\eta_h, \tau_h))| \leq \beta_h \|(\omega, \sigma)\|_X \|(\eta_h, \tau_h)\|_X, \quad \forall x \in X_{\#}, \forall y_h \in X_h. \quad (3.3.73)$$

\square

Theorem 3.3.7 (BNB stability FEEC). *For the FEEC Nitsche Hodge Laplace method (3.3.56), there exists $\gamma > 0$ independent of h such that*

$$\exists \gamma > 0 : \quad \sup_{y_h \neq 0} \frac{B(x_h, y_h)}{\|y_h\|_X} \geq \gamma \|x_h\|_X, \quad \forall x_h \in X_h. \quad (3.3.74)$$

Proof. By [Bonnet10, Thm. 2.1], we choose the following linear operator T to show T -coercivity, as we did in the vector proxy case.

$$\sup_{(\eta_h, \tau_h) \neq 0} B((\omega_h, \sigma_h); (\eta_h, \tau_h)) \geq B((\omega_h, \sigma_h); T((\omega_h, \sigma_h))) = B\left((\omega_h, \sigma_h); \left(\omega_h, \sigma_h - \frac{1}{2C_{P_2}^2} \varphi\right)\right). \quad (3.3.75)$$

We apply linearity of the bilinear form B and decompose it to the differential form analogon of 3.3.27

$$B\left((\omega_h, \sigma_h); \left(\omega_h, \sigma_h - \frac{1}{2C_{P_2}^2} \varphi\right)\right) = B((\omega_h, \sigma_h); (\omega_h, \sigma_h)) + \frac{1}{2C_{P_2}^2} B((\omega_h, \sigma_h); (0, -\varphi)). \quad (3.3.76)$$

Bounding the first term in (3.3.76)

$$B((\omega_h, \sigma_h), (\omega_h, \sigma_h)) = a_h(\omega_h, \omega_h) + \|\sigma_h\|_{L^2(\Omega)}^2 \quad (3.3.77)$$

$$= \|\mathbf{d}\omega_h\|_{L^2(\Omega)}^2 - 2\langle (\mathbf{d}\omega_h)^{\text{nor}}, \omega_h^{\text{tan}} \rangle_{L^2(\Gamma)} + \frac{C_w}{h} \|\omega_h^{\text{tan}}\|_{L^2(\Gamma)}^2 + \|\sigma_h\|_{L^2(\Omega)}^2. \quad (3.3.78)$$

We bound the mixed boundary term by Cauchy-Schwartz, Young's inequality and Lemma 3.1.2

$$-\langle (\mathbf{d}\omega_h)^{\text{nor}}, \omega_h^{\text{tan}} \rangle_{L^2(\Gamma)} \geq -\frac{1}{2\epsilon} \|(\mathbf{d}\omega_h)^{\text{nor}}\|_{L^2(\Gamma)}^2 - \frac{\epsilon}{2} \|\omega_h^{\text{tan}}\|_{L^2(\Gamma)}^2 \quad (3.3.79)$$

$$\geq -\frac{C_{\text{tr}_1}^2}{2h\epsilon} \|\mathbf{d}\omega_h\|_{L^2(\Omega)}^2 - \frac{\epsilon}{2} \|\omega_h^{\text{tan}}\|_{L^2(\Gamma)}^2, \quad (3.3.80)$$

$$\text{Pick } \epsilon = \frac{2C_{\text{tr}_1}^2}{h},$$

$$\geq -\frac{1}{4} \|\mathbf{d}\omega_h\|_{L^2(\Omega)}^2 - \frac{C_{\text{tr}_1}^2}{h} \|\omega_h^{\text{tan}}\|_{L^2(\Gamma)}^2. \quad (3.3.81)$$

Using the obtained estimate

$$B((\omega_h, \sigma_h), (\omega_h, \sigma_h)) \geq \frac{1}{2} \|\mathbf{d}\omega_h\|_{L^2(\Omega)}^2 + \left(\frac{C_w}{h} - \frac{2C_{\text{tr}_1}^2}{h}\right) \|\omega_h^{\text{tan}}\|_{L^2(\Gamma)}^2 + \|\sigma_h\|_{L^2(\Omega)}^2, \quad (3.3.82)$$

$$\text{Pick } C_w = 4C_{\text{tr}_1}^2,$$

$$\geq \frac{1}{2} \|\mathbf{d}\omega_h\|_{L^2(\Omega)}^2 + \frac{2C_{\text{tr}_1}^2}{h} \|\omega_h^{\text{tan}}\|_{L^2(\Gamma)}^2 + \|\sigma_h\|_{L^2(\Omega)}^2, \quad (\text{SPD}\square). \quad (3.3.83)$$

We make use of inverse inequality 2.4.4 to obtain the following bound

$$\|(\mathbf{d}\omega_h)^{\text{nor}}\|_{L^2(\Gamma)}^2 \leq \frac{C_{\text{tr}_2}^2}{h} \|\mathbf{d}\omega_h\|_{L^2(\Omega)}^2. \quad (3.3.84)$$

We can further bound the bilinear form with this estimate and with theorem 2.4.5

$$B((\omega_h, \sigma_h), (\omega_h, \sigma_h)) \geq \frac{1}{4} \|\mathbf{d}\omega_h\|_{L^2(\Omega)}^2 + \frac{h}{4C_{\text{tr}_2}^2} \|(\mathbf{d}\omega_h)^{\text{nor}}\|_{L^2(\Gamma)}^2 + \frac{2C_{\text{tr}_1}^2}{h} \|\omega_h^{\text{tan}}\|_{L^2(\Gamma)}^2 + \|\sigma_h\|_{L^2(\Omega)}^2 \quad (3.3.85)$$

$$\begin{aligned} &\geq \frac{1}{4} \|\mathbf{d}\omega_h\|_{L^2(\Omega)}^2 + \frac{h}{4C_{\text{tr}_2}^2} \|(\mathbf{d}\omega_h)^{\text{nor}}\|_{L^2(\Gamma)}^2 + \frac{2C_{\text{tr}_1}^2}{h} \|\omega_h^{\text{tan}}\|_{L^2(\Gamma)}^2 \\ &\quad + \frac{1}{2} \|\sigma_h\|_{L^2(\Omega)}^2 + \frac{C_{\text{inv}}^2 h}{2} \|\mathbf{d}\sigma_h\|_{L^2(\Omega)}^2. \end{aligned} \quad (3.3.86)$$

Due to the Hodge decomposition 2.2.13 and the Poincaré inequality 2.2.14 we have the following bounds

$$\|\mathbf{d}\omega_h\|_{L^2(\Omega)}^2 = \|\mathbf{d}\omega_h^\perp\|_{L^2(\Omega)}^2 + \|\mathbf{d}\mathbf{d}\varphi_h\|_{L^2(\Omega)}^2 = \|\mathbf{d}\omega_h^\perp\|_{L^2(\Omega)}^2, \quad (3.3.87)$$

$$\|\omega_h^\perp\|_{L^2(\Omega)}^2 \leq C_{P_1}^2 \|\mathbf{d}\omega_h^\perp\|_{L^2(\Omega)}^2. \quad (3.3.88)$$

which yields

$$\begin{aligned} B((\omega_h, \sigma_h), (\omega_h, \sigma_h)) &\geq \frac{1}{8} \|\mathbf{d}\omega_h\|_{L^2(\Omega)}^2 + \frac{1}{8C_{P_1}^2} \|\omega_h^\perp\|_{L^2(\Omega)}^2 + \frac{h}{4C_{\text{tr}_2}^2} \|(\mathbf{d}\omega_h)^{\text{nor}}\|_{L^2(\Gamma)}^2 \\ &\quad + \frac{2C_{\text{tr}_1}^2}{h} \|\omega_h^{\text{tan}}\|_{L^2(\Gamma)}^2 + \frac{1}{2} \|\sigma_h\|_{L^2(\Omega)}^2 + \frac{C_{\text{inv}}^2 h}{2} \|\mathbf{d}\sigma_h\|_{L^2(\Omega)}^2. \end{aligned} \quad (3.3.89)$$

Bounding the second term of 2.4.3

$$B((\omega_h, \sigma_h), (0, -\varphi_h)) = b(\varphi_h, \omega_h) - c(\sigma_h, \varphi_h) \quad (3.3.90)$$

$$= \langle \omega_h, \mathbf{d}\varphi_h \rangle_{L^2(\Omega)} - \langle \sigma_h, \varphi_h \rangle_{L^2(\Omega)} \quad (3.3.91)$$

$$= \langle \omega_h^\perp, \mathbf{d}\varphi_h \rangle_{L^2(\Omega)} + \langle \mathbf{d}\varphi_h, \mathbf{d}\varphi_h \rangle_{L^2(\Omega)} - \langle \sigma_h, \varphi_h \rangle_{L^2(\Omega)} \quad (3.3.92)$$

$$= \|\mathbf{d}\varphi_h\|_{L^2(\Omega)}^2 - \langle \sigma_h, \varphi_h \rangle_{L^2(\Omega)} \quad (3.3.93)$$

$$\geq \|\mathbf{d}\varphi_h\|_{L^2(\Omega)}^2 - \frac{1}{2\epsilon} \|\sigma_h\|_{L^2(\Omega)}^2 - \frac{\epsilon}{2} \|\varphi_h\|_{L^2(\Omega)}^2, \quad (3.3.94)$$

$$\text{Pick } \epsilon = \frac{1}{C_{P_2}^2},$$

$$B((\omega_h, \sigma_h), (0, -\varphi_h)) \geq \|\mathbf{d}\varphi_h\|_{L^2(\Omega)}^2 - \frac{C_{P_2}^2}{2} \|\sigma_h\|_{L^2(\Omega)}^2 - \frac{1}{2C_{P_2}^2} \|\varphi_h\|_{L^2(\Omega)}^2. \quad (3.3.95)$$

Due to the Hodge decomposition 2.2.13 we have

$$-\|\varphi_h\|_{L^2(\Omega)}^2 \geq -C_{P_2}^2 \|\mathbf{d}\varphi_h\|_{L^2(\Omega)}^2. \quad (3.3.96)$$

Which allows us to give the following bound

$$B((\omega_h, \sigma_h), (0, -\varphi_h)) \geq \frac{1}{2} \|\mathbf{d}\varphi_h\|_{L^2(\Omega)}^2 - \frac{C_{P_2}^2}{2} \|\sigma_h\|_{L^2(\Omega)}^2. \quad (3.3.97)$$

Gathering all bounds

$$B\left((\omega_h, \sigma_h); \left(\omega_h, \sigma_h - \frac{1}{2C_{P_2}^2} \varphi_h\right)\right) = B((\omega_h, \sigma_h), (\omega_h, \sigma_h)) + \frac{1}{2C_{P_2}^2} B((\omega_h, \sigma_h), (0, -\varphi_h)) \quad (3.3.98)$$

$$\begin{aligned} &\geq \frac{1}{8} \|\mathbf{d}\omega_h\|_{L^2(\Omega)}^2 + \frac{1}{8C_{P_1}^2} \|\omega_h^\perp\|_{L^2(\Omega)}^2 + \frac{h}{4C_{\text{tr}_2}^2} \|(\mathbf{d}\omega_h)^{\text{nor}}\|_{L^2(\Gamma)}^2 \\ &\quad + \frac{2C_{\text{tr}_1}^2}{h} \|\omega_h^{\text{tan}}\|_{L^2(\Gamma)}^2 + \frac{1}{2} \|\sigma_h\|_{L^2(\Omega)}^2 + \frac{C_{\text{inv}}^2 h}{2} \|\mathbf{d}\sigma_h\|_{L^2(\Omega)}^2 \\ &\quad + \frac{1}{2C_{P_2}^2} \left(\frac{1}{2} \|\mathbf{d}\varphi_h\|_{L^2(\Omega)}^2 - \frac{C_{P_2}^2}{2} \|\sigma_h\|_{L^2(\Omega)}^2 \right). \end{aligned} \quad (3.3.99)$$

$$\begin{aligned}
B\left((\omega_h, \sigma_h); \left(\omega_h, \sigma_h - \frac{1}{2C_{P_2}^2} \varphi_h\right)\right) &\geq \frac{1}{8} \|\mathbf{d}\omega_h\|_{L^2(\Omega)}^2 + \frac{1}{8C_{P_1}^2} \|\omega_h\|_{L^2(\Omega)}^2 + \frac{1}{4C_{P_2}^2} \|\mathbf{d}\varphi_h\|_{L^2(\Omega)}^2 \\
&\quad + \frac{h}{4C_{\text{tr}_2}^2} \|(\mathbf{d}\omega_h)^{\text{nor}}\|_{L^2(\Gamma)}^2 + \frac{2C_{\text{tr}_1}^2}{h} \|\omega_h^{\text{tan}}\|_{L^2(\Gamma)}^2 \\
&\quad + \frac{1}{4} \|\sigma_h\|_{L^2(\Omega)}^2 + \frac{C_{\text{inv}}^2 h}{2} \|\mathbf{d}\sigma_h\|_{L^2(\Omega)}^2.
\end{aligned} \tag{3.3.100}$$

$$\gamma = \min\left(\frac{1}{8}, \frac{1}{8C_{P_1}^2}, \frac{1}{4C_{\text{tr}_2}^2}, 2C_{\text{tr}_1}^2, \frac{C_{\text{inv}}}{2}, \frac{1}{4C_{P_2}^2}\right). \tag{3.3.101}$$

Which lets us conclude the proof

$$\begin{aligned}
B\left((\omega_h, \sigma_h); \left(\omega_h, \sigma_h - \frac{1}{2C_{P_2}^2} \varphi_h\right)\right) &\geq \gamma (\|\mathbf{d}\omega_h\|_{L^2(\Omega)}^2 + \|\omega_h\|_{L^2(\Omega)}^2 + h \|(\mathbf{d}\omega_h)^{\text{nor}}\|_{L^2(\Gamma)}^2 \\
&\quad + \frac{1}{h} \|\omega_h^{\text{tan}}\|_{L^2(\Gamma)}^2 + \|\sigma_h\|_{L^2(\Omega)}^2 + h \|\mathbf{d}\sigma_h\|_{L^2(\Omega)}^2)
\end{aligned} \tag{3.3.102}$$

$$= \gamma \|(\omega_h, \sigma_h)\|_X^2 \tag{3.3.103}$$

□

3.4 Consistency

3.4.1 1-form vector proxy consistency

As before, we present the vector proxy consistency result first. If one considers the vector Laplacian $-\nabla^2 \mathbf{u} = \mathbf{f}$, then applies the Hodge decomposition to it and introduces auxiliary variable $p = -\operatorname{div} \mathbf{u}$, then one arrives at the formulation below, which inherits the vector Laplacian's regularity properties.

Theorem 3.4.1 (1-form vector proxy consistency). *Let $(\mathbf{u}, p) \in [H^2(\Omega)]^3 \times H^1(\Omega)$ solve*

$$\nabla \times (\nabla \times \mathbf{u}) + \nabla p = \mathbf{f}, \quad \text{in } \Omega, \quad (3.4.1)$$

$$\nabla \cdot \mathbf{u} + p = 0, \quad \text{in } \Omega, \quad (3.4.2)$$

$$\mathbf{u} = \mathbf{g}, \quad \text{on } \Gamma. \quad (3.4.3)$$

Then (\mathbf{u}, p) satisfies the weak mixed method for 1-form vector proxies

$$B((\mathbf{u}, p), (\mathbf{v}_h, q_h)) = \mathcal{F}((\mathbf{v}_h, q_h)), \quad \forall (\mathbf{v}_h, q_h) \in X_h. \quad (3.4.4)$$

With

$$\begin{aligned} \mathcal{F}((\mathbf{v}_h, q_h)) &= \langle \mathbf{f}, \mathbf{v}_h \rangle_{L^2(\Omega)} + \langle \gamma_n(\mathbf{v}_h), \gamma_{\parallel}(\mathbf{g}) \rangle_{L^2(\Gamma)} + \frac{C_w}{h} \langle \gamma_{\parallel}(\mathbf{g}), \gamma_{\parallel}(\mathbf{v}_h) \rangle_{L^2(\Gamma)} \\ &\quad + \langle \mathbf{g} \cdot \mathbf{n}, q_h \rangle_{L^2(\Gamma)}. \end{aligned} \quad (3.4.5)$$

Proof. If we plug in the left hand side of (3.4.1) into the first term of (3.4.5), we obtain

$$\mathcal{F}((\mathbf{v}_h, q_h)) = \langle \mathbf{f}, \mathbf{v}_h \rangle_{L^2(\Omega)} + \dots \quad (3.4.6)$$

$$= \langle \nabla \times (\nabla \times \mathbf{u}) + \nabla p, \mathbf{v}_h \rangle_{L^2(\Omega)} + \dots \quad (3.4.7)$$

$$= \langle \nabla \times (\nabla \times \mathbf{u}), \mathbf{v}_h \rangle_{L^2(\Omega)} + \langle \nabla p, \mathbf{v}_h \rangle_{L^2(\Omega)} + \dots \quad (3.4.8)$$

On the first term in (3.4.8) we do integration by parts and use Lemma 3.1.4 on the resulting boundary term

$$\mathcal{F}((\mathbf{v}_h, q_h)) = \langle \nabla \times \mathbf{u}, \nabla \times \mathbf{v}_h \rangle_{L^2(\Omega)} + \langle \gamma_n(\mathbf{u}), \mathbf{v}_h \rangle_{L^2(\Gamma)} + \langle \nabla p, \mathbf{v}_h \rangle_{L^2(\Omega)} + \dots \quad (3.4.9)$$

$$= \langle \nabla \times \mathbf{u}, \nabla \times \mathbf{v}_h \rangle_{L^2(\Omega)} + \langle \gamma_n(\mathbf{u}), \gamma_{\parallel}(\mathbf{v}_h) \rangle_{L^2(\Gamma)} + \langle \nabla p, \mathbf{v}_h \rangle_{L^2(\Omega)} + \dots \quad (3.4.10)$$

We can use (3.4.3) in the terms of (3.4.5) where \mathbf{g} occurs to obtain

$$\mathcal{F}((\mathbf{v}_h, q_h)) = a_h(\mathbf{u}, \mathbf{v}_h) + b(\mathbf{v}_h, p) + \langle \mathbf{u} \cdot \mathbf{n}, q_h \rangle_{L^2(\Gamma)}. \quad (3.4.11)$$

Undoing integration by parts on the $\text{div}(\mathbf{u})$ term which can be done due to the regularity of \mathbf{u} and use equation 3.4.2

$$\langle \mathbf{u} \cdot \mathbf{n}, q_h \rangle_{L^2(\Gamma)} = \langle \text{div}(\mathbf{u}), q_h \rangle_{L^2(\Omega)} + \langle \mathbf{u}, \nabla q_h \rangle_{L^2(\Omega)} \quad (3.4.12)$$

$$= \langle \mathbf{u}, \nabla q_h \rangle_{L^2(\Omega)} - \langle p, q_h \rangle_{L^2(\Omega)}. \quad (3.4.13)$$

Which concludes the proof

$$\mathcal{F}((\mathbf{v}_h, q_h)) = a_h(\mathbf{u}, \mathbf{v}_h) + b(\mathbf{v}_h, p) + b(\mathbf{u}, q_h) - c(p, q_h) \quad (3.4.14)$$

$$= B((\mathbf{u}, p), (\mathbf{v}_h, q_h)), \quad \forall (\mathbf{v}_h, q_h) \in X_h. \quad (3.4.15)$$

□

3.4.2 FEEC consistency

Theorem 3.4.2 (FEEC consistency). *Let $V_h \subset H\Lambda^k(\Omega)$ and $Q_h \subset H\Lambda^{k-1}(\Omega)$.*

Let also $(\omega, \sigma) \in H^2\Lambda^k(\Omega) \times H^1\Lambda^{k-1}(\Omega)$ solve

$$\delta \mathbf{d}\omega + \mathbf{d}\sigma = f, \quad \text{in } \Omega, \quad (3.4.16)$$

$$\delta \omega - \sigma = 0, \quad \text{in } \Omega, \quad (3.4.17)$$

$$\omega = g, \quad \text{on } \Gamma. \quad (3.4.18)$$

Then (ω, σ) solve the FEEC Nitsche Hodge Laplace mixed method

$$B_h((\omega, \sigma), (\eta_h, \tau_h)) = \mathcal{F}((\eta_h, \tau_h)), \quad \forall (\eta_h, \tau_h) \in V_h \times Q_h. \quad (3.4.19)$$

With

$$\mathcal{F}((\eta_h, \tau_h)) = \langle f, \eta_h \rangle_{L^2(\Omega)} - \langle (\mathbf{d}\eta_h)^{\text{nor}}, g^{\text{tan}} \rangle_{L^2(\Gamma)} + \frac{C_w}{h} \langle g^{\text{tan}}, \eta_h^{\text{tan}} \rangle_{L^2(\Gamma)} + \langle g^{\text{nor}}, \tau_h^{\text{tan}} \rangle_{L^2(\Gamma)}. \quad (3.4.20)$$

Proof. We use the lefthand side of (3.4.16) and integration by parts to obtain

$$\mathcal{F}((\eta_h, \tau_h)) = \langle f, \eta_h \rangle_{L^2(\Omega)} - \langle (\mathbf{d}\eta_h)^{\text{nor}}, g^{\text{tan}} \rangle_{L^2(\Gamma)} + \frac{C_w}{h} \langle g^{\text{tan}}, \eta_h^{\text{tan}} \rangle_{L^2(\Gamma)} + \langle g^{\text{nor}}, \tau_h^{\text{tan}} \rangle_{L^2(\Gamma)} \quad (3.4.21)$$

$$= \langle \delta \mathbf{d}\omega + \mathbf{d}\sigma, \eta_h \rangle_{L^2(\Omega)} + \dots \quad (3.4.22)$$

$$= \langle \delta \mathbf{d}\omega, \eta_h \rangle_{L^2(\Omega)} + \langle \mathbf{d}\sigma, \eta_h \rangle_{L^2(\Omega)} + \dots \quad (3.4.23)$$

$$= \langle \mathbf{d}\omega, \mathbf{d}\eta_h \rangle_{L^2(\Omega)} + \langle (\mathbf{d}\omega)^{\text{nor}}, (\eta_h)^{\text{tan}} \rangle_{L^2(\Gamma)} + \langle \mathbf{d}\sigma, \eta_h \rangle_{L^2(\Omega)} + \dots \quad (3.4.24)$$

Now we use (3.4.18) to replace the g 's and we get

$$\mathcal{F}((\eta_h, \tau_h)) = a_h(\omega, \eta_h) + b(\sigma, \eta_h) + \langle \omega^{\text{nor}}, \tau_h^{\text{tan}} \rangle_{L^2(\Gamma)}. \quad (3.4.25)$$

To get the last term that is the inner product on the boundary, we use the integration by parts formula

$$\langle \omega^{\text{nor}}, \tau_h^{\text{tan}} \rangle_{L^2(\Gamma)} = \langle \omega, \mathbf{d}\tau_h \rangle_{L^2(\Omega)} - \langle \delta\omega, \tau_h \rangle_{L^2(\Omega)}. \quad (3.4.26)$$

We can now use (3.4.17) to replace $\delta\omega$ with σ

$$\mathcal{F}((\eta_h, \tau_h)) = a_h(\omega, \eta_h) + b(\sigma, \eta_h) + b(\omega, \tau_h) - c(\sigma, \tau_h) \quad (3.4.27)$$

$$= B_h((\omega, \sigma), (\eta_h, \tau_h)), \quad \forall (\eta_h, \tau_h) \in V_h \times Q_h. \quad (3.4.28)$$

Which concludes the FEEC consistency proof. \square

3.5 A priori error analysis

We start by presenting the a-priori error analysis in the exterior calculus framework. So far we have proven boundedness 3.3.6, stability 3.3.7 and consistency 3.4.2, which are all the components needed to derive the error bounds.

Definition 3.5.1 (Smoothness of solutions). In the following sections we always assume $(\omega, \sigma) \in H^r \Lambda^k(\Omega) \times H^l \Lambda^{k-1}(\Omega)$ to be the exact solutions, where l, r are the degrees of the finite element polynomial spaces, such that we can make use of theorem 2.4.6. Note that they are always chosen such that $l = r$, they are distinguished merely to track where the rates are coming from.

Find $x_h \in X_h \subset X = H\Lambda^k(\Omega) \times H\Lambda^{k-1}(\Omega)$ such that

$$B(x_h, y_h) = \mathcal{F}(y_h), \quad \forall y_h \in X_h. \quad (3.5.1)$$

Due to the consistency result 3.4.2, we can derive the Galerkin orthogonality for our method immediately.

Lemma 3.5.2 (Galerkin orthogonality). *Let $x \in X$ solve (3.4.16) and also have regularity as in definition 3.3.2.*

$$B(x - x_h, y_h) = B(x, y_h) - B(x_h, y_h) = \mathcal{F}(y_h) - \mathcal{F}(y_h) = 0, \quad \forall y_h \in X_h. \quad (3.5.2)$$

3.5.1 A suboptimal error bound

For problem (3.5.1) we present the following Theorem

Theorem 3.5.3 (Convergence). *Let x and x_h be the continuous and discrete solution to (3.3.56) respectively and let z_h be arbitrary, then there exists $C > 0$ independent of h such that*

$$\|x - x_h\|_X \leq Ch^{-1} \inf_{z_h \in X_h} \|x - z_h\|_X \leq Ch^{r-\frac{3}{2}} + Ch^{l-1}. \quad (3.5.3)$$

Proof. Let $z_h \in X_h$ be arbitrary. Then we can use Galerkin orthogonality 3.5.2 and continuity 3.3.6 to show

$$\begin{aligned} B(z_h - x_h, y_h) &= B(z_h - x_h + x - x, y_h) = B(z_h - x, y_h) + B(x - x_h, y_h) = B(z_h - x, y_h) \\ &\leq \beta_h \|z_h - x\|_X \|y_h\|_X, \quad \forall y_h \in X_h. \end{aligned} \quad (3.5.4)$$

We use stability 3.3.7 and 3.5.4

$$\|z_h - x_h\|_X \leq \gamma^{-1} \sup_{0 \neq y_h \in X_h} \frac{|B(z_h - x_h, y_h)|}{\|y_h\|_X} = \gamma^{-1} \sup_{0 \neq y_h \in X_h} \frac{|B(z_h - x, y_h)|}{\|y_h\|_X}. \quad (3.5.5)$$

We introduce the error $e = x - x_h$, add and subtract our arbitrary z_h and apply the triangle inequality

$$\|e\|_X = \|x - x_h\|_X = \|x - x_h + z_h - z_h\|_X \leq \|x - z_h\|_X + \|z_h - x_h\|_X. \quad (3.5.6)$$

We bound the last term with (3.5.5) and apply continuity 3.3.6 to its numerator to obtain

$$\begin{aligned} \|e\|_X &\leq \|x - z_h\|_X + \gamma^{-1} \sup_{0 \neq y_h \in X_h} \frac{|B(z_h - x, y_h)|}{\|y_h\|_X} \\ &\leq \left(1 + \frac{\beta_h}{\gamma}\right) \|x - z_h\|_X \end{aligned} \quad (3.5.7)$$

$$\leq Ch^{-1} \inf_{z_h \in X_h} \|x - z_h\|_X, \quad (3.5.8)$$

$$= Ch^{-1} \inf_{(\eta_h, \tau_h) \in X_h} \|\omega - \eta_h\|_{\#} + \|\sigma - \tau_h\|_{L^2(\Omega)} + h \|\mathbf{d}(\sigma - \tau_h)\|_{L^2(\Omega)}. \quad (3.5.9)$$

Exploring the infimum in the hashtag norm

$$\begin{aligned} \inf_{\eta_h \in V_h} \|\omega - \eta_h\|_{\#} &= \inf_{\eta_h \in V_h} \|\mathbf{d}(\omega - \eta_h)\|_{L^2(\Omega)} + \|\omega - \eta_h\|_{L^2(\Omega)} \\ &\quad + h^{-\frac{1}{2}} \|(\omega - \eta_h)^{\tan}\|_{L^2(\Gamma)} + h^{\frac{1}{2}} \|(\mathbf{d}\omega - \mathbf{d}\eta_h)^{\text{nor}}\|_{L^2(\Gamma)}, \end{aligned} \quad (3.5.10)$$

$$\begin{aligned} \text{using theorem 2.4.6} \quad &\leq Ch^r |\mathbf{d}\omega|_{H^r \Lambda^{k+1}(\Omega)} + Ch^r |\omega|_{H^r \Lambda^k(\Omega)} \\ &\quad + Ch^{r-\frac{1}{2}} |\omega^{\tan}|_{H^r \Lambda^k(\Gamma)} + Ch^{r+\frac{1}{2}} |(\mathbf{d}\omega)^{\text{nor}}|_{H^r \Lambda^{k+1}(\Gamma)}, \end{aligned} \quad (3.5.11)$$

$$\leq Ch^{r-\frac{1}{2}}. \quad (3.5.12)$$

We collect the terms again

$$\|e\|_X \leq Ch^{r-\frac{3}{2}} + Ch^{-1} \inf_{\tau_h \in Q_h} (\|\sigma - \tau_h\|_{L^2(\Omega)} + h\|\mathbf{d}(\sigma - \tau_h)\|_{L^2(\Omega)}) \quad (3.5.13)$$

$$\text{using theorem 2.4.6} \quad \leq Ch^{r-\frac{3}{2}} + Ch^{-1} (Ch^l |\sigma|_{H^l \Lambda^{k-1}(\Omega)} + Ch^{l+1} |\mathbf{d}\sigma|_{H^l \Lambda^k(\Omega)}) \quad (3.5.14)$$

$$= Ch^{r-\frac{3}{2}} + Ch^{l-1}. \quad (3.5.15)$$

□

3.5.2 A sharp error bound for the 1-form 2D method

In the proof for the BNB continuity 3.3.6, we obtained an h dependent constant which is not desirable since it decreases the error bound an entire order before the exploration of the approximation properties. We make use of an auxiliary result needed to get rid of the h^{-1} factor. This auxiliary result is only valid for $\mathbf{u} \in \mathbf{H}^0(\text{curl}, \Omega)$, which is why we first need to define the vector Laplacian in the context of a boundary lifting. The vector Laplacian can be written as

$$-\Delta \mathbf{u} = \mathbf{f}, \text{ in } \Omega, \quad \mathbf{u}|_\Gamma = \mathbf{g}.$$

Let $\mathbf{w} \in [H^r(\Omega)]^2$ such that $\mathbf{w}|_\Gamma = \mathbf{g}$ and $-\Delta \mathbf{w} = \mathbf{0}$ then we have

$$\mathbf{u}_0 = \mathbf{u} - \mathbf{w} \implies \mathbf{u}_0|_\Gamma = \mathbf{u}|_\Gamma - \mathbf{w}|_\Gamma = \mathbf{g} - \mathbf{g} = \mathbf{0}.$$

Then we can rewrite our problem in the following way

$$-\Delta \mathbf{u}_0 = \mathbf{f}, \text{ in } \Omega, \quad \mathbf{u}_0|_\Gamma = \mathbf{0}, \quad \forall \mathbf{u}_0 \in [H_0^r(\Omega)]^2. \quad (3.5.16)$$

We require r to be at least as high such that $\mathbf{u}_0 \in \mathbf{H}_0(\text{curl}, \Omega) \subset [H_0^r(\Omega)]^2$.

Theorem 3.5.4. *Following D. Arnold et. al [Arnold12], there exists a projection operator $\pi_{V_h^0}$ such that*

$$\mathbf{v}_h^0 = \pi_{V_h^0} \mathbf{v}, \quad \pi_{V_h^0} : \mathbf{H}_0(\text{curl}, \Omega) \longrightarrow V_h^0 \subset V_h^{\text{ND}1}. \quad (3.5.17)$$

Then, for $\Omega \subset \mathbb{R}^2$ we have the following bound

$$\langle \mathbf{u} - \mathbf{v}_h^0, \nabla q_h \rangle_{L^2(\Omega)} \leq Ch^{-\frac{1}{2} - \frac{1}{t}} \|\mathbf{u} - \mathbf{v}_h^0\|_{L^t(\Omega)} \|q_h\|_{L^2(\Omega)}, \quad (3.5.18)$$

$$\forall \mathbf{u} \in \mathbf{H}_0(\text{curl}, \Omega) \cap L^t(\Omega).$$

And there holds

$$\inf_{\mathbf{v}_h^0 \in V_h^0} Ch^{-\frac{1}{2} - \frac{1}{t}} \|\mathbf{u} - \mathbf{v}_h^0\|_{L^t(\Omega)} \|q_h\|_{L^2(\Omega)} \leq Ch^{r-\frac{1}{2} - \frac{1}{t}} \|\mathbf{u}\|_{L^t(\Omega)} \|q_h\|_{L^2(\Omega)}. \quad (3.5.19)$$

Proof. Similar to proof of [Arnold12, Thm. 3.5]. □

Theorem 3.5.5 (1-form 2D optimal a-priori error bound). *Let $\mathbf{u}_0 \in [H_0^r(\Omega)]^2$, obtained from the lifting as shown in (3.5.16) be the exact solution to the lifted 2D vector Laplacian and let (\mathbf{u}_h, p_h) be the discrete solution to the corresponding method. Then there exists $C > 0$ such that*

$$\|(\mathbf{u}_0 - \mathbf{u}_h, p - p_h)\|_X = Ch^{r-\frac{1}{2}} + Ch^l. \quad (3.5.20)$$

Proof.

$$\|e\|_X \leq \|x - z_h\|_X + \gamma^{-1} \sup_{0 \neq y_h \in X_h} \frac{|B(z_h - x, y_h)|}{\|y_h\|_X}. \quad (3.5.21)$$

Now instead of applying continuity, we write the entire bilinear form B , and bound it.

$$\|(\mathbf{u}_0 - \mathbf{u}_h, p - p_h)\|_X \leq \|(\mathbf{u}_0 - \mathbf{v}_h, p - q_h)\|_X + \gamma^{-1} \sup_{0 \neq (\mathbf{w}_h, s_h) \in X_h} \frac{|B((\mathbf{v}_h - \mathbf{u}_0, q_h - p), (\mathbf{w}_h, s_h))|}{\|(\mathbf{w}_h, s_h)\|_X}. \quad (3.5.22)$$

$$\begin{aligned} |B((\mathbf{v}_h - \mathbf{u}_0, q_h - p), (\mathbf{w}_h, s_h))| &= |a_h(\mathbf{v}_h - \mathbf{u}_0, \mathbf{w}_h) + b(\mathbf{w}_h, q_h - p) - b(\mathbf{v}_h - \mathbf{u}_0, s_h) + c(q_h - p, s_h)| \\ &\leq |a_h(\mathbf{u}_0 - \mathbf{v}_h, \mathbf{w}_h)| + |b(\mathbf{w}_h, p - q_h)| + |b(\mathbf{u}_0 - \mathbf{v}_h, s_h)| + |c(p - q_h, s_h)| \\ &\leq \|(\mathbf{u}_0 - \mathbf{v}_h, p - q_h)\|_X \|(\mathbf{w}_h, s_h)\|_X + \|(\mathbf{w}_h, s_h)\|_X \|\nabla(p - q_h)\|_{L^2(\Omega)} \\ &\quad + |b(\mathbf{u}_0 - \mathbf{v}_h, s_h)| + \|(\mathbf{u}_0 - \mathbf{v}_h, p - q_h)\|_X \|(\mathbf{w}_h, s_h)\|_X. \end{aligned} \quad (3.5.23)$$

We identify the bilinear form b with second argument s_h as the troublemaker. Since the gradient of s_h in the X -norm has an h factor, we cannot bound it from above by the X -norm. Using theorem 3.5.4, let $t = |\log(h)|$, then we have

$$\langle \mathbf{u}_0 - \pi_{V_h^0} \mathbf{u}_0, \nabla q_h \rangle_{L^2(\Omega)} \leq \langle \mathbf{u}_0 - \mathbf{v}_h^0, \nabla q_h \rangle_{L^2(\Omega)} \leq Ch^{-\frac{1}{2} - \frac{1}{|\log(h)|}} \|\mathbf{u}_0 - \mathbf{v}_h^0\|_{L^{|\log(h)|}(\Omega)} \|q_h\|_{L^2(\Omega)}. \quad (3.5.24)$$

In the next steps we assume that with $h \rightarrow 0$, the fraction $\frac{1}{|\log(h)|}$ becomes more and more negligible while $|\log(h)| \rightarrow \infty$. This result allows us to bound our bilinear form b from (3.5.23).

$$b(\mathbf{u}_0 - \mathbf{v}_h^0, s_h) = \langle \mathbf{u}_0 - \pi_{V_h^0} \mathbf{u}_0, \nabla s_h \rangle_{L^2(\Omega)} \leq Ch^{-\frac{1}{2}} \|\mathbf{u}_0 - \mathbf{v}_h^0\|_{L^\infty(\Omega)} \|s_h\|_{L^2(\Omega)} \quad (3.5.25)$$

$$\leq Ch^{-\frac{1}{2}} \|\mathbf{u}_0 - \mathbf{v}_h^0\|_{L^\infty(\Omega)} \|(\mathbf{w}_h, s_h)\|_X. \quad (3.5.26)$$

Now our bound on the bilinear form B becomes

$$|B((\mathbf{v}_h - \mathbf{u}_0, q_h - p), (\mathbf{w}_h, s_h))| \leq \|(\mathbf{w}_h, s_h)\|_X (2\|(\mathbf{u}_0 - \mathbf{v}_h, p - q_h)\|_X \quad (3.5.27)$$

$$+ \|\nabla(p - q_h)\|_{L^2(\Omega)} + Ch^{-\frac{1}{2}} \|\mathbf{u}_0 - \mathbf{v}_h^0\|_{L^\infty(\Omega)}) \quad (3.5.28)$$

The obtained result plugged into (3.5.22) yields

$$\begin{aligned} \|(\mathbf{u}_0 - \mathbf{u}_h, p - p_h)\|_X &\leq \|(\mathbf{u}_0 - \mathbf{v}_h, p - q_h)\|_X + \gamma^{-1} 2 \|(\mathbf{u}_0 - \mathbf{v}_h, p - q_h)\|_X \\ &\quad + \gamma^{-1} \|\nabla(p - q_h)\|_{L^2(\Omega)} + C\gamma^{-1} h^{-\frac{1}{2}} \|\mathbf{u}_0 - \mathbf{v}_h^0\|_{L^\infty(\Omega)} \end{aligned} \quad (3.5.29)$$

$$\|(\mathbf{u}_0 - \mathbf{u}_h, p - p_h)\|_X \leq + \inf_{\mathbf{0} \neq (\mathbf{v}_h, q_h)} \left((1 + 2\gamma^{-1}) \|(\mathbf{u}_0 - \mathbf{v}_h, p - q_h)\|_X + \gamma^{-1} \|\nabla(p - q_h)\|_{L^2(\Omega)} \right) \quad (3.5.30)$$

$$+ Ch^{r-\frac{1}{2}} \|\mathbf{u}_0\|_{L^\infty(\Omega)} \quad (3.5.31)$$


From (3.5.14) and (3.5.12) we already know the approximation properties under the X norm to be $\leq Ch^{r-\frac{1}{2}} + Ch^l$. The last term in (3.5.30) is also $\leq Ch^l$, therefore we conclude

$$\|(\mathbf{u}_0 - \mathbf{u}_h, p - p_h)\|_X \leq Ch^{r-\frac{1}{2}} + Ch^l. \quad (3.5.32)$$

□

Chapter 4

Numerical Experiments

In this chapter we present our numerical results, starting with the 2D 1-forms, followed by the 3D 1-forms and 2-forms. All the numerical experiments were implemented in  NGSolve, which is a high performance finite element method library with a frontend in Python and a backend in C++. It is developed and maintained by Prof. Dr. J. Schöberl and his Team at the institute of Analysis and Scientific Computing (ASC) at the Technical University of Vienna since already more than two decades. All the results can be recreated locally by cloning <https://github.com/tellocam/nitscheDirichletHodgeLaplace>. There are detailed instructions on how to run the experiments either with Docker or with a script `run.sh` that creates a virtual environment with conda. The repository runs all methods and shows convergence plots in the X -norm with coarse meshes and low orders. For all the experiments we set $r = l$, in the plots the rates are distinguished except in the X norm, there we just use r .

4.1 Discrete Hodge Laplace for $\Lambda^1(\Omega)$ in \mathbb{R}^2

for the 2D method, the convergence analysis was done on the unit square with structured meshes.

Listing 4.1: Structured unit square mesh creation

```
1  from ngsolve import *
2  from ngsolve.meshes import MakeStructured2DMesh
3  n = Int(1/h)
4  mesh = MakeStructured2DMesh(quads=False, nx=n, ny=n)
```

Listing 4.2: Structured unit square mesh creation

```
1  H_curl = HCurl(mesh, order=r, type1=True)  # For 1-forms, H(curl) space
2  H_1 = H1(mesh, order=l)                  # For 0-forms, H1 space
3  fes = H_1 * H_curl                        # Finite element space
4  (p, u), (q, v) = fes.TnT()                # TnT -> Test and Trial
```

Note that the finite element space is a product space. If the `HCurl` function is not given the argument `type1=True`, it will automatically use type 2 Nédélec elements, which is generally preferred but we actually want the trimmed spaces.

For the boundary integrals the normal vector, the tangent vector and the local meshsize are required.

Listing 4.3: Structured unit square mesh creation

```

1      n = specialcf.normal(mesh.dim)           # Normal vector
2      t = specialcf.tangential(mesh.dim)        # Tangent vector
3      h = specialcf.mesh_size                   # Local meshsize
4      dS = ds(skeleton=True, definedon=mesh.Boundaries("."*)) # BND diff
5      f = CF(GCurl(GCurl(g)) - GGrad(GDiv(g)))   # HL of g

```

The dS is the boundary differential NGSolve requires to assemble the boundary integrals correctly. the argument `definedon=mesh.Boundaries("."*)` does this for all the strings that `mesh.GetBoundaries()` would return. The argument `skeleton=True` allows the integrator to obtain information of the adjacent volume element, otherwise this integral would be zero since the trace of an $HCurl$ function is only tangential, which is orthogonal to the normal. The last line computes the left hand side of (3.4.1) which we use as a manufactured solution \mathbf{f} to do the convergence experiments. The functions `GCurl`, `GGrad` and `GDiv` are shown in appendix C, they make use of NGSolve's automatic differentiation capabilities of `coefficient` functions, since we cannot use differential operators that are applied to test and trial functions. The following $\mathbf{g} \in C^\infty(\Omega)$ is used in the 2D experiments

$$\mathbf{g} = \begin{pmatrix} \sin(x) \cos(\frac{1}{4}y) \\ -\sin(3y) \cos(\frac{3}{2}x) \end{pmatrix}. \quad (4.1.1)$$

We can proceed with the instantiation of the forms (3.3.63) on the product space in listing 4.2 to let NGSolve create the sparsity pattern to reserve the required memory.

Listing 4.4: Instatiation of bilinear form B and adding of volume integrals

```

1      B = BilinearForm(fes)
2
3      B += grad(p) * v * dx                     # Volume integrals of B
4      B += curl(u) * curl(v) * dx               # rot u * rot v
5      B += u * grad(q) * dx
6      B += - p * q * dx

```

Adding integrals to the bilinear form according to (2.6.18).

Listing 4.5: Boundary term in bilinear form B

```

1      gamma_n_u = -curl(u)*t                     # Gamma_n and Gamma_parallel
2      gamma_n_v = -curl(v)*t                     # terms appearing in
3      gamma_p_v = v - n*(v*n)                   # the boundary integrals
4      gamma_p_u = u - n*(u*n)
5
6      B += gamma_n_v * gamma_p_u * dS             # Bnd. integrals of B
7      B += gamma_p_v * gamma_n_u * dS
8      B += (C_w/h) * gamma_p_v * gamma_p_u * dS

```


Just as defined in 2.5.2, we have the 2D-version of γ_n . In 2D, the NGSolve curl operator returns the scalar rotation rot if given a vector field and a vectorfield if given a scalarfield.

Adding integrals to \mathcal{F} . Note that we do not require the differential dS for the boundary integral in line 5 of listing 4.6, since q is from the Lagrange space and therefore the integral non-zero.

Listing 4.6: Instatiation of Linear form \mathcal{F} and adding of right hand side terms

```

1      F = LinearForm( fes )
2
3      gamma_p_g = g - n*(g*n)                                # Tangential comp. of g
4
5      F += f * v * dx                                          # f is HL of g
6      F += (C_w / h) * gamma_p_g * gamma_p_v * dS
7      F += gamma_n_v * gamma_p_g * dS
8      F += (g*n) * q * ds

```

For large systems, the parallel assembly is useful, although in this convergence analysis, there were only 16k DOF's for the 5th order and the finest mesh.

Listing 4.7: Assembly of B and \mathcal{F} , solving of the linear system

```

1      with TaskManager():                                     # Assemble and solve
2                                                                # in parallel
3      B.Assemble()
4      F.Assemble()
5      sol = GridFunction( fes )                               # Instatiation of
6                                                                #solution vector
7      res = F.vec - B.mat * sol.vec                           # Residual
8      inv = B.mat.Inverse( freedofs=fes.FreeDofs(),           # Direct solving
9                          inverse="pardiso")                  # with PARDISO
10     sol.vec.data += inv * res                                # solution shift
11                                                                # by residual
12     gf_p , gf_u = sol.components                             # Solutions u_h, p_h

```

With gf_u and gf_p , one can now visualize and compute errors

Listing 4.8: Error computation and preliminary visualization

```

1      L2_error_u = sqrt( Integrate((g - gf_u)**2*dx, mesh))    # Vol L2 err
2      L2_error_u_n = sqrt( Integrate((g*n - gf_u*n)**2*dS) mesh) # Bnd L2 err
3                                                                # normal err
4      Draw( gf_u )                                             # Visualize

```

Note that the visualizations that are shown with the `Draw()` command are mostly used for preliminary visualizations. All the visualizations in this thesis have been done with PARAVIEW. The data for PARAVIEW (or pyvista) can easily be generated with code shown in listing 4.9.

Listing 4.9: VTK data generation for PARAVIEW

```
1      vtk = VTKOutput(mesh, coefs=[gf_u, gf_p], names=["u", "p"],
2                          filename="vtkFile", subdivision=0)
3      vtk.Do()
```

4.1.1 First order solution visualizations

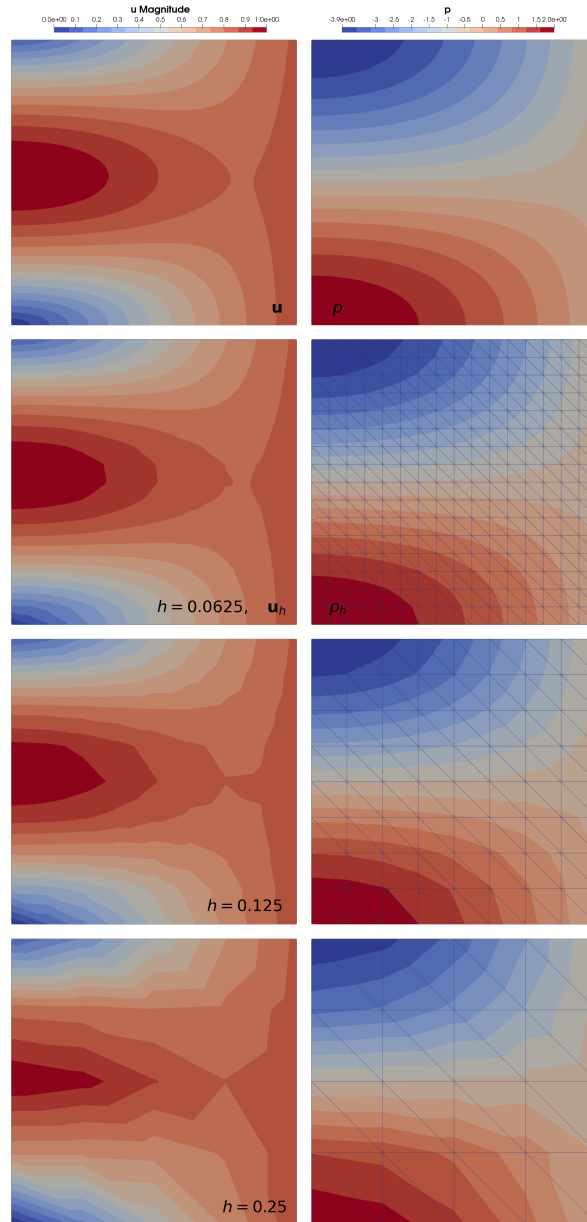


Figure 4.1: The two figures on top are the analytical solutions \mathbf{u} and p (\mathbf{g} and $-\text{div } \mathbf{g}$). Below them we show the approximation \mathbf{u}_h and p_h respectively with increasing meshsize $h = \{0.0625, 0.125, 0.25\}$. The solutions p have the meshlines as an opaque overlay.

In figure 4.1 one can observe the convergence towards the analytical solution in Ω as well as on Γ . We support this argument with convergence rate plots but first we investigate the behavior of the penalty parameter C_w on the errors in Ω as well as on Γ .

4.1.2 Nitsche penalty parameter C_w impact on errors

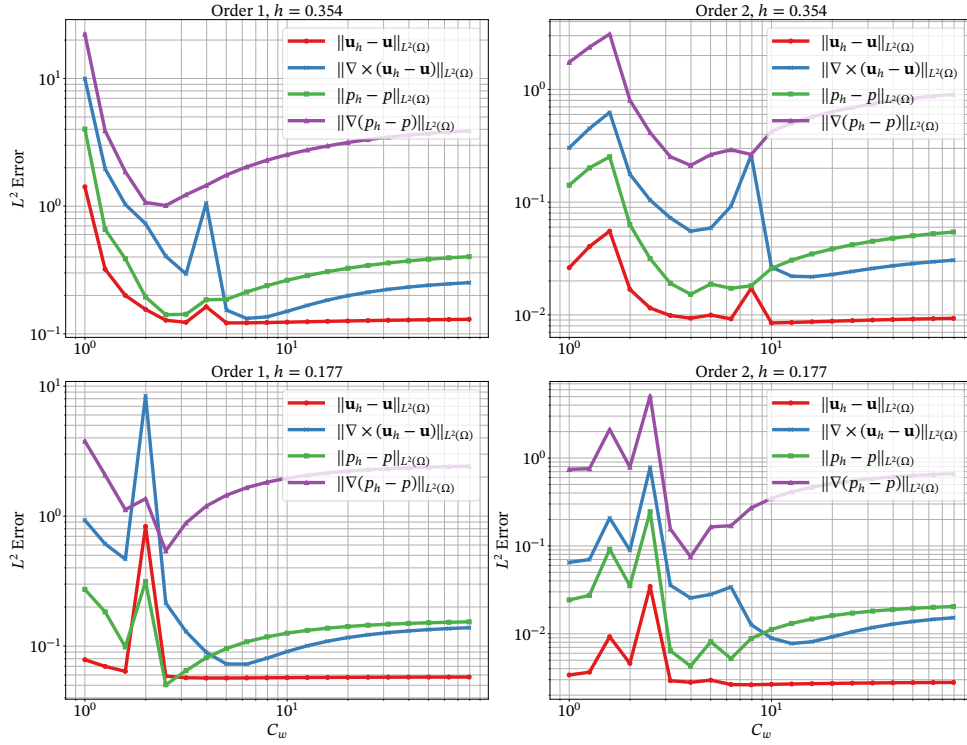


Figure 4.2: L^2 errors over Nitsche penalty parameter C_w for constant order and meshwidth h per plot for the 2D 1-form vector proxy method. From figures left to right, we have increasing order. From top to bottom, we have decreasing meshsize.

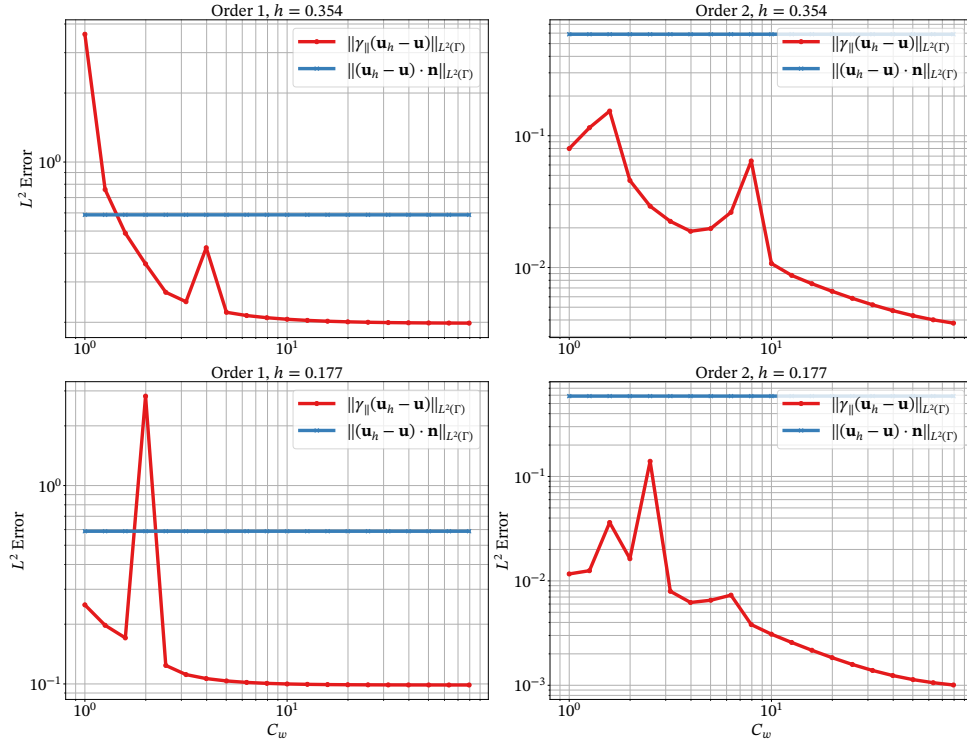


Figure 4.3: Nitsche penalty parameter C_w impact on the relevant errors on the boundary Γ . 1-form 2D proxy method, Same plotting arrangement as in figure 4.2.

We observe the experimental manifestation of the statement "for sufficiently large C_w " in figure 4.2. In fact, for this method if we chose $C_w = 12$ we observe optimal convergence rates under the X norm for all orders and meshsizes.

4.1.3 h -convergence rates in the L^2 norms

Note that for all the error rates, also for all other methods, we automatically identify the C_w value that minimizes the L^2 error of \mathbf{u}_h per order to do the h convergence plots.

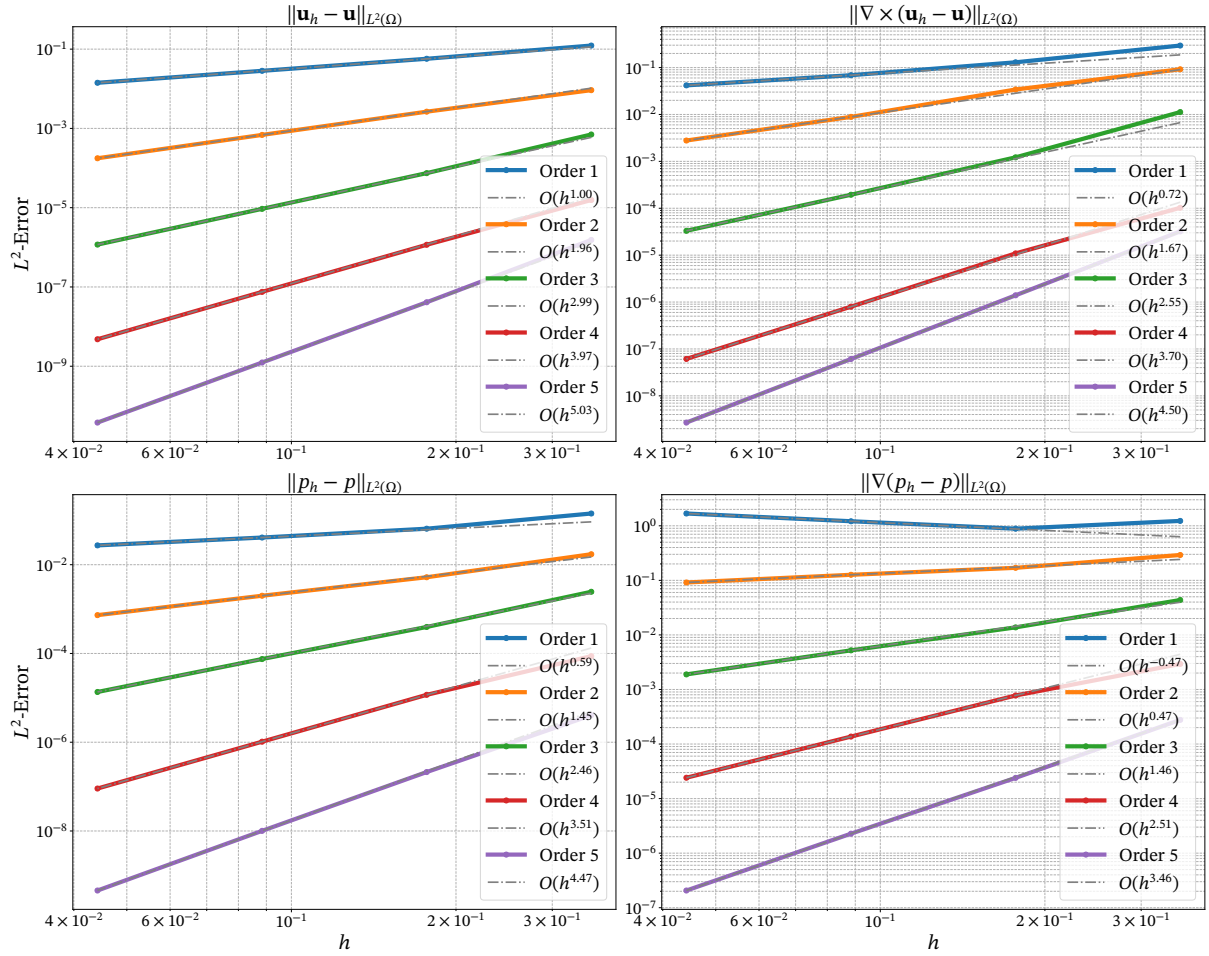


Figure 4.4: Relevant L^2 errors for the 1-form 2D proxy method. Up to order 5 and every order with interpolated rate in dash-dotted gray.

Observed L^2 convergence rates for 2D 1-forms. Except for first order we observe

$$\|\mathbf{u}_h - \mathbf{u}\|_{L^2(\Omega)} \leq Ch^r,$$

$$\|p_h - p\|_{L^2(\Omega)} \leq Ch^{l-\frac{1}{2}},$$

$$\|\nabla \times (\mathbf{u}_h - \mathbf{u})\|_{L^2(\Omega)} \leq Ch^{r-\frac{1}{2}},$$

$$\|\nabla(p_h - p)\|_{L^2(\Omega)} \leq Ch^{l-\frac{3}{2}}.$$

4.1.4 h -convergence in the $\#$ -norm and its components

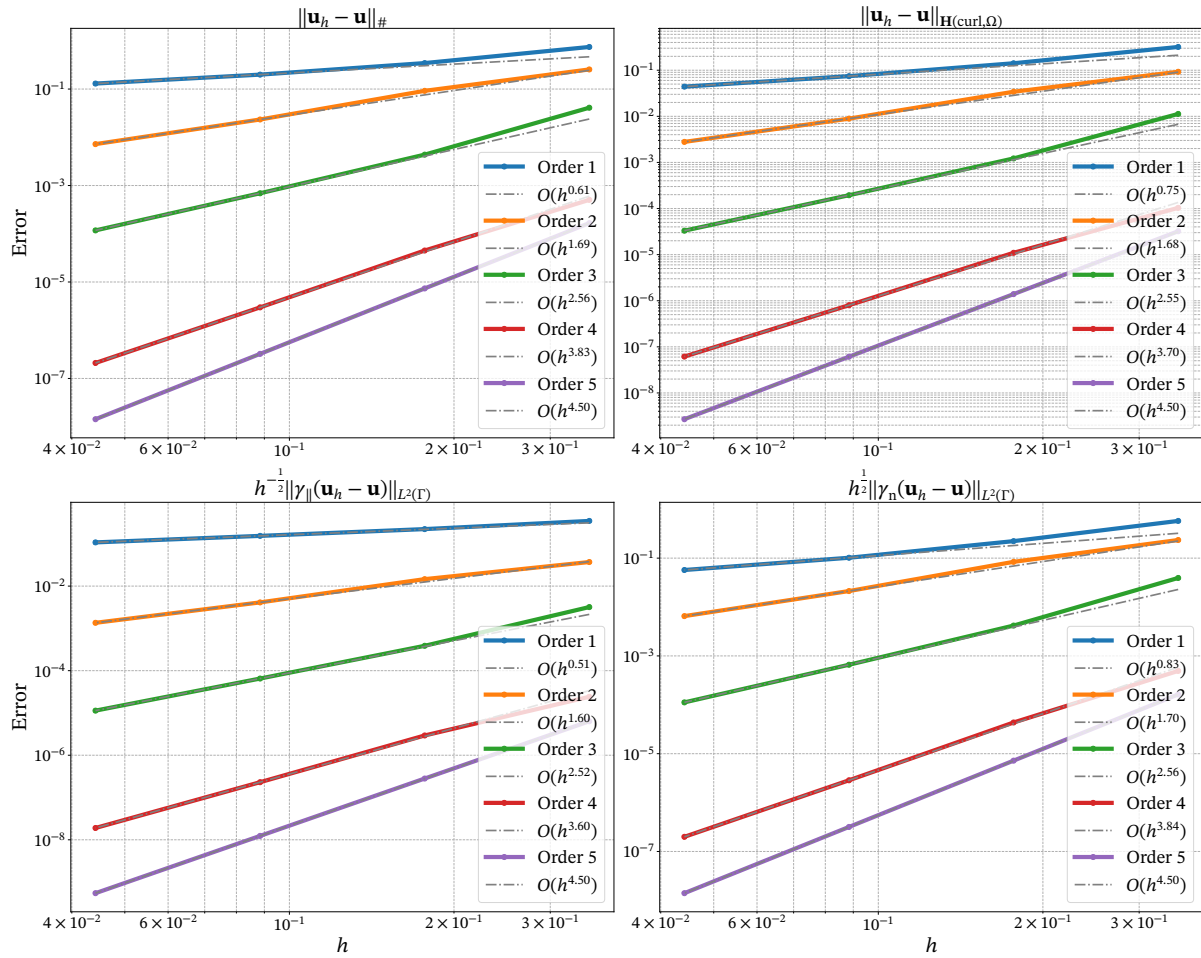


Figure 4.5: The $\#$ error and its components for the 1-form 2D proxy method. Up to order 5 and every order with interpolated rate in dash-dotted gray.

Observed convergence rate in the $\#$ -norm and its components for 2D 1-forms. Except for first order we observe

$$\|\mathbf{u}_h - \mathbf{u}\|_{\#} \leq Ch^{r-\frac{1}{2}},$$

$$h^{-\frac{1}{2}} \|\gamma_{\parallel}(\mathbf{u}_h - \mathbf{u})\|_{L^2(\Gamma)} \leq Ch^{r-\frac{1}{2}},$$

$$\|\mathbf{u}_h - \mathbf{u}\|_{H(\text{curl}, \Omega)} \leq Ch^{r-\frac{1}{2}},$$

$$h^{\frac{1}{2}} \|\gamma_n(\mathbf{u}_h - \mathbf{u})\|_{L^2(\Gamma)} \leq Ch^{r-\frac{1}{2}}.$$

4.1.5 h -convergence in the X -norm and its components

Below we present the most relevant experimental convergence result for the 2D 1-form method.

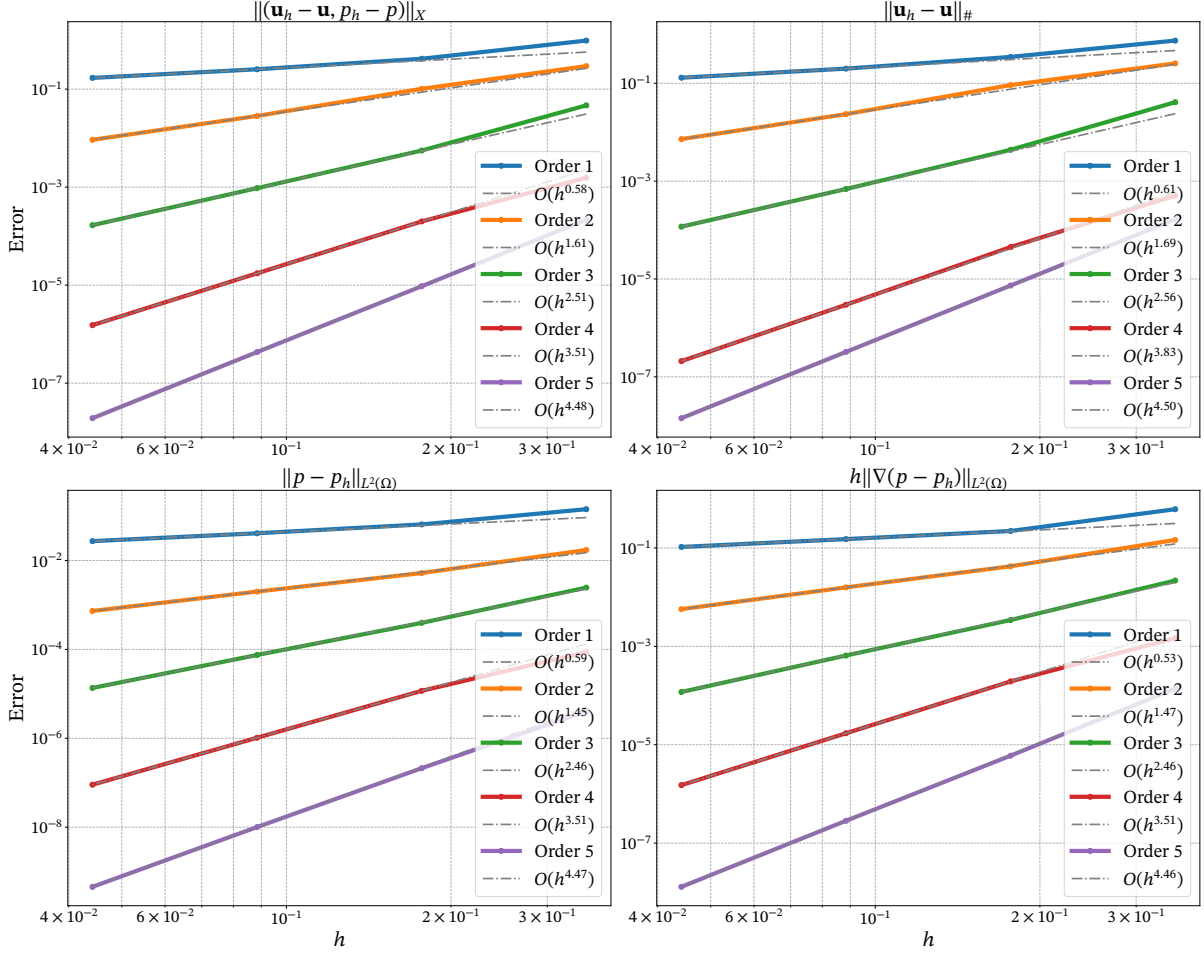


Figure 4.6: The X error and its components for the 1-form 2D proxy method. Up to order 5 and every order with interpolated rate in dash-dotted gray.

Observed convergence rate in the X norm and its components for 2D 1-forms. We observe

$$\|(\mathbf{u}_h - \mathbf{u}, p - p_h)\|_X \leq Ch^{r-\frac{1}{2}},$$

$$\|p_h - p\|_{L^2(\Omega)} \leq Ch^{l-\frac{1}{2}},$$

$$\|\mathbf{u}_h - \mathbf{u}\|_{\#} \leq Ch^{r-\frac{1}{2}},$$

$$h\|\nabla(p_h - p)\|_{L^2(\Omega)} \leq Ch^{l-\frac{1}{2}}.$$

The X -error converges as the a-priori error estimate in Theorem 3.5.5 predicted, rendering the theoretical result optimal for the 2D 1-forms case.

4.2 Discrete Hodge Laplace for $\Lambda^1(\Omega)$ in \mathbb{R}^3

For the 1-forms in 3D, we use the following manufactured solution

$$\mathbf{g} = \begin{pmatrix} 7 \sin(x) \cos(y) \sin(2z) \\ -\cos(x) \sin(\frac{1}{3}x) \cos(z) \\ 4 \cos(\frac{1}{8}x) \cos(y) \sin(z) \end{pmatrix}, \quad p = \nabla \cdot \mathbf{g}. \quad (4.2.1)$$

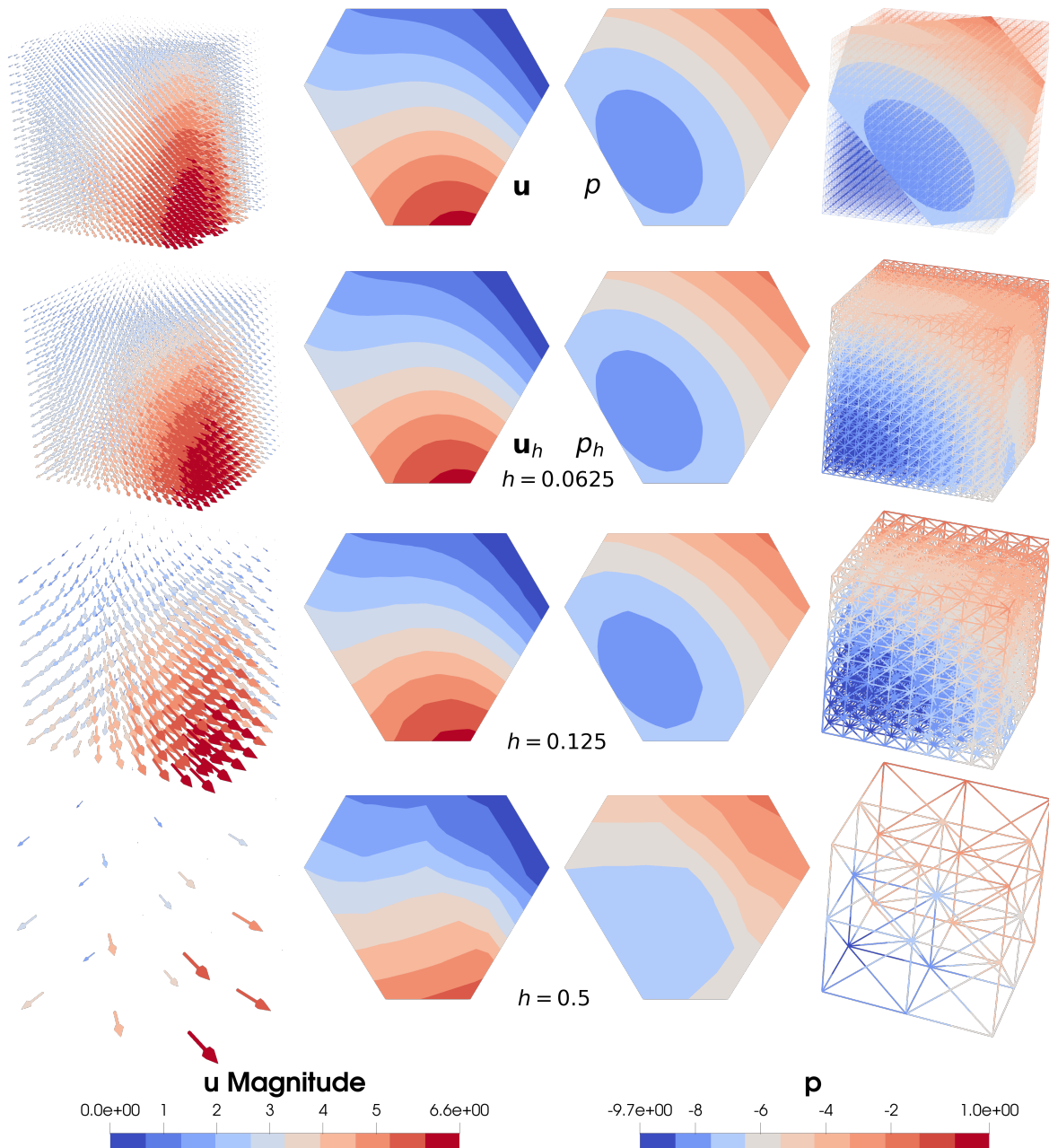


Figure 4.7: The top row shows the manufactured solutions (\mathbf{g}, p) ; its rightmost image displays the plane where the unit brick is cut to show the solutions in the 2 middle columns. The left column shows the vector field \mathbf{u} , while the right column displays the mesh colored by the magnitude of p .

In the listing below, we show the components of the code that differ from the 2D case.

Listing 4.10: Parts of 3D 1-forms code that differ from 2D

```

1      B += - curl(u) * Cross(n, v) * dS          # = gamma_n_u*gamma_p_v
2      B += - Cross(n, u) * curl(v) * dS          # = gamma_p_u*gamma_n_v
3      B += (C_w / h) * Cross(n, u) * Cross(n, v) * dS
4
5      F += (C_w / h) * Cross(n, g) * Cross(n, v) * dS
6      F += - Cross(n, g) * curl(v) * dS
7      F += g * n * q * ds

```

we opted to use the GMRes solver, and use the diagonal elements of the blockmatrices as preconditioner. This decision was made since the problems became quite large, for order 3 and $h = 0.055$ we already have 600k DOF's. At this size, one also benefits from the parallel assembly. The 3D experiments for 1-forms and for 2-forms were run a cluster with specifications documented in appendix B.

Listing 4.11: Assembly and solving of 3D 1-forms method

```

1      from ngsolve.solvers import GMRes
2      with TaskManager():
3          B.Assemble()
4          F.Assemble()
5          sol = GridFunction(fes)
6          blocks = fes.CreateSmoothingBlocks()
7          prebj = B.mat.CreateBlockSmoother(blocks)  # block-Jacobi precondition
8          GMRes(A=B.mat,
9                x=sol.vec,
10               b=F.vec, pre = prebj,
11               printrates="\r",
12               maxsteps = 10000,                    # 10k iters. because
13                                                    # low tolerance
14               tol=1e-8)                             # tol = sqrt(1e-16)
15      gf_p , gf_u = sol.components

```

4.2.1 Nitsche penalty parameter C_w impact on errors

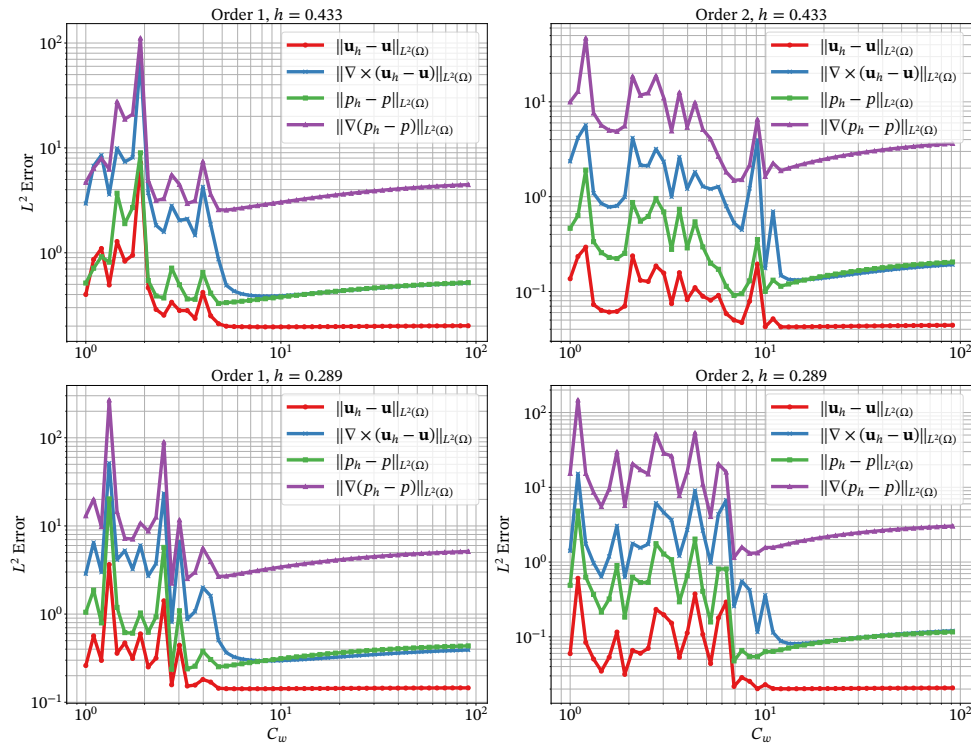


Figure 4.8: L^2 error over Nitsche penalty parameter C_w for constant order and meshwidth h for the 3D 1-form vector proxy method. From figures left to right, we have increasing order. From top to bottom, we have decreasing meshsize.

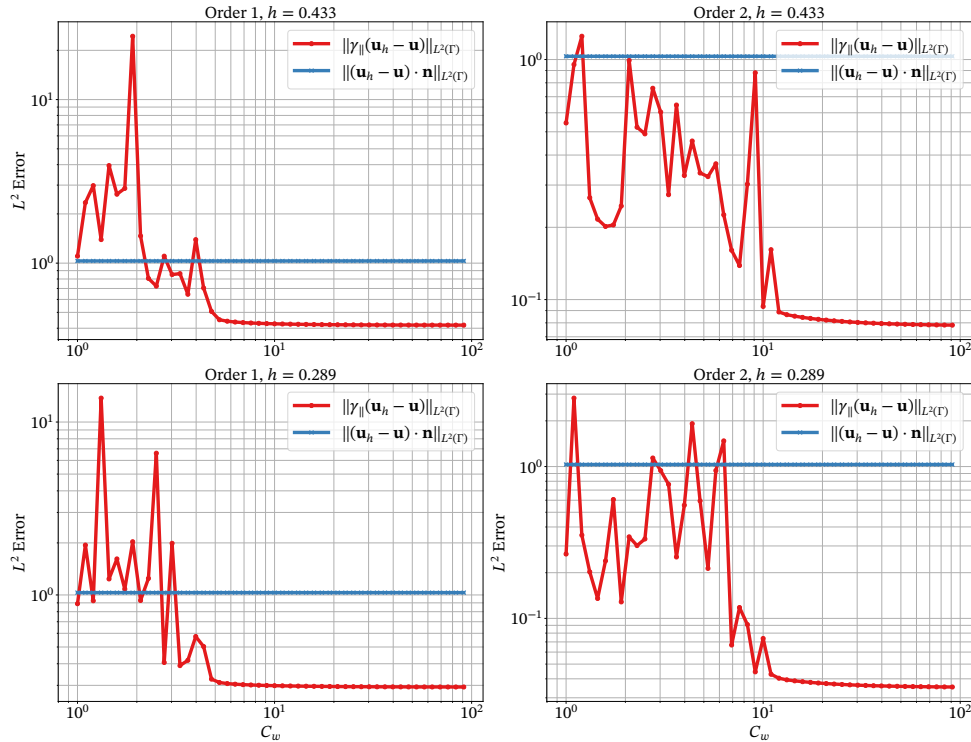


Figure 4.9: Nitsche penalty parameter C_w impact on the relevant errors on the boundary Γ . 1-form 3D proxy method, Same plotting arrangement as in figure 4.8.

4.2.2 h -convergence in the L^2 norms

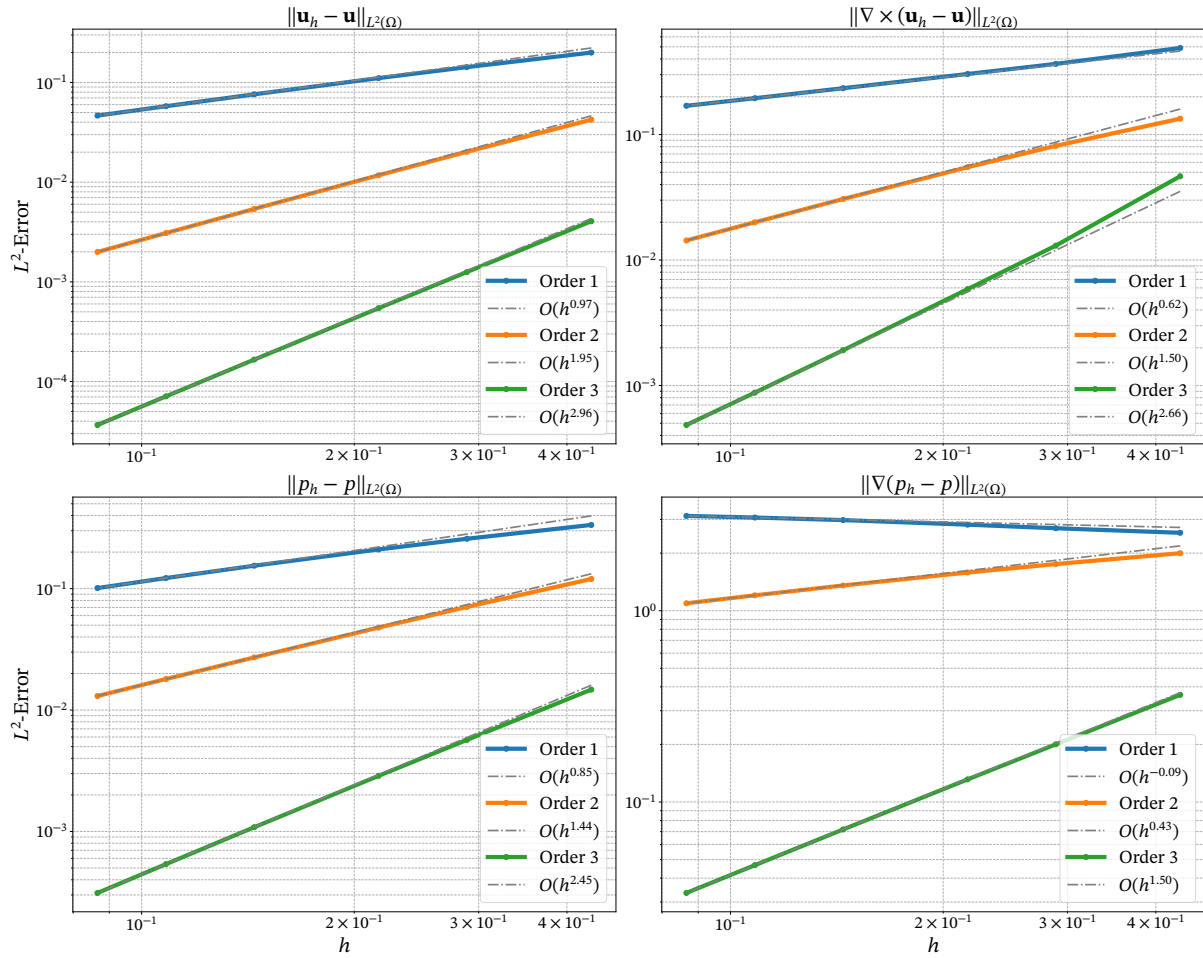


Figure 4.10: Relevant L^2 errors for the 1-form 3D proxy method. Up to order 3 and every order with interpolated rate in dash-dotted gray.

Observed L^2 convergence rates for 3D 1-forms. Except for first order, we observe

$$\begin{aligned} \|\mathbf{u}_h - \mathbf{u}\|_{L^2(\Omega)} &\leq Ch^r, & \|\nabla \times (\mathbf{u}_h - \mathbf{u})\|_{L^2(\Omega)} &\leq Ch^{r-\frac{1}{2}}, \\ \|p_h - p\|_{L^2(\Omega)} &\leq Ch^{l-\frac{1}{2}}, & \|\nabla(p_h - p)\|_{L^2(\Omega)} &\leq Ch^{l-\frac{3}{2}}. \end{aligned}$$

The observed L^2 convergence rates for 3D 1-forms coincide with the observed L^2 convergence rates for 2D 1-forms.

4.2.3 h -convergence in the # norm

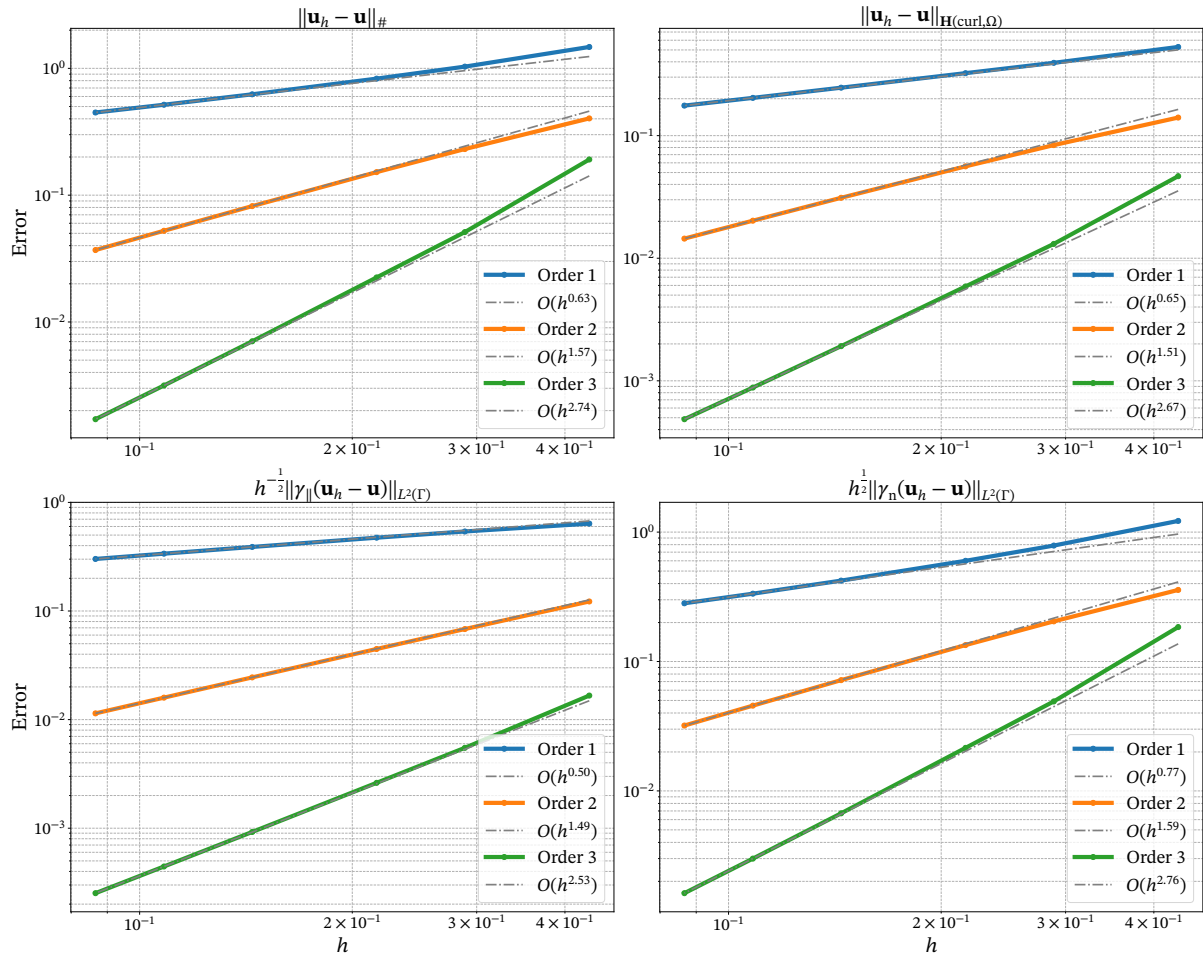


Figure 4.11: The # error and its components for the 1-form 3D proxy method. Up to order 3 and every order with interpolated rate in dash-dotted gray.

Observed convergence rates in the #-norm for 3D 1-forms. Except for first order, we observe

$$\|\mathbf{u}_h - \mathbf{u}\|_{\#} \leq Ch^{r-\frac{1}{2}},$$

$$h^{-\frac{1}{2}} \|\gamma_{\parallel}(\mathbf{u}_h - \mathbf{u})\|_{L^2(\Gamma)} \leq Ch^{r-\frac{1}{2}},$$

$$\|\mathbf{u}_h - \mathbf{u}\|_{\mathbf{H}(\text{curl}, \Omega)} \leq Ch^{r-\frac{1}{2}},$$

$$h^{\frac{1}{2}} \|\gamma_n(\mathbf{u}_h - \mathbf{u})\|_{L^2(\Gamma)} \leq Ch^{r-\frac{1}{2}}.$$

The observed rates in the #-norm for 3D 1-forms coincide with the observed rates in the #-norm for 2D 1-forms.

4.2.4 h -convergence in the X norm

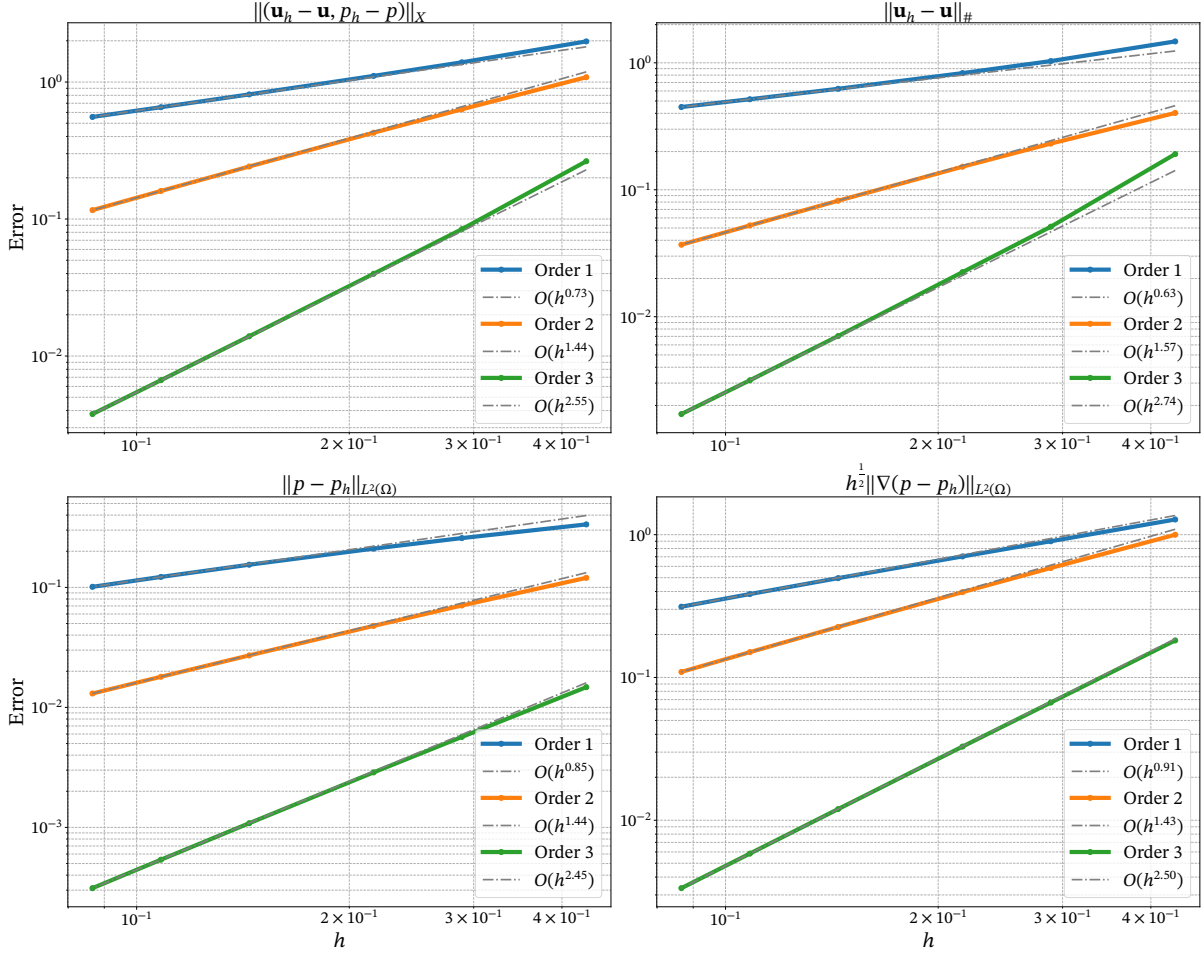


Figure 4.12: The X error and its components for the 1-form 3D proxy method. Up to order 3 and every order with interpolated rate in dash-dotted gray.

Observed convergence rates in the X -norm for 3D 1-forms. we observe

$$\|(\mathbf{u}_h - \mathbf{u}, p - p_h)\|_X \leq Ch^{r-\frac{1}{2}},$$

$$\|p_h - p\|_{L^2(\Omega)} \leq Ch^{l-\frac{1}{2}},$$

$$\|\mathbf{u}_h - \mathbf{u}\|_{\#} \leq Ch^{r-\frac{1}{2}},$$

$$h\|\nabla(p_h - p)\|_{L^2(\Omega)} \leq Ch^{l-\frac{1}{2}}.$$

The observed rates in the X -norm for 3D 1-forms coincide with the observed rates in the X -norm for 2D 1-forms. However, this rate is half an order off from the a-priori estimate from Theorem 3.5.3, which renders the theoretical result suboptimal.

4.3 Discrete Hodge Laplace for $\Lambda^2(\Omega)$ in \mathbb{R}^3

The manufactured solution \mathbf{g} is the same as in the 1-forms 3D method for comparability reasons.

$$\mathbf{g} = \begin{pmatrix} 7 \sin(x) \cos(y) \sin(2z) \\ -\cos(x) \sin(\frac{1}{3}x) \cos(z) \\ 4 \cos(\frac{1}{8}x) \cos(y) \sin(z) \end{pmatrix}, \quad \mathbf{p} = \nabla \times \mathbf{g}. \quad (4.3.1)$$

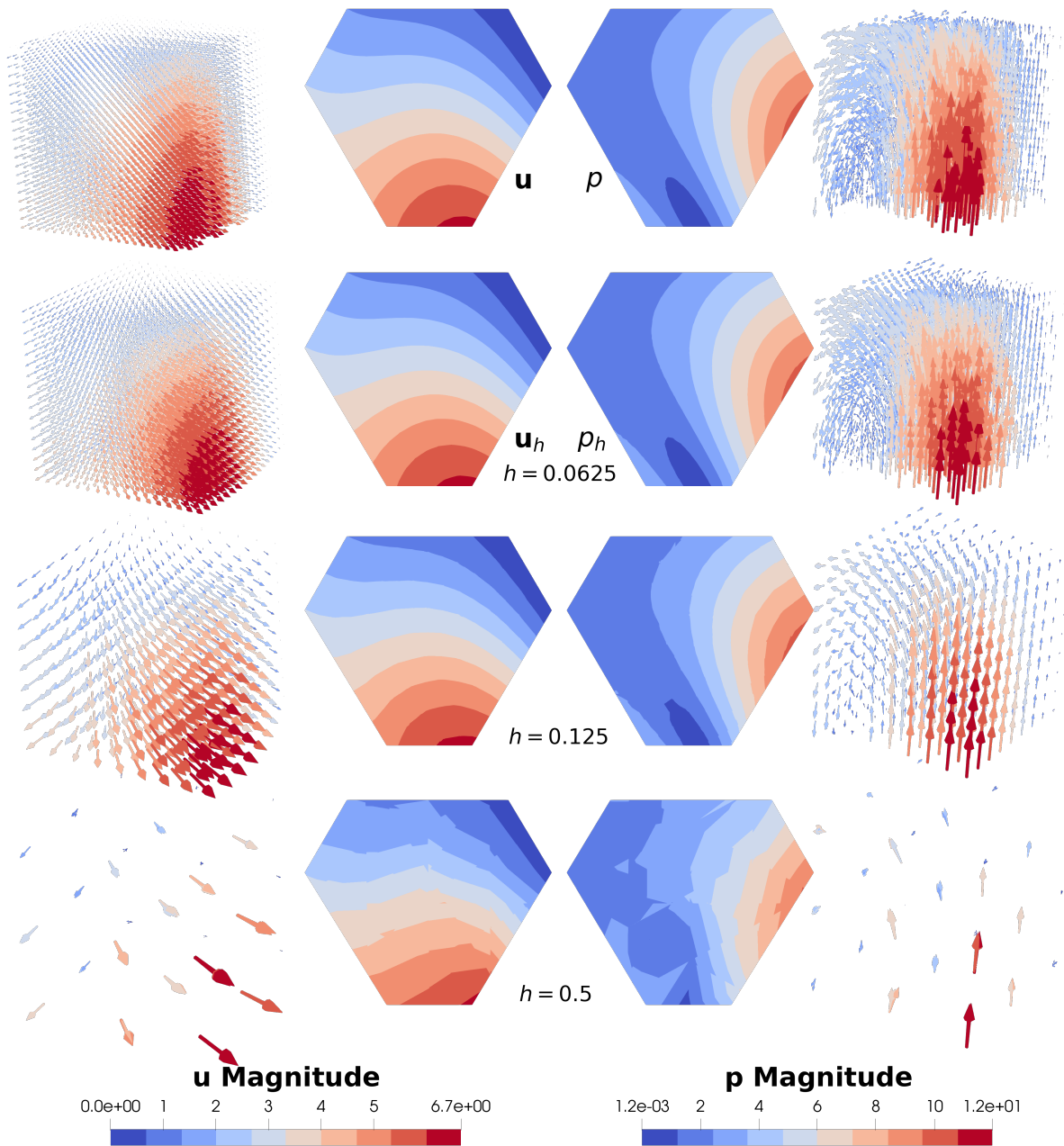


Figure 4.13: The top row shows the manufactured solution (\mathbf{g}, \mathbf{p}) . The left column shows the vector field \mathbf{u} and the right one shows the vectorfield \mathbf{p} . The cut sections presented in the 2 middle columns are cut in the same way as in figure 4.7

Note that for unknown reason's, the lowest order Raviart-Thomas elements in NGSolve, start their numbering with 0. Hence the order - 1 argument in the HDiv instantiation. We assemble and solve the arising system identical to listing 4.11 and run it on the cluster with documented specifications in appendix B.

Listing 4.12: 2-forms 3D method code

```

1   H_curl = HCurl(mesh, order=order, type1=True)
2   H_div = HDiv(mesh, order=order-1, RT=True)
3   fes = H_div * H_curl
4   (u, p), (v, q) = fes.TnT()
5
6   n = specialcf.normal(mesh.dim)
7   h = specialcf.mesh_size
8   dS = ds(skeleton=True, definedon=mesh.Boundaries(".*"))
9   f = CF(GCurl(GCurl(g)) - GGrad(GDiv(g)))
10
11  B, F = BilinearForm(fes), LinearForm(fes)
12
13  B += curl(p) * v * dx
14  B += div(u) * div(v) * dx
15  B += curl(q) * u * dx
16  B += - p * q * dx
17
18  B += - div(u) * (v*n) * dS
19  B += - div(v) * (u*n) * dS
20  B += (C_w/h) * (v*n) * (u*n) * dS
21
22  F += f * v * dx
23  F += - div(v) * (g*n) * dS
24  F += (C_w/h) * (g*n) * (v*n) * dS
25  F += Cross(n, q) * g * dS

```

4.3.1 Nitsche penalty parameter C_w impact on errors

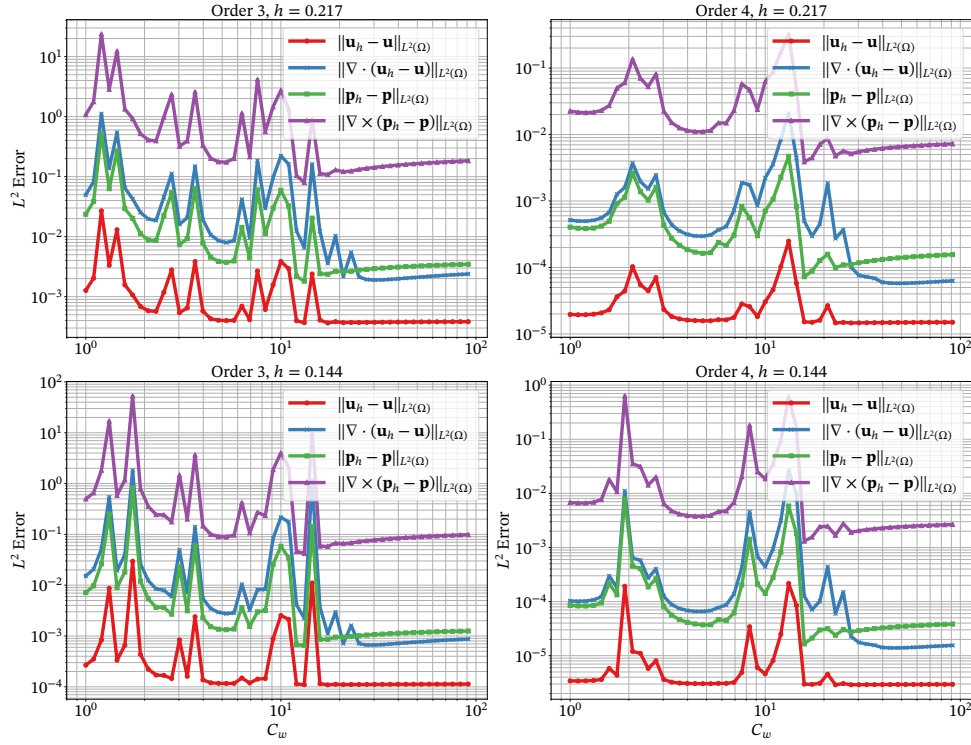


Figure 4.14: L^2 error over Nitsche penalty parameter C_w for constant order and meshwidth h for the 3D 2-form vector proxy method. From figures left to right, we have increasing order. From top to bottom, we have decreasing meshsize.

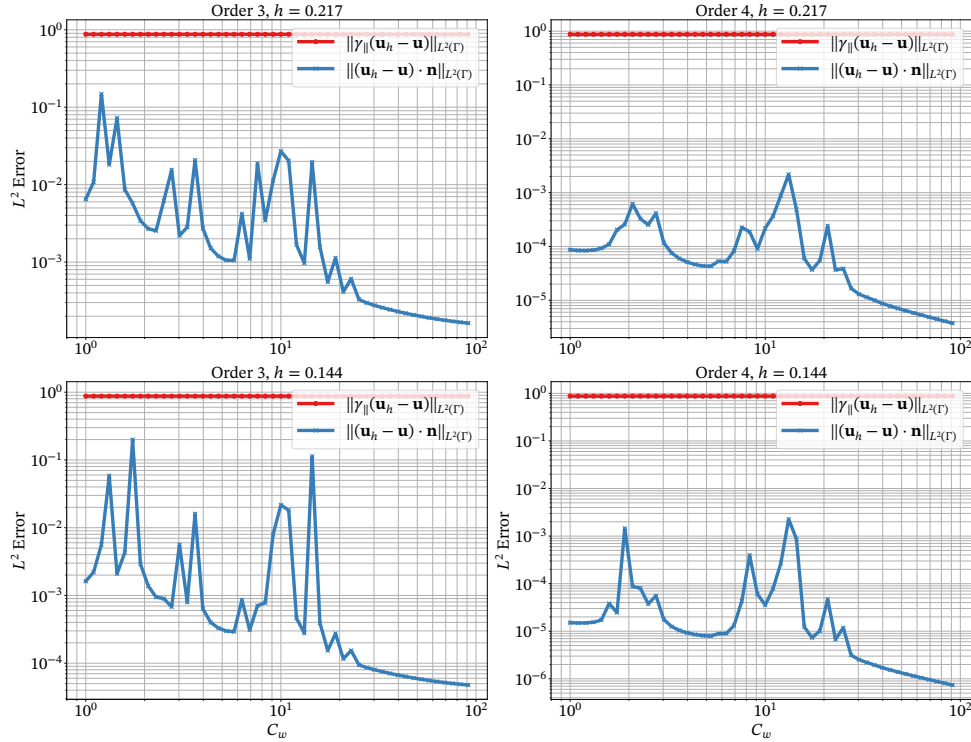


Figure 4.15: Nitsche penalty parameter C_w impact on the relevant errors on the boundary Γ . 2-form 3D proxy method, Same plotting arrangement as in figure 4.14. We observe reversed behavior as in figure 4.9 and 4.3.

4.3.2 h -convergence in the L^2 -norms

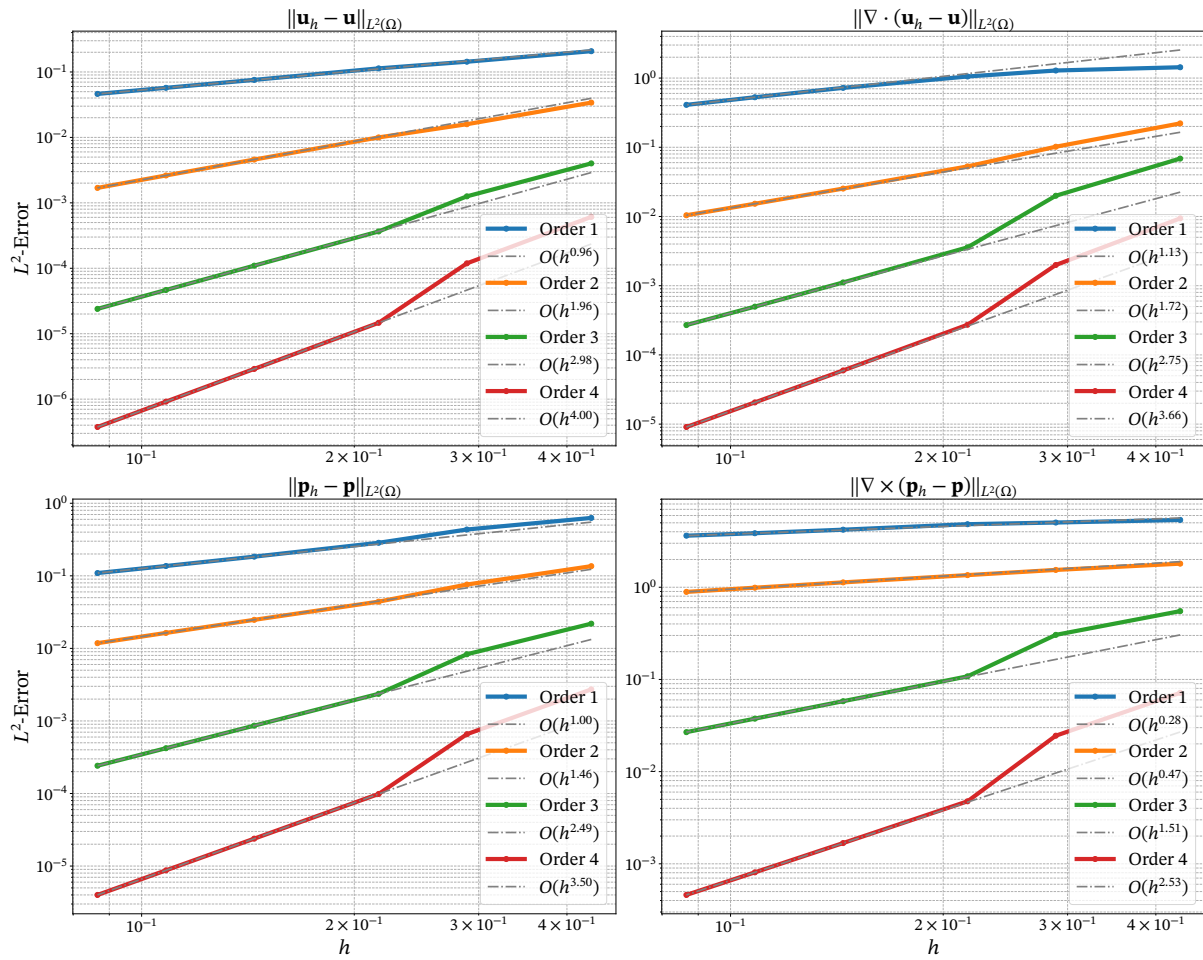


Figure 4.16: Relevant L^2 errors for the 2-form 3D proxy method. Up to order 4 and every order with interpolated rate in dash-dotted gray.

Observed L^2 convergence rates for 3D 2-forms. Except for the first order we observe

$$\begin{aligned} \|\mathbf{u}_h - \mathbf{u}\|_{L^2(\Omega)} &\leq Ch^r, & \|\nabla \cdot (\mathbf{u}_h - \mathbf{u})\|_{L^2(\Omega)} &\leq Ch^{r-\frac{1}{2}}, \\ \|\mathbf{p}_h - \mathbf{p}\|_{L^2(\Omega)} &\leq Ch^{l-\frac{1}{2}}, & \|\nabla \times (\mathbf{p}_h - \mathbf{p})\|_{L^2(\Omega)} &\leq Ch^{l-\frac{3}{2}}. \end{aligned}$$

The L^2 rates observed for the 2D 1-forms, coincide with the L^2 rates observed for the 2D as well as the 3D 1-forms.

4.3.3 h -convergence in the $\#$ -norm

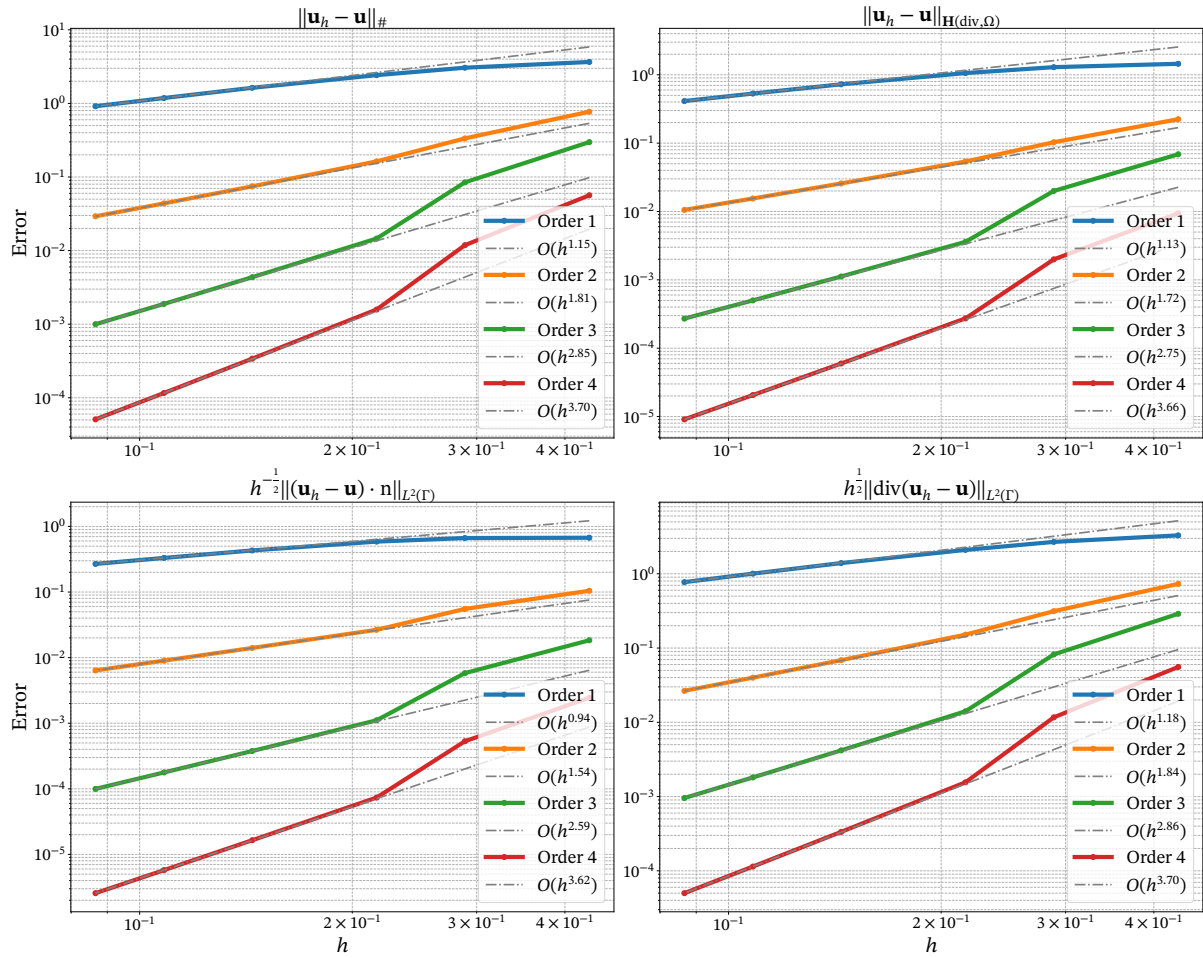


Figure 4.17: The $\#$ error and its components for the 2-form 3D proxy method. Up to order 4 and every order with interpolated rate in dash-dotted gray.

Observed convergence rates in the $\#$ -norm for 3D 2-forms. Except for the first order we observe

$$\|\mathbf{u}_h - \mathbf{u}\|_{\#} \leq Ch^{r-\frac{1}{2}},$$

$$h^{-\frac{1}{2}} \|(\mathbf{u}_h - \mathbf{u}) \cdot \mathbf{n}\|_{L^2(\Gamma)} \leq Ch^{r-\frac{1}{2}},$$

$$\|\mathbf{u}_h - \mathbf{u}\|_{\mathbf{H}(\text{div}, \Omega)} \leq Ch^{r-\frac{1}{2}},$$

$$h^{\frac{1}{2}} \|\nabla \cdot (\mathbf{u}_h - \mathbf{u})\|_{L^2(\Gamma)} \leq Ch^{r-\frac{1}{2}}.$$

The rates observed in the $\#$ -norm for the 3D 2-forms, coincide with the rates in the $\#$ -norm observed for the 2D as well as the 3D 1-forms.

4.3.4 h -convergence in the X -norm

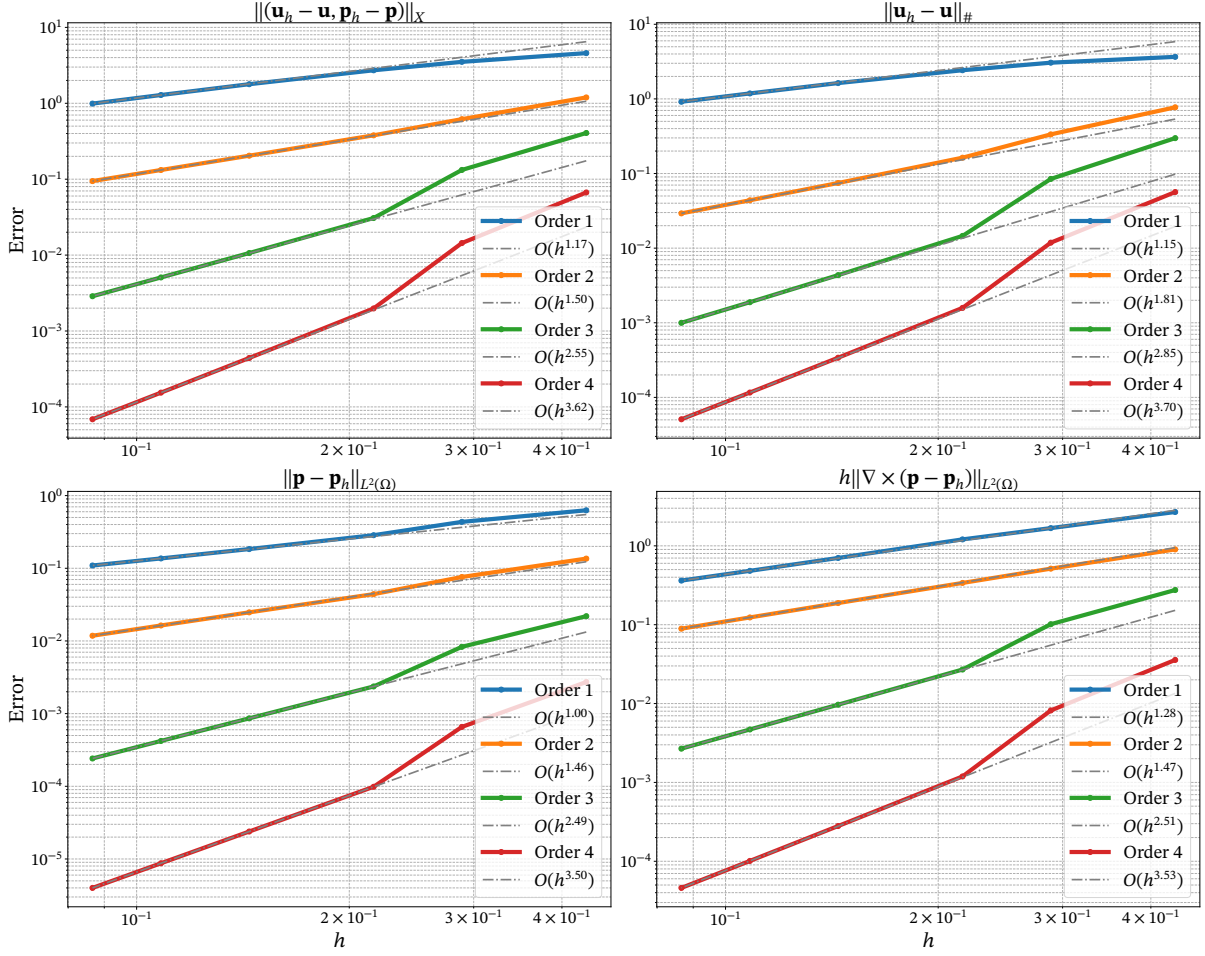


Figure 4.18: The X error and its components for the 2-form 3D proxy method. Up to order 4 and every order with interpolated rate in dash-dotted gray.

Observed convergence rates in the X -norm for 3D 2-forms. Except for the first order we observe

$$\|(\mathbf{u}_h - \mathbf{u}, \mathbf{p} - \mathbf{p}_h)\|_X \leq Ch^{r-\frac{1}{2}},$$

$$\|\mathbf{p}_h - \mathbf{p}\|_{L^2(\Omega)} \leq Ch^{l-\frac{1}{2}},$$

$$\|\mathbf{u}_h - \mathbf{u}\|_{\#} \leq Ch^{r-\frac{1}{2}},$$

$$h\|\nabla \times (\mathbf{p}_h - \mathbf{p})\|_{L^2(\Omega)} \leq Ch^{l-\frac{1}{2}}.$$

The rates observed in the X -norm for the 3D 2-forms, coincide with the rates in the X -norm observed for the 2D as well as the 3D 1-forms. Like for the 3D 1-forms, this shows as well the proven bound from Theorem 3.5.3 is suboptimal.

4.4 Experiments with non-convex geometries

In this part we want to showcase the ability of all the methods to handle non-convex geometries. The standard example being the reentrant corner or L-shaped domain in 2D and its equivalent in 3D, where one substracts a smaller cube from a larger cube without the new geometry having any holes or hollow parts. Holes and hollow parts should also be possible to handle, however the analysis in this thesis only covers trivial domains. For all the following experiments, we divide the domain boundary Γ as follows

$$\Gamma_D = \Gamma_{D1} \cup \Gamma_{D2}, \quad \Gamma = \Gamma_D \cup \Gamma \setminus \Gamma_D.$$

4.4.1 Singularities in reentrant corners

We want to point out, that with full Dirichlet boundary conditions, our methods do not create any singularities, however we can omit the Dirichlet terms (for 1-forms that is the natural normal right hand side term and the Nitsche tangential terms) and omit adding $-\langle \mathbf{u}_h \cdot \mathbf{n}, q \rangle_{\Gamma \setminus \Gamma_D}$ to the bilinear form B , just for the sake of witnessing the singularities. Figure 4.19 was obtained by setting

$$C_w = 10, \quad \mathbf{u}_h|_{\Gamma_{D1}} = -\frac{1}{10}\mathbf{n}, \quad \mathbf{u}_h|_{\Gamma_{D2}} = \frac{1}{10}\mathbf{n}, \quad \mathbf{f} = (5, -3).$$

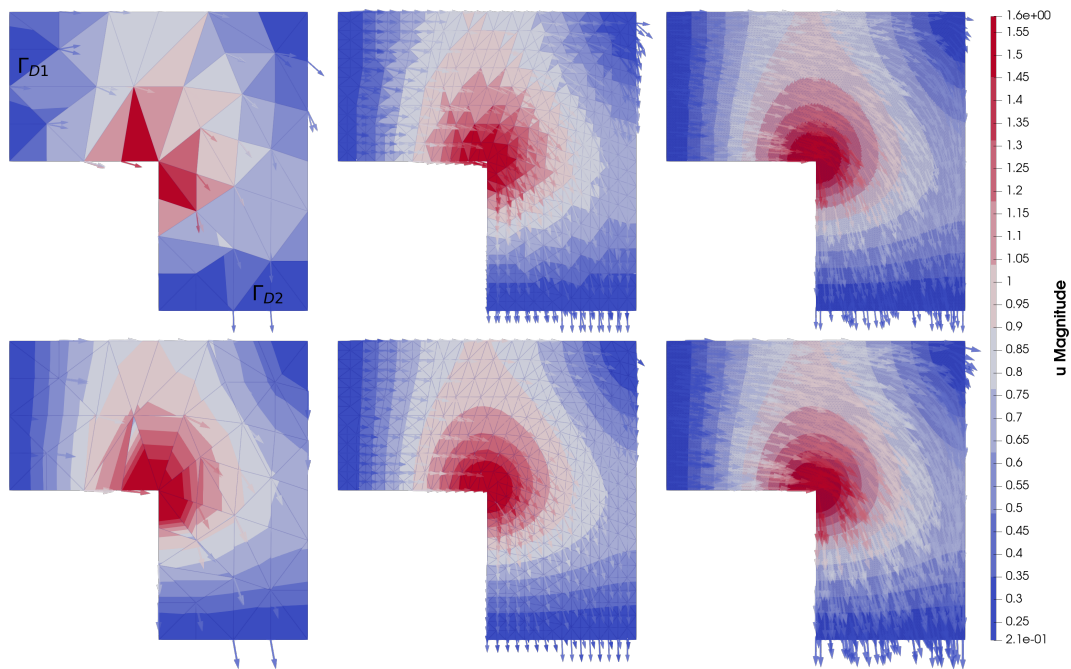


Figure 4.19: In the top left L-shaped domain the Dirichlet boundaries Γ_{D1} and Γ_{D2} are indicated. From left to right for both rows, the unstructured mesh goes from coarse to fine. In the top row we used first order elements for both spaces, and second order in the second row. One can clearly identify the singularities at the reentrant corner in all configurations.

4.4.2 Reentrant corner 1-forms in 2D

In this experiment we have the same configuration with one addition, that is the zero Dirichlet enforcement on $\Gamma \setminus \Gamma_D$. The boundary conditions are the same as in a 2D pipe flow example with Γ_{D1} as an inlet, Γ_{D2} as an outlet with prescribed velocity and "no-slip" boundary conditions at $\Gamma \setminus \Gamma_D$.

$$C_w = 100, \quad \mathbf{u}_h|_{\Gamma_{D1}} = -\frac{1}{10}\mathbf{n}, \quad \mathbf{u}_h|_{\Gamma_{D2}} = \frac{1}{10}\mathbf{n}, \quad \mathbf{u}_h|_{\Gamma \setminus \Gamma_D} = \mathbf{0}, \quad \mathbf{f} = (3, -3).$$

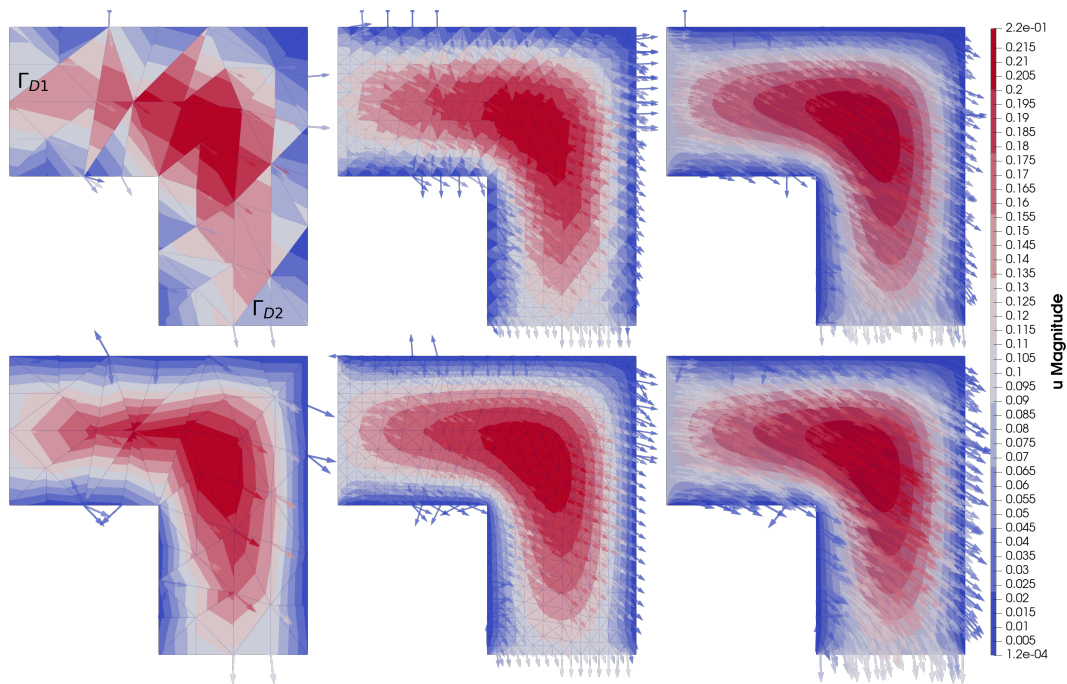


Figure 4.20: In the top left L-shaped domain the Dirichlet boundaries Γ_{D1} and Γ_{D2} are indicated again. From left to right for both rows, the unstructured mesh goes from coarse to fine. In the top row we used first order elements for both spaces, and second order in the second row. One cannot observe any singularity in the reentrant corner.

4.4.3 3D Reentrant corner geometry experiments

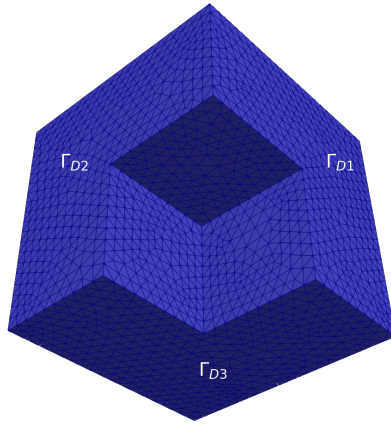


Figure 4.21: 3D reentrant corner geometry with illustrated boundaries. The origin is in the inner vertex of the reentrant corner. The normal vector on Γ_{D1} points in $-x$ direction, on Γ_{D2} in $-y$ and on Γ_{D3} in $-z$ direction.

In figures 4.7 and 4.13, we have observed that we solve the vector laplacian with two different mixed methods. In this section we show not only that there do not occur singularities in the reentrant corner for both 3D methods, but that we also obtain the same result when applying the same boundary conditions. We set up the problem as follows:

$$\Gamma_D = \Gamma_{D1} \cup \Gamma_{D2} \cup \Gamma_{D3}, \quad \Gamma = \Gamma_D \cup \Gamma \setminus \Gamma_D,$$

$$C_w = 100, \quad \mathbf{f} = (3, -3, -3),$$

$$\mathbf{u}|_{\Gamma_{D1}} = -\frac{1}{10}\mathbf{n}, \quad \mathbf{u}|_{\Gamma_{D2}} = \frac{1}{10}\mathbf{n},$$

$$\mathbf{u}|_{\Gamma_{D3}} = \frac{1}{10}\mathbf{n}, \quad \mathbf{u}|_{\Gamma \setminus \Gamma_D} = \mathbf{0}.$$

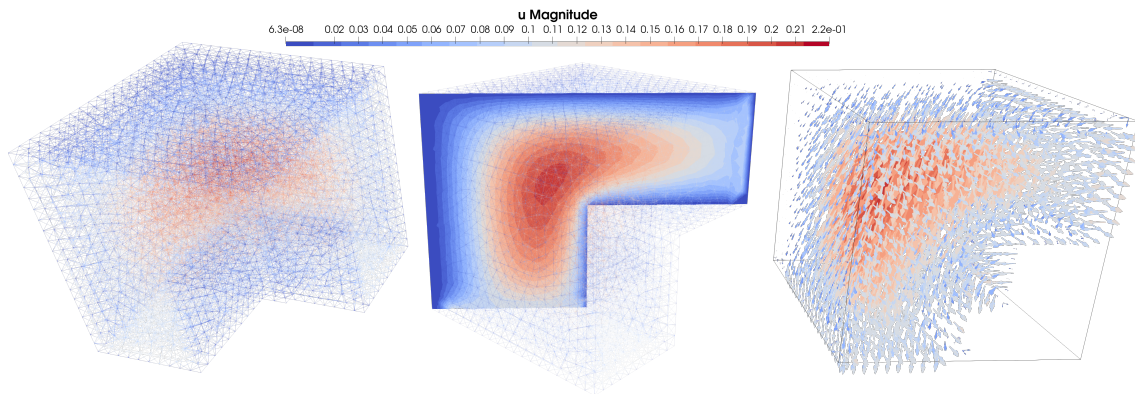


Figure 4.22: 1-forms 3D method (2.6.18). \mathbf{u} magnitude colored mesh, cut section that shows a similar result as in 4.20, vectorfield \mathbf{u} . No singularity occurring at the reentrant corner.

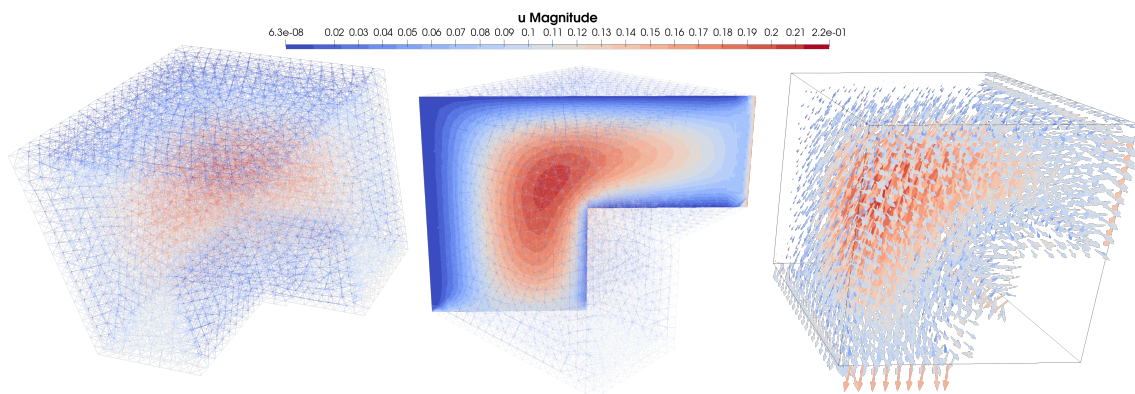


Figure 4.23: 2-forms 3D method (2.6.20). \mathbf{u} magnitude colored mesh, cut section that shows a similar result as in 4.20, vectorfield \mathbf{u} . No singularity occurring at the reentrant corner.

4.5 Perturbation factor experiments

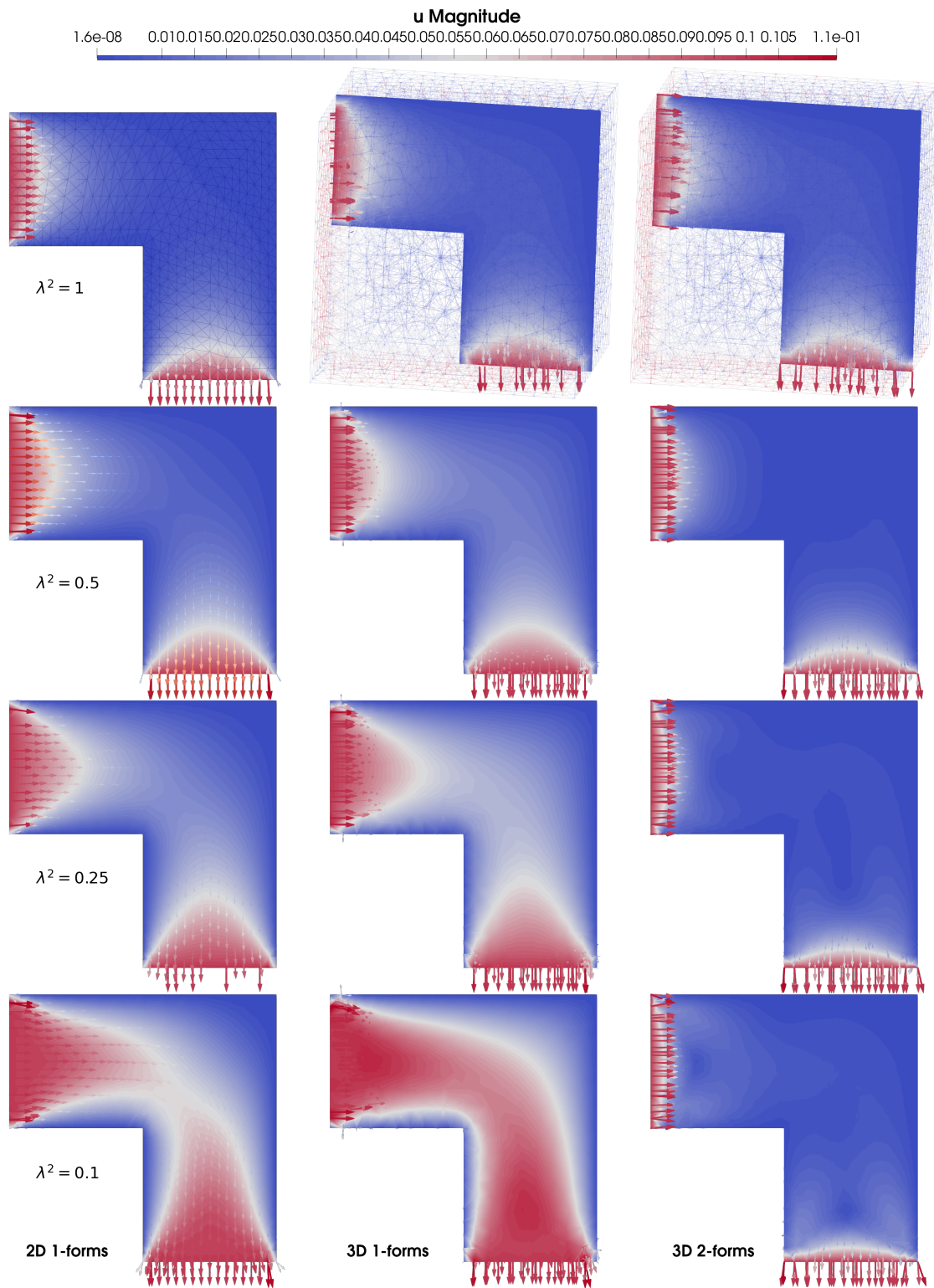


Figure 4.24: Perturbation factor experiments for all methods, with boundary conditions and general setup as in the previous experiment, see boxes on the following page. For both 1-forms methods, we clearly see developing flow, with decreasing λ^2 . For the 2-forms method, additional experiments need to be done.

By establishing Theorem 3.2.2 for the 1-form discretisation, we obtain a theoretical guarantee that the method is stable for every perturbation parameter $\lambda^2 > 0$ in (3.2.2). The result can be interpreted as follows:

- $\lambda^2 = 1$: The scheme reduces to the Hodge Laplace formulation for 1-forms and with minor modifications to the equations of linear elasticity.
- $\lambda^2 \rightarrow 0^+$: the formulation converges to the velocity-vorticity-pressure formulation of the incompressible Stokes equations.
- Intermediate λ^2 : offer a possible pathway to modelling compressible flow.

In figure 4.24 we present numerical results for several choices of λ^2 . The experimental setup mirrors the previous study, except that the forcing term is set to zero so that all three formulations can be compared directly and the isolated influence of λ^2 can be observed. The geometries and boundary-condition labels are identical to those used earlier.

2D 1-forms experiment setup

$$\begin{aligned} \text{order} &= 2, \quad C_w = 100, \quad \mathbf{f} = \mathbf{0} \\ \mathbf{u}_h|_{\Gamma_{D1}} &= -\frac{1}{10}\mathbf{n}, \quad \mathbf{u}_h|_{\Gamma_{D2}} = \frac{1}{10}\mathbf{n}, \\ \mathbf{u}_h|_{\Gamma \setminus \Gamma_D} &= \mathbf{0}. \end{aligned}$$

3D 1-forms and 2-forms experiment setup

$$\begin{aligned} \text{order} &= 2, \quad C_w = 100, \quad \mathbf{f} = \mathbf{0} \\ \mathbf{u}_h|_{\Gamma_{D1}} &= -\frac{1}{10}\mathbf{n}, \quad \mathbf{u}_h|_{\Gamma_{D2}} = \frac{1}{10}\mathbf{n}, \\ \mathbf{u}_h|_{\Gamma_{D3}} &= \frac{1}{10}\mathbf{n}, \quad \mathbf{u}_h|_{\Gamma \setminus \Gamma_D} = \mathbf{0}. \end{aligned}$$

Note that the stability proof for $\lambda^2 > 0$ is only valid for 1-forms in 2D and 3D. However, we suspect that this stability proof with Theorem 3.2.2 can also be done for the Nitsche Hodge Laplace method for 2-forms 2.6.20.

Chapter 5

Conclusion & Outlook

The main theoretical results of this thesis are Theorem 3.3.6 (FEEC continuity), Theorem 3.3.7 (FEEC stability), Theorem 3.4.2 (FEEC consistency), Theorem 3.5.3 (sub-optimal FEEC convergence) and Theorem 3.5.5 (optimal 2D 1-form convergence). Our theoretical results are supported by numerical experiments we have conducted. In all experiments, we observe the rate $\mathcal{O}(h^{r-\frac{1}{2}}) + \mathcal{O}(h^l)$ in the X norm. For the 2D 1-forms case, this coincides with the theoretical result we have obtained. For the other experiments, there is a gap of half an order to the a-priori bound.

We assume, that there exists a more elegant way than Theorem 3.5.4, to achieve an optimal a-priori error bound for the 2D 1-forms case, most likely an approach in the FEEC framework that allows us to prove an a-priori error result valid for all correctly employable proxy spaces. We will try to close this gap in upcoming work.

Furthermore, Theorem 3.2.2 possibly allows us to simulate compressible flow problems, due to the stability of the 1-forms method for positive λ^2 . The numerical experiments conducted with the perturbation factor λ^2 seem to suggest so, however, more analysis needs to be done to understand how to model incompressible flow. Another application is elasticity, which can also be explored with all the methods. The difference is strictly that in the 2-forms case, the normal component of the Dirichlet boundary condition is applied with the Nitsche penalization and the tangential component is incorporated into the variational formulation naturally, whereas in the 1-forms method it is the other way around. This behavior is nicely illustrated in figures 4.9 and 4.15 and can obviously be seen in the variational formulations in (2.6.20) and (2.6.18).

We would like to further explore the modelling capabilities of our framework in the context of linear elasticity. Extending the current theoretical results to non-trivial domains (e.g., domains with holes and voids) is essential, without this generalisation, the elasticity application remains of limited practical value. Accordingly, a first direction for future work is to carry out this extension.

In addition, the linear systems that arise become increasingly ill-conditioned as the mesh is refined, an observation made at the outset of this thesis. Developing effective preconditioners for the proposed methods therefore is a second promising direction for further study.

References

- [Ern21b] A. Ern and J.-L. Guermond, *Finite Elements II: Galerkin Approximation, Elliptic and Mixed PDEs*. Springer, 2021. DOI: 10.1007/978-3-030-56923-5.
- [Arnold12] D. N. Arnold, R. S. Falk, and J. Gopalakrishnan, “Mixed finite element approximation of the vector laplacian with dirichlet boundary conditions,” *Mathematical Models and Methods in Applied Sciences*, vol. 22, no. 09, 2012. DOI: 10.1142/s0218202512500248.
- [Boon24] W. M. Boon, R. Hiptmair, W. Tonnon, and E. Zampa, “H(curl)-based approximation of the stokes problem with slip boundary conditions,” *arXiv preprint*, 2024. arXiv: 2407.13353. [Online]. Available: <https://arxiv.org/abs/2407.13353>.
- [Wang25] H. Wang, L. Wang, G. Zhu, and C. Xiong, “Rot-div mixed finite element method of two dimensional hodge laplacian problem,” *Computers & Mathematics with Applications*, vol. 184, pp. 134–152, 2025, ISSN: 0898-1221. DOI: <https://doi.org/10.1016/j.camwa.2025.02.005>.
- [Bossavit88] A. Bossavit, “Whitney forms: A class of finite elements for three-dimensional computations in electromagnetism,” *Physical Science, Measurement and Instrumentation, Management and Education - Reviews, IEE Proceedings A*, vol. 135, pp. 493–500, Dec. 1988. DOI: 10.1049/ip-a-1:19880077.
- [Raviart77] P. A. Raviart and J. M. Thomas, “A mixed finite element method for 2-nd order elliptic problems,” in *Mathematical Aspects of Finite Element Methods*, I. Galligani and E. Magenes, Eds., Berlin, Heidelberg: Springer Berlin Heidelberg, 1977, pp. 292–315, ISBN: 978-3-540-37158-8.
- [Nédélec80] J. Nédélec, “Mixed finite elements in \mathbb{R}^3 .,” *Numerische Mathematik*, vol. 35, pp. 315–342, 1980. [Online]. Available: <http://eudml.org/doc/186293>.
- [Brezzi91] F. Brezzi and M. Fortin, *Mixed and Hybrid Finite Element Methods*, ser. Springer Series in Computational Mathematics 15. Springer New York, 1991, ISBN: 3-540-97582-9.
- [Hiptmair01] R. Hiptmair, “Discrete hodge operators,” *Numerische Mathematik*, vol. 90, no. 2, pp. 265–289, Dec. 2001, ISSN: 0945-3245. DOI: 10.1007/s002110100295. [Online]. Available: <https://doi.org/10.1007/s002110100295>.
- [Arnold18] D. N. Arnold, *Finite Element Exterior Calculus*. Society for Industrial and Applied Mathematics, 2018. DOI: 10.1137/1.9781611975543.
- [Arnold06] D. N. Arnold, R. S. Falk, and R. Winther, “Finite element exterior calculus, homological techniques, and applications,” *Acta Numerica*, vol. 15, pp. 1–155, 2006.

- [Brezzi85] F. Brezzi, J. J. Douglas, and L. Marini, “Two families of mixed finite elements for second order elliptic problems.,” *Numerische Mathematik*, vol. 47, pp. 217–236, 1985.
- [Ciarlet72] P. G. Ciarlet and P.-A. Raviart, “General Lagrange and Hermite interpolation in R^n with applications to finite element methods,” *Arch. Rational Mech. Anal.*, vol. 46, pp. 177–199, 1972, ISSN: 0003-9527.
- [Ern21a] A. Ern and J.-L. Guermond, *Finite Elements I: Approximation and Interpolation*. Springer, 2021. DOI: 10.1007/978-3-030-56341-7.
- [Buffa02] A. Buffa, M. Costabel, and D. Sheen, “On traces for $h(\text{curl}, \omega)$ in lipschitz domains,” *Journal of Mathematical Analysis and Applications*, vol. 276, no. 2, pp. 845–867, 2002, ISSN: 0022-247X. DOI: [https://doi.org/10.1016/S0022-247X\(02\)00455-9](https://doi.org/10.1016/S0022-247X(02)00455-9). [Online]. Available: <https://www.sciencedirect.com/science/article/pii/S0022247X02004559>.
- [Boffi13] D. Boffi, F. Brezzi, and M. Fortin, *Mixed Finite Element Methods and Applications*, ser. Springer Series in Computational Mathematics. Springer Berlin Heidelberg, 2013, ISBN: 9783642365195. [Online]. Available: <https://books.google.at/books?id=mRhAAAAAQBAJ>.
- [Boon25] W. M. Boon, R. Hiptmair, W. Tonnon, and E. Zampa, “ $H(\text{curl})$ -based approximation of the stokes problem with dirichlet boundary conditions,” *in preparation*, 2025.
- [Nečas62] J. Nečas, “Sur une méthode pour résoudre les équations aux dérivées partielles du type elliptique, voisine de la variationnelle,” *Annali della Scuola Normale Superiore di Pisa - Classe di Scienze*, vol. 16, no. 4, pp. 305–326, 1962. [Online]. Available: <http://eudml.org/doc/83288>.
- [Babuška62] I. BABUSKA, “Error-bounds for finite element method.,” *Numerische Mathematik*, vol. 16, pp. 322–333, 1970/71. [Online]. Available: <http://eudml.org/doc/132037>.
- [Bonnet10] A. Bonnet-Ben Dhia, P. Ciarlet, and C. Zwölf, “Time harmonic wave diffraction problems in materials with sign-shifting coefficients,” *Journal of Computational and Applied Mathematics*, vol. 234, no. 6, pp. 1912–1919, 2010, Eighth International Conference on Mathematical and Numerical Aspects of Waves (Waves 2007), ISSN: 0377-0427. DOI: <https://doi.org/10.1016/j.cam.2009.08.041>. [Online]. Available: <https://www.sciencedirect.com/science/article/pii/S0377042709005196>.

Appendix A

In-silico environment 1

The experiments were done on a WSL system running Ubuntu 20.04.2 LTS with NGSolve v6.2.2402.

Table A.1: Hardware Specifications

Specification	Detail
Architecture	x86_64
CPU op-mode(s)	32-bit, 64-bit
Address sizes	46 bits physical, 48 bits virtual
Byte Order	Little Endian
CPU(s)	20
On-line CPU(s) list	0–19
Vendor ID	GenuineIntel
Model name	12th Gen Intel(R) Core(TM) i9-12900H
CPU family	6
Model	154
Thread(s) per core	2
Core(s) per socket	10
Socket(s)	1
Caches (sum of all):	
L1d	480 KiB (10 instances)
L1i	320 KiB (10 instances)
L2	12.5 MiB (10 instances)
L3	24 MiB (1 instance)
RAM	64 GB DDR5, 4800MHz

Appendix B

In-silico environment 2


The experiments were done on a WSL system running Ubuntu 22.04.05 LTS with NGSolve v6.2.2402.

Table B.1: Hardware Specifications

Specification	Detail
Architecture	x86_64
CPU op-mode(s)	32-bit, 64-bit
Address sizes	46 bits physical, 48 bits virtual
Byte Order	Little Endian
CPU(s)	52
On-line CPU(s) list	0-51
Vendor ID	GenuineIntel
Model name	Intel(R) Xeon(R) Platinum 8270 CPU @ 2.70GHz
CPU family	6
Model	85
Thread(s) per core	1
Core(s) per socket	26
Socket(s)	2
Caches (sum of all):	
L1d	1.6 MiB (52 instances)
L1i	1.6 MiB (52 instances)
L2	52 MiB (52 instances)
L3	71.5 MiB (2 instances)
NUMA node(s):	2
Numa node0 CPU(s):	0-25
Numa node1 CPU(s):	26-51
RAM	384 GB DDR4, 2933MHz (12 x 32GB)

Appendix C

Differential operators on \mathbf{g}

Listing C.1: 1-form 3D proxy method Python code in  NGSolve

```

1  def JacobianOfCF(cf):
2      #Function to compute the Jacobi Matrix of vector cf
3      Jac_u_3D = CF((
4          cf[0].Diff(x), cf[0].Diff(y), cf[0].Diff(z),
5          cf[1].Diff(x), cf[1].Diff(y), cf[1].Diff(z),
6          cf[2].Diff(x), cf[2].Diff(y), cf[2].Diff(z)
7      ), dims=(3, 3))
8      return Jac_u_3D
9
10 def GGrad(cf):
11     # Function to compute the gradient of a scalar Coefficient Function
12     gg = [cf.Diff(coords[i]) for i in range(mesh.dim)]
13     return CF(tuple(gg))
14
15 def GCurl(cf):
16     #Function to compute the curl or rot of cf using Jacobian
17     if cf.dim == 1:
18         curl_rot_u = CF((cf.Diff(y), - cf.Diff(x)))
19         return curl_rot_u
20     elif mesh.dim == 2:
21         rot_u = CF(cf[1].Diff(x) - cf[0].Diff(y))
22         return rot_u
23     elif mesh.dim == 3:
24         Jac_u = JacobianOfCF(cf)
25         curl_u = CF((Jac_u[2,1] - Jac_u[1,2],
26                     Jac_u[0,2] - Jac_u[2,0],
27                     Jac_u[1,0] - Jac_u[0,1]))
28         return curl_u
29
30 def GDiv(cf):
31     # Function to compute the divergence of a vector coefficient function
32     gd = [cf[i].Diff(coords[i]) for i in range(cf.dim)]
33     return CF(sum(gd))

```

Declaration of originality

The signed declaration of originality is a component of every written paper or thesis authored during the course of studies. In consultation with the supervisor, one of the following three options must be selected:

- ☒ I confirm that I authored the work in question independently and in my own words, i.e. that no one helped me to author it. Suggestions from the supervisor regarding language and content are excepted. I used no generative artificial intelligence technologies¹.
- ☐ I confirm that I authored the work in question independently and in my own words, i.e. that no one helped me to author it. Suggestions from the supervisor regarding language and content are excepted. I used and cited generative artificial intelligence technologies².
- ☐ I confirm that I authored the work in question independently and in my own words, i.e. that no one helped me to author it. Suggestions from the supervisor regarding language and content are excepted. I used generative artificial intelligence technologies³. In consultation with the supervisor, I did not cite them.

Title of paper or thesis:

Nitsche-based enforcement of Dirichlet boundary conditions for the Hodge Laplacian

Authored by:

If the work was compiled in a group, the names of all authors are required.

Last name(s):

Tello Fachin

First name(s):

Camilo

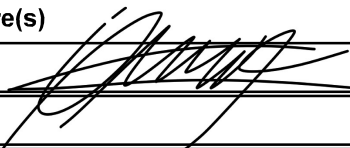
With my signature I confirm the following:

- I have adhered to the rules set out in the Citation Guide.
- I have documented all methods, data and processes truthfully and fully.
- I have mentioned all persons who were significant facilitators of the work.

I am aware that the work may be screened electronically for originality.

Place, date

Zürich, 31.03.2025

Signature(s)

If the work was compiled in a group, the names of all authors are required. Through their signatures they vouch jointly for the entire content of the written work.

¹ E.g. ChatGPT, DALL E 2, Google Bard

² E.g. ChatGPT, DALL E 2, Google Bard

³ E.g. ChatGPT, DALL E 2, Google Bard